ON SOME MATHEMATICAL ASPECTS OF DEFORMATIONS OF INHOMOGENEOUS ELASTIC MATERIALS

by

JEFFRY KUSUMA

Drs. (Matematika), Universitas Hasanuddin

Thesis submitted for the Degree of

Doctor of Philosophy

at The University of Adelaide

Department of Applied Mathematics

May, 1992

CONTENTS

SUMMARY

Two types of inhomogeneous elastic materials are considered in this thesis. The first type of material is made up of different regions with the elastic coefficients constant in each region. For the second type of material the elastic coefficients vary continuously with the spatial coordinates.

The thesis may be thought of as being composed of three parts. In the first part, the one-dimensional propagation of waves through an inhomogeneous elastic material is considered. Numerical solutions for certain materials are obtained by using the finite difference method. In the second part of the thesis, axially symmetric and spherically symmetric deformations problems of inhomogeneous materials are considered by employing analytical techniques. In the final and major part of the thesis, we consider some antiplane and plane deformation problems for isotropic and anisotropic inhomogeneous elastic materials. In the antiplane and plane problems emphasis is placed on the development of the boundary element method for the numerical solution of particular boundary value problems. The kernel of the integral equation for some specific materials is derived so that the standard boundary element method may be employed.

SIGNED STATEMENT

I declare that the thesis contains no material which has been accepted for the award of any other degree or diploma in any University and that, to the best of my knowledge and belief, the thesis contains no material previously published or written by another person, except where due reference is made in the text of the thesis.

I consent to the thesis being made available for photocopying and loan if applicable if accepted for the award of the degree.

Jeffry Kusuma

ACKNOWLEDGEMENTS

I wish to thank my supervisor Dr. D.L. Clements for his encouragement and valuable advice, as well as his numerous helpful suggestions and corrections during the work for this thesis.

The author gratefully acknowledge the support of IDP (International Development Program) scholarship from March 1989 to January 1990 and AIDAB (Australian International Development Assistance Bureau) scholarship from January 1990 to April 1992.

Finally, but most importantly, the work presented in this thesis would never have been completed without the undying love, encouragement, support and patience of my parents and family. Although they did not understand what I was doing, they have provided the greatest contribution to this thesis.

CHAPTER 1

INTRODUCTION

The foundation of the mathematical theory of elasticity dates back to the seventeenth century when Robert Hooke stated that the extension of springlike solid bodies, produced by the tensile forces, is proportional to the applied force. Such a relation which is known as a stress–strain relation has been developed extensively over the last two centuries due to the growing demand for the elastic analysis of many problems involving solid bodies. A large number of books and theories have been written on the subject involving homogeneous materials (see for example Green and Zerna [34], Love [47]. Muskhelishvli [53], Sokolnikoff [71]). The solution of boundary value problems for such materials has been widely investigated. Several methods have been developed such as the use of integral transforms (see for example Sneddon [68], [69], [70], Tranter [77]), special functions (see for example Sneddon [70], Watson [80]) and complex variable methods (see for example Muskhelishvli [53]). More recently with the help of modern computational equipment, numerical methods such as finite elements, finite differences (see for example Yang and Lee [88]), the boundary element method (BIEM) (see for example Abdrabbo and Mahmoud [1], Ang [3], [4], Cheng [9], Clements [10], [11], [12], [13], [14], [16], [19], Coleman [20], Cruse [22], Ligget [46], Rangogni [59], [60], Rizzo [61) and the combination of the finite element and boundary element method (see for example Wearing and Sheikh [81]) have been used extensively to solve a number of boundary value problems for homogeneous elastic materials.

The study of boundary value problem involving inhomogeneous materials is also of great importance in applications. In comparison with the homogeneous case relatively little has been done in this area. Problems of this type are of considerable

practical importance in view of the fact that inhomogeneous materials such as fibre reinforced and composite materials have wide applications in modern technology especially in engineering.

The solution of many problems for inhomogeneous materials presents considerable mathematical difficulty. However for laminated materials a number of solutions exist. For example, recent investigations presented by Sun et al [74] have described the dynamic behaviour of a laminated composite. Following this work, several researchers have studied the propagation of waves in a composite with periodic structure. Nayfeh and Nasser [56] investigated elastic waves in inhomogeneous periodic materials. Using the variational method, Kohn et al [43] studied wave dispersion in composite media. More recently, Yang and Lee [88] developed a numerical method to analyse the modes of Floquet waves.

Some work has been done and a number of papers published on the subject of linear elasticity involving inhomogeneous materials with continuous variation of the elastic parameter. In particular some progress has been made in applying the boundary element method to such problems. Since Rizzo [61] approached the classical elastostatic problem using the boundary integral method, the boundary integral element method has become a more and more accepted tool for the fast and accurate numerical solution of problems for homogeneous media. In comparison with the other commonly used numerical methods, the obvious advantage of the boundary integral element technique is that the only quantities that have to be specifically determined in the numerical solution process are the boundary values. Once these have been obtained, the basic unknowns at any interior point may be found by the use of an appropriate integral relation. Very recently, by using the radial basis functions approach, Coleman [20] has employed the boundary element method to solve the Helmholtz equation with variable coefficients. Other boundary element techniques involving the evaluation of the area integral have also been developed (see

for example Cruse [22]). However such as approach employs the unknown interior points which means the boundary element method is less effective. To employ the standard boundary element method, it is necessary to find a suitable kernel of the integral equation. Unfortunately, the kernel of the integral equation is often very hard to find. This is particularly true for elastic problems involving inhomogeneous materials. The two dimensional Laplace equation with variable coefficients which appear in anti–plane deformation problems involving inhomogeneous materials has been successfully approached by Clements [10] using the boundary element method. However this approach still needs to be developed since the variable coefficient which is considered in his paper only varies with one spatial coordinate.

In this thesis, we review and develop several analytical and numerical methods for solving problems in the theory of linear elasticity of inhomogeneous materials. In chapter 2, the propagation of waves through one dimensional deformations of inhomogeneous materials is discussed through the WKBJ method. The results of the perturbation technique for specific problems are compared also with the results from the Floquet theory. The propagation of Floquet waves through inhomogeneous periodic materials is also investigated numerically in this chapter by using the finite difference method. Chapters 3 and 4 discuss axially symmetric deformations and spherically symmetric deformations respectively. Analytical solutions are derived by the integral transform method and the method of separation of variables. Numerical solutions for some problems are obtained by the two point boundary value method. Chapter 5 deals with anti–plane deformation problems for isotropic materials. Analytical solutions are derived through the method of separation of variables and the numerical solution through the boundary integral element method (BIEM) combined with the perturbation technique. The development of the boundary element method for certain classes of shear moduli for the materials is centred around finding a suitable kernel for the integral equation. Several problems and their numerical results

are compared with their analytical results in order to verify the accuracy of the numerical procedure. In chapter 6 we consider anti–plane deformations for anisotropic materials. The development of the boundary element method again centres on finding a suitable kernel for the integral equation so that the standard boundary element method can be directly applied. Chapter 7 deals with plane deformations for inhomogeneous materials. The numerical results obtained by coupling the boundary integral element method (BIEM) and the perturbation technique are compared with the numerical results using the two point boundary value method. Several numerical results relating to stress intensity factors are also discussed in this chapter. In chapter 8, the integral equation formulations for anisotropic inhomogeneous elastic materials developed in chapter 6 are used in considering the surface effects due to incident plane polarised SH waves.

CHAPTER 2

ONE–DIMENSIONAL ELASTIC DEFORMATIONS

2.1 Introduction

One–dimensional elastic deformations for inhomogeneous materials are considered in this chapter. Such materials, including composite materials, have become an important ingredient in many modern engineering structures. The propagation of elastic waves in such materials has, therefore, been discussed by a number of writers using different theories and approaches. For example by using WKB method Kohn [42] has discussed the propagation of small frequency waves in composite materials.

In the present chapter, we consider the propagation of large frequency waves through inhomogeneous materials with constant cross section as well as with variable cross section using the WKB or WKBJ method (named after Wentzel, Kramers, Brillouin and Jeffreys) in which the large frequency wave solutions can be compared with their approximations. Using the perturbation method, we consider the propagation of waves through specific materials with relatively small variation of the Young modulus and the density. For two layered composite materials, the analysis of the Floquet waves has been discussed by Yang and Lee [88] using the finite difference approximation. Here we extend their work by including inhomogeneous materials in section 2.5. The numerical results for two layered composite cells are then compared with the exact solutions.

2.2 Basic equations

We consider a semi-infinite rod with constant cross section A as shown in Figure 2.1. By applying Newton's law to the force through the cross section A at a point x and $x + \delta x$ we obtain

$$A\left[\sigma(x+\delta x) - \sigma(x)\right] = \rho \delta x A \frac{\partial^2 u}{\partial t^2}, \tag{2.2.1}$$

Here ρ denotes the mass of the inhomogeneous rod at the point x, u denotes the displacement and σ denotes the force at the relevant points. As usual we can make δx arbitrarily small, thus by using the stress strain relation $\sigma = \eta \partial u/\partial x$ equation (2.2.1) reduces to the wave equation for the inhomogeneous semi infinite rod

$$\frac{1}{\rho}\frac{\partial}{\partial x}\left(\eta \frac{\partial u}{\partial x}\right) = \frac{\partial^2 u}{\partial t^2}, \tag{2.2.2}$$

where η denotes the Young modulus or the elasticity coefficient.

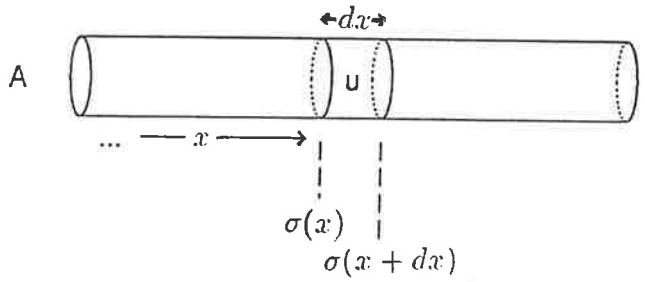

Figure 2.1
Semi-infinite rod with constant cross section A

In the case when η and ρ are constants, equation (2.2.2) simply becomes the well known one-dimensional wave equation

$$C^2 \frac{\partial^2 u}{\partial x^2} = \frac{\partial^2 u}{\partial t^2}, \tag{2.2.3}$$

where $C^2 = \eta/\rho$.

If the cross section varies then by applying Newton's law, we obtain

$$A(x+\delta x)\sigma(x+\delta x) - A(x)\sigma(x) = \frac{1}{2}\rho\delta x\{A(x+\delta x) + A(x)\}\frac{\partial^2 u}{\partial t^2}. \tag{2.2.4}$$

Expanding $A(x+\delta x)$ and $\sigma(x+\delta x)$ using Taylor's series and taking the limit as δx tends to zero gives

$$\frac{1}{\rho A}\frac{\partial}{\partial x}\left(A\eta\frac{\partial u}{\partial x}\right) = \frac{\partial^2 u}{\partial t^2}. \tag{2.2.5}$$

2.3 Waves in inhomogeneous rods

Consider equation (2.2.5) for wave propagation along the x axis in an elastic inhomogeneous medium with varying cross section

$$\frac{1}{\rho A}\frac{\partial}{\partial x}\left(A\eta\frac{\partial u}{\partial x}\right) = \frac{\partial^2 u}{\partial t^2}, \tag{2.3.1}$$

where $u(x,t)$ is the particle displacement, $\eta = \eta(x)$ is the elasticity coefficient, $A = A(x)$ is the area of cross section, $\rho = \rho(x)$ is the mass density. Yih [90] express that the solution of (2.3.1) may exist in the form

$$u(x,t) = f(x)\exp\left[\imath(g(x) - \omega t)\right], \tag{2.3.2}$$

also Clements [10] suggests that a simple spatial transformation might simplify equation (2.3.1). Thus if we assume the displacement takes the form

$$u(x,t) = U(x)\left[A(x)\eta(x)\right]^{-\frac{1}{2}}\exp[-\imath\omega t], \tag{2.3.3}$$

where $\imath^2 = -1$ and ω is a constant, then by substituting equation (2.3.3) into equation (2.3.1) we obtain

$$\frac{\partial^2 U}{\partial x^2} + \omega^2\left[\frac{\rho}{\eta} - \frac{\Lambda}{\omega^2}\right]U = 0, \tag{2.3.4}$$

where

$$\Lambda(x) = \frac{1}{2}(A\eta)''(A\eta)^{-1} - \frac{1}{4}(A\eta)'^2(A\eta)^{-2}. \tag{2.3.5}$$

Equation (2.3.3) shows that the condition $(\frac{\rho}{\eta} - \frac{\Lambda}{\omega^2}) > 0$ is sufficient for U to have a periodic solution. As is known, unless $(\frac{\rho}{\eta} - \frac{\Lambda}{\omega^2})$ equal a constant, equation (2.3.2) does not admit a progressive wave solution since the inhomogeneity of the materials induces wave reflection. However, an approximate solution can be obtained which exhibits many of the properties of a progressive wave under certain restricted conditions. Furthermore suppose we can set

$$U(x) = T(x)\exp[\imath S(x)], \tag{2.3.6}$$

where T and S are real valued functions which are to be determined. By substituting equation (2.3.6) into equation (2.3.4) we obtain

$$T'' - TS'^2 + \left(\frac{\omega^2\rho}{\eta} - \Lambda\right)T + (2T'S' + TS'')\imath = 0. \tag{2.3.7}$$

This condition only holds if the real and imaginary parts of the complex number vanish. That is

$$T'' - TS'^2 + \left(\frac{\omega^2\rho}{\eta} - \Lambda\right)T = 0, \tag{2.3.8}$$

$$2T'S' + TS'' = 0, \tag{2.3.9}$$

or

$$T^2S' = \text{constant}. \tag{2.3.10}$$

The power in complex notation is given by

$$P = \Re\left\{A\eta\frac{\partial u}{\partial x}\right\}\Re\left\{\frac{\partial u}{\partial t}\right\}, \tag{2.3.11}$$

where $\Re$ denotes the real part of the relevant argument or

$$P = \frac{1}{2}\omega A\eta T^2S' - \frac{1}{2}\omega A\eta T\left\{T'\sin 2(S+\omega t) + TS'\cos 2(S+\omega t)\right\}, \tag{2.3.12}$$

where

$$\mathcal{T} = T(A\eta)^{-\frac{1}{2}}. \tag{2.3.13}$$

Using equation (2.3.10) since ω is a constant, the time average power per unit volume is then given by

$$\begin{aligned} \overline{P} &= \lim_{\alpha \to 0} \left\{ \frac{1}{\alpha} \int_0^{\alpha} P(t)\, dt \right\} \\ &= \frac{1}{2}\omega T^2 S' \end{aligned} \tag{2.3.14}$$

which means that the time average of the power flow P over the unit volume is constant. By assuming that $(\frac{\rho}{\eta} - \frac{\Lambda}{\omega^2})$ is such that T is a slowly varying function of x, and hence that T''/T tends to zero or can be neglected then from equation (2.3.8) we obtain

$$S' = \pm\omega \left[\frac{\rho}{\eta} - \frac{\Lambda}{\omega^2} \right]^{\frac{1}{2}}. \tag{2.3.15}$$

Also equation (2.3.10) gives

$$T = T_0 \left[\frac{\rho}{\eta} - \frac{\Lambda}{\omega^2} \right]^{-\frac{1}{4}}, \tag{2.3.16}$$

where T_0 is a constant. Thus finally by using (2.3.16), (2.3.15), (2.3.6) and (2.3.3) we obtain

$$u(x,t) = T_0(A\eta)^{-\frac{1}{2}} \left[\frac{\rho}{\eta} - \frac{\Lambda}{\omega^2} \right]^{-\frac{1}{4}} \exp\left[i\omega \left(t \pm \int_0^x \left[\frac{\rho(\alpha)}{\eta(\alpha)} - \frac{\Lambda(\alpha)}{\omega^2} \right]^{\frac{1}{2}} d\alpha \right) \right]. \tag{2.3.17}$$

For large ω, equation (2.3.4) can be approximated by

$$\frac{\partial^2 U}{\partial x^2} + \frac{\omega^2 \rho}{\eta} U = 0, \tag{2.3.18}$$

so that the solution for the displacement in (2.3.17) reduces to

$$u(x,t) = T_0(A\eta)^{-\frac{1}{2}} \left(\frac{\eta}{\rho} \right)^{\frac{1}{4}} \exp[i\omega(t \pm \int_0^x \left(\frac{\rho}{\eta} \right)^{\frac{1}{2}} d\alpha)]. \tag{2.3.19}$$

Another method for the comparison of results in the case of large ω will be discussed next. Following Nayfeh and Nasser [56], if we write $U(x)$ as

$$U(x) = \exp[\omega \int_0^x Q\, d\alpha], \tag{2.3.20}$$

then by substituting this into equation (2.3.4) we obtain Riccati's equation

$$\frac{1}{\omega}Q' + Q^2 + \frac{\rho}{\eta} - \frac{\Lambda}{\omega^2} = 0. \tag{2.3.21}$$

Suppose ω is large and Q can be written in the form

$$Q = Q_0 + \frac{Q_1}{\omega} + \frac{Q_2}{\omega^2} + \cdots \tag{2.3.22}$$

By using three terms of the series only, we now determine Q_0, Q_1, and Q_2 by substituting (2.3.22) into equation (2.3.21). This gives

$$\begin{aligned} Q_0^2 + \frac{\rho}{\eta} &= 0, \\ Q_0' + 2Q_0Q_1 &= 0, \\ Q_1' + Q_1^2 + 2Q_0Q_2 - \Lambda &= 0, \end{aligned} \tag{2.3.23}$$

or

$$\begin{aligned} Q_0 &= \pm \frac{i}{C}, \\ Q_1 &= \mp \frac{1}{2}C(\frac{1}{C})', \\ Q_2 &= \mp \frac{1}{2}Cf_i \pm \frac{1}{4}C^2(\frac{1}{C})'' \pm \frac{3}{8}C^3(\frac{1}{C})'^2, \end{aligned} \tag{2.3.24}$$

where $C = \sqrt{\eta/\rho}$. By using (2.3.24), (2.3.22), (2.3.20) and (2.3.3) we finally obtain

$$u(x,t) = T_0\left[A\eta\right]^{-\frac{1}{2}} C^{\frac{1}{2}} \exp\left[i\omega\left\{t \pm \int_0^x [\frac{1}{C} - \frac{fC}{\omega^2} - \frac{C^3}{8\omega^2}(\frac{2}{C}(\frac{1}{C})'' - 3(\frac{1}{C})'^2)]\, d\alpha\right\}\right]. \tag{2.3.25}$$

Equation (2.3.19) and equation (2.3.25) are similar for large values of ω since the terms containing ω^{-2} are negligible.

Of particular interest is the case where $\eta = \eta_0$, $A = A_0$, $\rho = \rho_0(x+a)^n$ where η_0, A_0, ρ_0 and a are constants. We obtain

$$\Lambda(x) = 0. \tag{2.3.26}$$

Equation (2.3.17) becomes

$$u(x,t) = T_0 A_0^{-\frac{1}{2}} (\eta_0\rho_0)^{-\frac{1}{4}} (x+a)^{-\frac{n}{4}} \exp\left[i\omega\left\{t \pm \frac{\sqrt{\rho_0/\eta_0}}{n/2+1}\left((x+a)^{\frac{n}{2}+1} - a^{\frac{n}{2}+1}\right)\right\}\right]. \tag{2.3.27}$$

We see here that for the case $n = -4$ the amplitude varies linearly with x while the wave speed also varies with respect to position according to the equation

$$V = \eta_0^{\frac{1}{2}} \rho_0^{-\frac{1}{2}} (x+a)^2. \tag{2.3.28}$$

In the case where $\Lambda(x) = 0$, $A = A_0$, $\eta = \eta_0(x+a)^2$ and $\rho = \rho_0(x+a)^2$ we obtain

$$u(x,t) = T_0 A_0^{-\frac{1}{2}} (\eta_0\rho_0)^{-\frac{1}{4}} (x+a)^{-1} \exp\left[i\omega\left\{t \pm \sqrt{\frac{\rho_0}{\eta_0}}x\right\}\right]. \tag{2.3.29}$$

Equation (2.3.29) shows that the wave speed is constant as well, while the amplitude is inversely proportional to x.

In the case of a homogeneous right circular cone, $A = A_0 x$, $\eta = \eta_0$, $\rho = \rho_0$, $\Lambda = -\frac{1}{4}x^{-2}$ we have the displacement in form

$$u(x,t) = T_0\left[A_0\eta_0 x\right]^{-\frac{1}{2}}\left[\frac{\rho_o}{\eta_0} + \frac{1}{4x^2\omega^2}\right]^{-\frac{1}{4}} \exp\left[i\omega\left(t \pm \int_0^x \left\{\frac{\rho_0}{\eta_0} + \frac{1}{4\alpha^2\omega^2}\right\}^{\frac{1}{2}} d\alpha\right)\right]. \tag{2.3.30}$$

If we apply a relatively large frequency ω, then equation (2.3.30) reduces to

$$u(x,t) = T_0 A_0^{-\frac{1}{2}} (\eta_0\rho_0)^{-\frac{1}{4}} x^{-1} \exp\left[i\omega\left\{t \pm \sqrt{\frac{\rho_0}{E_0}}x\right\}\right]. \tag{2.3.31}$$

2.4 Perturbation method

Motivated by Nayfeh and Nasser [56], we consider here an inhomogeneous materials with relatively small variations in Young's modulus and the mass density. If the Young's modulus and the mass density can be written as

$$\begin{aligned} \eta &= \eta_0 + \epsilon p(x), \\ \rho &= \rho_0 + \epsilon q(x), \end{aligned} \tag{2.4.1}$$

with ϵ is a small positive number, $p(x)$ and $q(x)$ are continuous functions then equation (2.3.4) can be written as

$$\frac{\partial^2 U}{\partial x^2} + \omega^2 \left[r_0 + \epsilon r_1 + \epsilon^2 r_2 + \cdots \right] U = 0, \tag{2.4.2}$$

where

$$\begin{aligned} r_0 &= \frac{\rho_0}{\eta_0}, \\ r_1 &= \frac{4\omega^2(q\eta_0 - p\rho_0) - 2\eta_0 p''}{4\omega^2 \eta_0^2}, \\ r_2 &= \frac{4\omega^2(p^2\rho_0/\eta_0 - pq) + 2pp'' + p'^2}{4\omega^2 \eta_0^2}. \end{aligned} \tag{2.4.3}$$

Furthermore, if we assume that

$$U = U_0 + \epsilon U_1 + \epsilon^2 U_2 + \cdots, \tag{2.4.4}$$

then by equating the coefficients of powers of ϵ we obtain

$$\begin{aligned} U_0'' + \omega^2 r_0 U_0 &= 0, \\ U_1'' + \omega^2 r_0 U_1 &= -\omega^2 r_1 U_0, \\ U_n'' + \omega^2 r_0 U_n &= -\omega^2 \sum_{i=0}^{n-1} r_{n-i} U_i, \qquad n = 2, 3, \cdots, \end{aligned} \tag{2.4.5}$$

Unless $p(x)$ and $q(x)$ are specified, equation (2.4.5) can not be solved. In their discussion of Harmonic media, Nayfeh and Nasser [56] have considered two specified cases. The first case is for materials with $\eta = \eta_0$, $\rho = \rho_0(1 + \epsilon \cos \theta x)$ and the second

case for materials with $\eta = \eta_0(1 - \epsilon\cos\theta x)$ and $\rho = \rho_0$, where η_0, ρ_0, θ are the material constants and ϵ is a small positive number. The first case is obtained by choosing $p(x) = 0$ and $q(x) = \rho_0 \cos\theta x$ so that equation (2.4.2) reduces to

$$\frac{\partial^2 U}{\partial y^2} + \frac{1}{a^2}(1 + \epsilon\cos y)U(y) = 0, \tag{2.4.6}$$

which is known as the classical Mathiew equation with $\theta x = y$, $a^2 = \eta_0\theta^2/\rho_0\omega^2$. The second case is obtained by choosing $p(x) = -\eta_0\cos\theta x$, $q(x) = 0$ so that equation (2.4.2) reduces to

$$\frac{\partial^2 U}{\partial y^2} + \frac{1}{a^2}\left[\frac{1}{1 - \epsilon\cos y} - \frac{\epsilon a^2\cos y}{2(1 - \epsilon\cos y)} + \frac{\epsilon^2 a^2 \sin^2 y}{4(1 - \epsilon\cos y)^2}\right]U(y) = 0, \tag{2.4.7}$$

which is a Hill equation (see Nayfeh and Nasser [56]). Here we note that any periodic functions of $p(x)$ and $q(x)$ will have a similar effect for two cases discussed above. For example by choosing the functions

$$\begin{aligned} p(x) &= \eta_0\cos\theta x, \\ q(x) &= \rho_0\cos\theta x, \end{aligned} \tag{2.4.8}$$

we obtain

$$\begin{aligned} r_0 &= \frac{\rho_0}{\eta_0}, \\ r_1 &= \frac{\theta^2\cos\theta x}{2\omega^2}, \\ r_2 &= -\frac{\theta^2(1 + 3\cos 2\theta x)}{8\omega^2}. \end{aligned} \tag{2.4.9}$$

By assuming the series in (2.4.4) converges very rapidly, we only consider three terms of (2.4.5). Thus

$$\begin{aligned} U_0'' + \frac{1}{a^2}U_0(y) &= 0, \\ U_1'' + \frac{1}{a^2}U_1(y) &= -\frac{1}{2}(\cos y)U_0, \\ U_2'' + \frac{1}{a^2}U_2(y) &= \frac{1}{8}(1 + 3\cos 2y)U_0 - \frac{1}{2}(\cos y)U_1, \end{aligned} \tag{2.4.10}$$

where $a^2 = \theta^2\eta_0/\omega^2\rho_0$.

The first equation (2.4.10) has a solution in the form

$$U_0 = A_0 \cos\frac{y}{a} + B_0 \sin\frac{y}{a}. \tag{2.4.11}$$

If the homogeneous solutions of the second and the third equation of (2.4.10) are

$$U_{1h} = A_1 \cos\frac{y}{a} + B_1 \sin\frac{y}{a}, \tag{2.4.12}$$

$$U_{2h} = A_2 \cos\frac{y}{a} + B_2 \sin\frac{y}{a}, \tag{2.4.13}$$

then the particular solution for the second equation (2.4.10) is

$$\begin{aligned} U_{1p} = d_2 &\left\{ A_0 \cos y(1+\frac{1}{a}) + B_0 \sin y(1+\frac{1}{a}) \right\} + \\ d_3 &\left\{ A_0 \cos y(1-\frac{1}{a}) - B_0 \sin y(1-\frac{1}{a}) \right\}, \end{aligned} \tag{2.4.14}$$

and for the third equation is

$$\begin{aligned} U_{2p} = d_1 &\left\{ A_0 y \sin\frac{y}{a} - B_0 y \cos\frac{y}{a} \right\} + \\ d_2 &\left\{ A_1 \cos y(1+\frac{1}{a}) + B_1 \sin y(1+\frac{1}{a}) \right\} + \\ d_3 &\left\{ A_1 \cos y(1-\frac{1}{a}) - B_1 \sin y(1-\frac{1}{a}) \right\} + \\ d_4 &\left\{ A_0 \cos y(2+\frac{1}{a}) + B_0 \sin y(2+\frac{1}{a}) \right\} + \\ d_5 &\left\{ A_0 \cos y(2-\frac{1}{a}) - B_0 \sin y(2-\frac{1}{a}) \right\}, \end{aligned} \tag{2.4.15}$$

where

$$\begin{aligned} d_1 &= \frac{-a}{4(a^2-4)}, \\ d_2 &= \frac{a}{4(a+2)}, \\ d_3 &= \frac{a}{4(a-2)}, \\ d_4 &= \frac{-a(3+a)}{32(a+1)(a+2)}, \\ d_5 &= \frac{a(3-a)}{32(a-1)(a-2)}. \end{aligned} \tag{2.4.16}$$

Thus the solution of U can be obtained in the form

$$U = C\cos\frac{y}{a} + D\sin\frac{y}{a} + \epsilon G_{1p} + \epsilon^2 G_{2p}, \tag{2.4.17}$$

where C and D are arbitrary constants and U_{1p} and U_{2p} are given in (2.4.12) and (2.4.13) respectively. From (2.4.11), (2.4.12), (2.4.13), (2.4.14) we can see that there exists a singular point at $a = 0$. The constants in (2.4.16) also show that there exists singular points which divide the domain a by the transition curve along which the solutions are periodic. These singular points are $a = \pm 2$, $a = \pm 1$. Other singular points can be obtained by expanding the perturbation parameter to a higher order. For the case near the singular point $a = 2$, we can write

$$a^2 = 4 + a_1\epsilon, \tag{2.4.18}$$

where $a_1 = O\{1\}$. If we consider two terms of the perturbation parameter only then equation (2.4.10) can be written as

$$\begin{aligned} U_0'' + \frac{1}{4}U_0 &= 0, \\ U_1'' + \frac{1}{4}U_1 &= (\frac{1}{16}a_1 - \frac{1}{2}\cos y)U_0, \end{aligned} \tag{2.4.19}$$

with solution

$$\begin{aligned} U_0 &= A_0\cos\frac{1}{2}y + B_0\sin\frac{1}{2}y, \\ U_{1h} &= A_1\cos\frac{1}{2}y + B_1\sin\frac{1}{2}y, \\ U_{1p} &= -B_0(\frac{1}{4} + \frac{1}{16}a_1)y\cos\frac{1}{2}y - A_0(\frac{1}{4} - \frac{1}{16}a_1)y\sin\frac{1}{2}y + \\ &\quad A_0\frac{1}{8}\cos\frac{3}{2}y + B_0\frac{1}{8}\sin\frac{3}{2}y, \end{aligned} \tag{2.4.20}$$

or

$$\begin{aligned} U = &\left\{A_0 + \epsilon(A_1 - B_0 y(\frac{1}{4} + \frac{1}{16}a_1))\right\}\cos\frac{1}{2}y + \frac{1}{8}A_0\cos\frac{3}{2}y + \\ &\left\{B_0 + \epsilon(B_1 - A_0 y(\frac{1}{4} - \frac{1}{16}a_1))\right\}\sin\frac{1}{2}y + \frac{1}{8}B_0\sin\frac{3}{2}y, \end{aligned} \tag{2.4.21}$$

which is always unstable since U grows infinitely with y. We obtain similar unstability for the other singular points. Thus the perturbation method above only gives good approximations if $a >> \epsilon$ and a is not close to the singular points.

2.5 Floquet waves in inhomogeneous periodic materials

In their study of the composite materials, Yang and Lee [88] have employed a forward difference approximation combined with an excellent numerical techniques for analysing the vibration modes of the composite. In the present section, we adopt their techniques in considering wave equation for inhomogeneous materials of constant cross section which are given by (2.2.2) and satisfy the periodicity of the materials

$$\begin{aligned} \eta(x+p) &= \eta(x), \\ \rho(x+p) &= \rho(x), \end{aligned} \tag{2.5.1}$$

where p is a periodicity constant, η and ρ are continuous functions of x and denote the Young's modulus and the density of the materials respectively.

By assuming the displacement takes the form of

$$u(x,t) = u(x)\exp[i\omega t], \tag{2.5.2}$$

equation (2.2.2) reduces to a second order ordinary differential equation

$$\frac{d}{dx}\left[\eta(x)\frac{du}{dx}\right] = -\rho(x)\omega^2 u. \tag{2.5.3}$$

If we consider only one period of the material, ranging from $x = a$ to $x = b$, then by introducing the new variables

$$\begin{aligned} X &= \frac{x-a}{p}, \\ U(X) &= \frac{u(x)}{p}, \\ E(X) &= \frac{\eta(x)}{\eta(x_1)}, \\ R(X) &= \frac{\rho(x)}{\rho(x_1)}, \end{aligned} \tag{2.5.4}$$

where $p = b - a$, equation (2.5.3) reduces to a dimensionless differential equation

$$\frac{d}{dX}\left[E(X)\frac{dU}{dX}\right] = -\frac{p^2\omega^2\rho(x_1)}{\eta(x_1)}R(X)U(X). \tag{2.5.5}$$

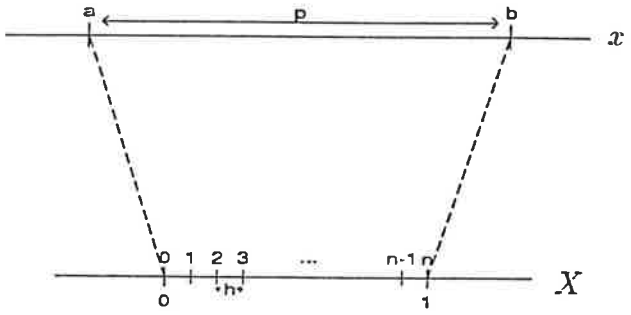

Figure 2.2

The X now, ranges from $X = 0$ to $X = 1$. Discretising X into n segments or $(n+1)$ discretisation points as in Figure 2.2, and also choosing

$$\begin{aligned} E_i &= E(X_i - \frac{h}{2}), \\ R_i &= \{R(X_i + \epsilon) + R(X_i - \epsilon)\}/2, \end{aligned} \tag{2.5.6}$$

where $h = 1/n$, ϵ is a small positive number, then by using the finite difference approximation, we obtain the relation

$$E_i U_{i-1} - (E_i + E_{i+1})U_i + E_{i+1}U_{i+1} = KR_iU_i, \tag{2.5.7}$$

where $i = 1, 2, \cdots, n$, and $K = -p^2\omega^2h^2\rho(x_1)/\eta(x_1)$.

By Floquet theory, the mode function $u(x)$ satisfies the quasi periodic conditions (see for example Nasser [55])

$$\begin{aligned} u(x+p) &= u(x)\exp[\imath pq], \\ u'(x+p) &= u'(x)\exp[\imath pq], \\ \sigma(x+p) &= \sigma(x)\exp[\imath pq] \end{aligned} \tag{2.5.8}$$

where q is the wave number which relates to the radial frequency ω.

Equation (2.5.7) provides n equations and $(n+2)$ unknowns, while equation (2.5.8) provides

$$\begin{aligned} U_{n+1} &= U_1 \exp[\imath pq], \\ U_0 &= U_n \exp[-\imath pq], \end{aligned} \tag{2.5.9}$$

Thus by using (2.5.1) and (2.5.9) in (2.5.7), we obtain

$$\begin{aligned} &-(E_1+E_2)U_1 + E_2U_2 + E_1e^{-\imath pq}U_n = KR_1U_1, \\ &E_iU_{i-1} - (E_i+E_{i+1})U_i + E_{i+1}U_{i+1} = KR_iU_i, \qquad i = 2,3,\cdots n-1 \\ &E_1e^{\imath pq}U_1 + E_nU_{n-1} - (E_n+E_1)U_n = KR_nU_n. \end{aligned} \tag{2.5.10}$$

In matrix form, equation (2.5.10) can be written as

$$\mathbf{AU} = K\mathbf{BU}, \tag{2.5.11}$$

where

$$\mathbf{A} = \begin{pmatrix} -E_1-E_2 & E_2 & 0 & \cdots & 0 & E_1e^{-\imath pq} \\ E_2 & -E_2-E_3 & E_3 & \cdots & 0 & 0 \\ 0 & E_3 & -E_3-E_4 & \cdots & 0 & 0 \\ \vdots & \vdots & \vdots & \ddots & \vdots & \vdots \\ 0 & 0 & 0 & \cdots & -E_{n-1}-E_n & E_n \\ E_1e^{\imath pq} & 0 & 0 & \cdots & E_n & -E_n-E_1 \end{pmatrix}$$

$\mathbf{U} = (U_1\ U_2\ \cdots\ U_{n-1}\ U_n)^T$, and $\mathbf{B}$ is a n-diagonal matrix with diagonal element $R_1, R_2, \cdots, R_n$.

Following Yang and Lee [88], since $\mathbf{B}$ is positive defenite, we may write $\mathbf{B} = \mathbf{B}^{\frac{1}{2}}\mathbf{B}^{\frac{1}{2}}$ where $\mathbf{B}^{\frac{1}{2}}$ is also a diagonal matrix. If we define

$$\mathbf{V} = \mathbf{B}^{\frac{1}{2}}\mathbf{U}, \tag{2.5.12}$$

then equation (2.5.11) reduces to ordinary eigenvalue problem

$$\mathbf{A}^*\mathbf{V} = K\mathbf{V}, \tag{2.5.13}$$

where $\mathbf{A}^* = \mathbf{B}^{-\frac{1}{2}}\mathbf{A}\mathbf{B}^{-\frac{1}{2}}$ is a Hermitian matrix with a real tridiagonal and two complex elements in $(1,n)$ and $(n,1)$ locations. All other elements of $\mathbf{A}^*$ are zeros.

If we write matrix $\mathbf{A}^*$ as

$$\mathbf{A}^* = \mathcal{A} + \mathbf{g}\mathbf{g}^{\mathbf{H}}, \tag{2.5.14}$$

where

$$\mathcal{A} = \begin{pmatrix} -\frac{E_1+E_2}{R_1} - 1 & \frac{E_2}{\sqrt{R_1R_2}} & 0 & \cdots & 0 & 0 \\ \frac{E_2}{\sqrt{R_1R_2}} & -\frac{E_2+E_3}{R_2} & \frac{E_3}{\sqrt{R_2R_3}} & \cdots & 0 & 0 \\ 0 & \frac{E_3}{\sqrt{R_2R_3}} & -\frac{E_3+E_4}{R_3} & \cdots & 0 & 0 \\ \vdots & \vdots & \vdots & \ddots & \vdots & \vdots \\ 0 & 0 & 0 & \cdots & -\frac{E_{n-1}+E_n}{R_{n-1}} & \frac{E_n}{\sqrt{R_{n-1}R_n}} \\ 0 & 0 & 0 & \cdots & \frac{E_n}{\sqrt{R_{n-1}R_n}} & -\frac{E_n+E_1}{R_n} - \frac{E_1^2}{R_1R_n} \end{pmatrix}, \tag{2.5.15}$$

$\mathbf{g} = (1\ 0\ \cdots\ 0\ \frac{E_1 e^{ipq}}{\sqrt{R_1R_n}})^T$ and $\mathbf{H}$ denotes the conjugate tranpose, then $\mathcal{A}$ is readily diagonalized by the implicit QL algorithm for a real symmetric matrix using shifts of origin (see for example Wilkinson and Reinsch [83]) such that we can write

$$\mathcal{A} = \mathbf{Q}\mathbf{\Lambda}\mathbf{Q}^T, \tag{2.5.16}$$

where $\mathbf{\Lambda}$ is a diagonal eigenvalues matrix which is arranged in ascending order

$$\mathbf{\Lambda}_1 < \mathbf{\Lambda}_2 < \mathbf{\Lambda}_3 \cdots < \mathbf{\Lambda}_n, \tag{2.5.17}$$

$\mathbf{Q}$ is an orthogonal matrix formed by the eigenvectors coresponding to the eigenvalues in $\mathbf{\Lambda}$.

Substituting (2.5.14) and (2.5.16) into (2.5.13) we obtain

$$(\mathbf{Q}\mathbf{\Lambda}\mathbf{Q}^T + \mathbf{g}\mathbf{g}^{\mathbf{H}})\mathbf{V} = K\mathbf{V}. \tag{2.5.18}$$

Let

$$\begin{aligned} \mathbf{h} &= \mathbf{Q}^T\mathbf{g}, \\ \mathbf{w} &= \mathbf{Q}^T\mathbf{V}, \end{aligned} \tag{2.5.19}$$

then equation (2.5.18) can be written as

$$(\mathbf{\Lambda} - K\mathbf{I} + \mathbf{h}\mathbf{h}^{\mathbf{H}})\mathbf{w} = 0, \tag{2.5.20}$$

which has a nontrivial solution if and only if

$$\det\,(\mathbf{\Lambda} - K\mathbf{I} + \mathbf{h}\mathbf{h}^{\mathbf{H}}) = 0. \tag{2.5.21}$$

The rank one modification on $\mathbf{A}^*$ has different eigenvalues from $\mathcal{A}$. Since $K \neq \Lambda_i$, $i = 1, 2, \cdots, n$ and $\det\,(\mathbf{\Lambda} - K\mathbf{I}) \neq 0$ then we can write (2.5.20) as

$$\det\,\left[\mathbf{I} + (\mathbf{\Lambda} - K\mathbf{I})^{-1}\mathbf{h}\mathbf{h}^{\mathbf{H}}\right] = 0. \tag{2.5.22}$$

After some algebraic manipulation, equation (2.5.22) can be written as a scalar characteristic equation

$$\phi(K) = 1 + \sum_{i=1}^{n} \frac{\mathbf{h}_i\overline{\mathbf{h}}_i}{\Lambda_i - K} = 0, \tag{2.5.23}$$

where the $\overline{\mathbf{h}}_i$ denotes the conjugate of $\mathbf{h}_i$. This function of K then can be solved for its roots for a certain specified accuracy especially for the smallest roots using an elementary methods such as the bisection method or Newton method. From a practical point of view, only the lowest few frequencies and mode shapes are of interest. This means that we do not have to solve for all zeros of K in (2.5.23). Let K_i be a known eigenvalue, equation (2.5.20) gives

$$(\mathbf{\Lambda} - K_i\mathbf{I})\mathbf{w}_i = -\mathbf{h}\mathbf{h}^{\mathbf{H}}\mathbf{w}_i. \tag{2.5.24}$$

Since $\mathbf{h}^{\mathbf{H}}\mathbf{w}_i$ is a scalar, we can write

$$\mathbf{w}_i = \gamma(\mathbf{\Lambda} - K_i\mathbf{I})^{-1}\mathbf{h}. \tag{2.5.25}$$

Using equations (2.5.11) and (2.5.18) we finally obtain

$$U_i = \gamma\mathbf{B}^{-\frac{1}{2}}\mathbf{Q}(\mathbf{\Lambda} - K_i\mathbf{I})^{-1}\mathbf{h}. \tag{2.5.26}$$

where γ is an arbitrary complex constant which can be determined by a given initial condition.

The strain now can be obtained through the relation

$$\mathbf{CU'} = \mathbf{D}, \tag{2.5.27}$$

where

$$\mathbf{C} = \begin{pmatrix} E_1 & -E_2 & 0 & \dots & 0 & 0 \\ 0 & E_2 & -E_3 & \dots & 0 & 0 \\ 0 & 0 & E_3 & \dots & 0 & 0 \\ \vdots & \vdots & \vdots & \ddots & \vdots & \vdots \\ 0 & 0 & 0 & \dots & E_{n-1} & -E_n \\ -E_1 e^{ipq} & 0 & 0 & \dots & 0 & E_n \end{pmatrix},$$

$$\mathbf{U'} = (\, U_1' \quad U_2' \quad U_3' \quad \cdots \quad U_n' \,)^T,$$

$$\mathbf{D} = \frac{p^2\omega^2\rho(x_1)h}{2\eta(x_1)} (\, R_1U_1 + R_2U_2 \quad \cdots \quad R_{n-1}U_{n-1} + R_nU_n \quad R_1U_1e^{ipq} + R_nU_n \,)^T,$$

and the stress follows immediately through the equation

$$\sigma(x) = \eta(x)\frac{du}{dx}. \tag{2.5.28}$$

In the case when the strain has been specified, then the displacement can be obtained by

$$\mathbf{FU} = \mathbf{G}, \tag{2.5.29}$$

where

$$\mathbf{F} = \begin{pmatrix} R_1 & R_2 & 0 & \dots & 0 & 0 \\ 0 & R_2 & R_3 & \dots & 0 & 0 \\ 0 & 0 & R_3 & \dots & 0 & 0 \\ \vdots & \vdots & \vdots & \ddots & \vdots & \vdots \\ 0 & 0 & 0 & \dots & R_{n-1} & R_n \\ R_1 e^{ipq} & 0 & 0 & \dots & 0 & R_n \end{pmatrix},$$

$$\mathbf{U} = (\, U_1 \quad U_2 \quad U_3 \quad \cdots \quad U_n \,)^T,$$

$$\mathbf{G} = \frac{2\eta(x_1)}{p^2\omega^2\rho(x_1)h} (\, E_1U_1' - E_2U_2' \quad \cdots \quad E_{n-1}U_{n-1}' - E_nU_n' \quad -E_1U_1'e^{ipq} + E_nU_n' \,)^T.$$

Problem 2.1 : A numerical example for a two layered composite cell

In order to verify the accuracy of the procedure above, we consider a two layered composite cell problem. Here the material is made up from many two layered composite cells as illustrated in Figure 2.3. Each cell consist of material one at both sides of the cell and material two which is located at the centre of the cell. If the cell and the material two have length a and b respectively, then the analytical solution of the mode which is found in the literature (see for example Sun et al [74], Yang and Lee [88]) may be written as

$$\cos(qa) = \cos\left(\frac{\omega(a-b)}{c_1}\right)\cos\left(\frac{\omega b}{c_2}\right) - \frac{1+r^2}{2r}\sin\left(\frac{\omega(a-b)}{c_1}\right)\sin\left(\frac{\omega b}{c_2}\right), \quad (2.5.30)$$

where $c_1 = (\eta_1/\rho_1)^{\frac{1}{2}}$, $c_2 = (\eta_2/\rho_2)^{\frac{1}{2}}$, $r = (\eta_2\rho_2/\eta_1\rho_1)^{\frac{1}{2}}$.

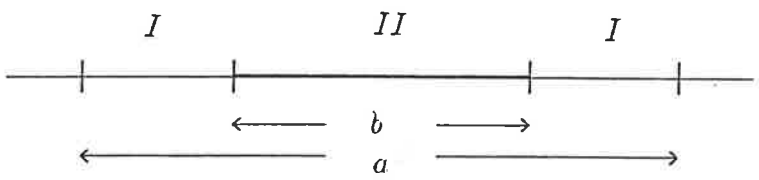

Figure 2.3
Two layered composite cell

If we further specify the materials with $\eta = \eta_2/\eta_1 = 4$ and $\theta = \rho_2/\rho_1 = 3$ and b/a = .5. Then by specifying the initial condition for the displacement $u = 1 + 0i$ in the middle of the cell and using 60 discretisation segments, we obtain the numerical results for displacement, strain and stress as in Table 2.1. The comparison between the analytical results which are given by solid lines and the numerical results which are given by the dots for the first six modes are in Figure 2.4.a.

Figure 2.4.b shows the similar comparison with materials specification $\eta = 50$, $\theta = 3$ and b/a = .5 (the composite material consists of two quite different materials). Both figures show that the first six modes of numerical solutions can be regarded as the exact solution. We note that a similar test problem and the numerical results for the first five mode can be found in Yang and Lee [88].

Problem 2.2 : Inhomogeneous cell

Here we extend the problem 2.1 by considering the material made up from many inhomogeneous cells. Each cell of the material has the non dimensionalised Young's modulus $\eta/\eta_0 = .5 + .02\cos x$ and mass density $\rho/\rho_0 = 2 + .02\cos x$, $-\pi \leq x \leq \pi$. Using 60 discretisation segments and specifying the initial condition for the displacement $u = 1 + 0i$ in the middle of the cell, we obtain the numerical results for displacement, strain and stress as in Table 2.2. The plot between the wave number qa and the radial frequency ω for the first three modes can be found in Figure 2.5.

Table 2.1

One dimensional Floquet waves in inhomogeneous materials

Mode = 1, QA = 1.5707963, Frequency = 2.3436633

No	u(x)		du/dx		$\sigma(x)$	
	Real	Imag	Real	Imag	Real	Imag
0	0.57112	-0.57112	1.70677	1.70677	5.12031	5.12031
6	0.73608	-0.39573	1.58692	1.79541	4.76077	5.38624
12	0.88757	-0.21311	1.43807	1.85123	4.31420	5.55370
18	0.97266	-0.09659	0.27212	0.47406	3.26546	5.68878
24	0.99314	-0.04863	0.13700	0.48405	1.64401	5.80856
30	1.00000	0.00000	0.00000	0.48739	0.00000	5.84867
36	0.99314	0.04863	-0.13700	0.48405	-1.64401	5.80856
42	0.97266	0.09659	-0.27212	0.47406	-3.26546	5.68878
48	0.88757	0.21311	-1.43807	1.85123	-4.31420	5.55370
54	0.73608	0.39573	-1.58692	1.79541	-4.76077	5.38624
60	0.57112	0.57112	-1.70677	1.70677	-5.12031	5.12031

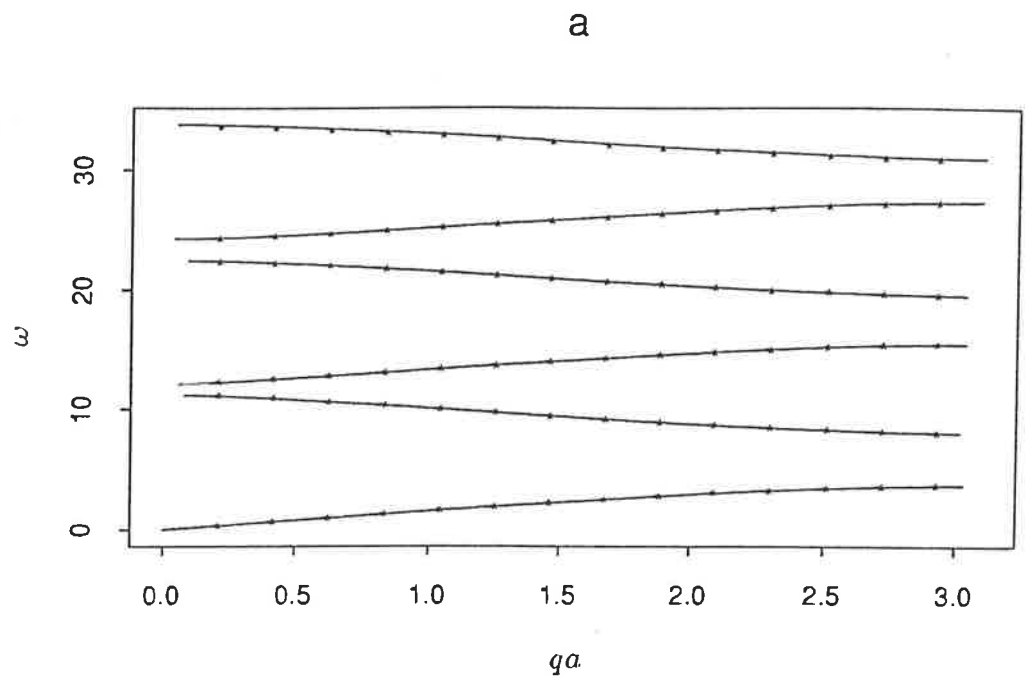

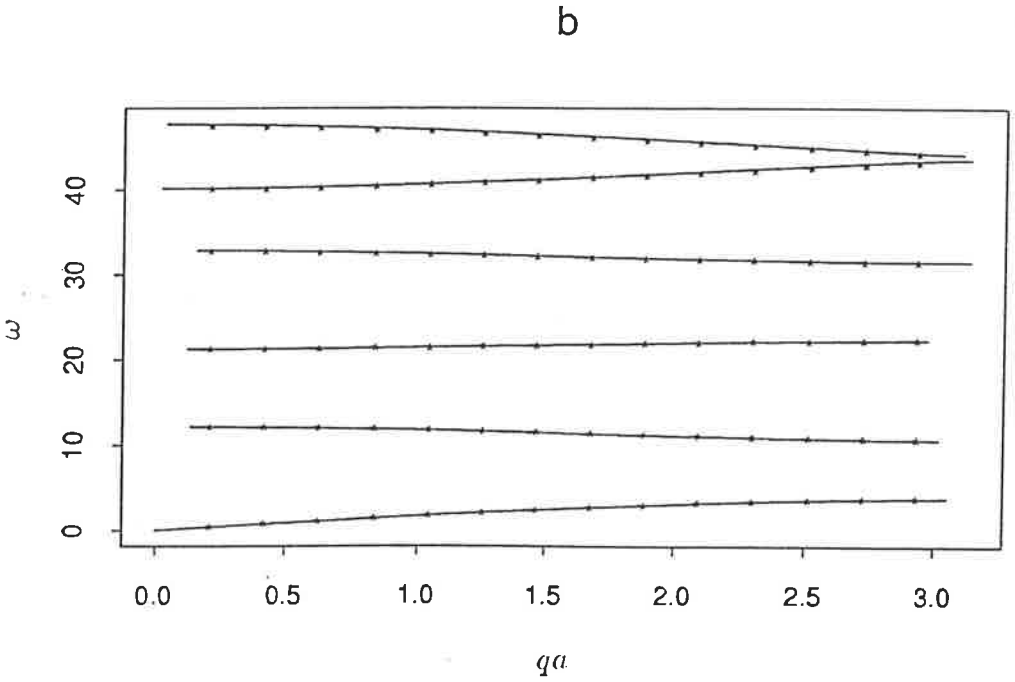

Figure 2.4
Comparison of the numerical and analytical results
for the first six modes of two layered composite cell

Table 2.2

One dimensional Floquet waves in inhomogeneous materials

Mode = 1, QA = 1.8849556, Frequency = 0.1499931

No	u(x)		du/dx		$\sigma(x)$	
	Real	Imag	Real	Imag	Real	Imag
0	0.58696	-0.80788	1.53081	1.11220	0.76235	0.55388
6	0.72870	-0.68298	1.29487	1.37773	0.64526	0.68655
12	0.84438	-0.53403	1.01189	1.59206	0.50522	0.79489
18	0.92989	-0.36651	0.69362	1.74839	0.34717	0.87510
24	0.98233	-0.18642	0.35238	1.84301	0.17674	0.92437
30	1.00000	0.00000	0.00000	1.87449	0.00000	0.94099
36	0.98233	0.18642	-0.35230	1.84256	-0.17674	0.92437
42	0.92989	0.36651	-0.69335	1.74769	-0.34717	0.87510
48	0.84438	0.53403	-1.01148	1.59143	-0.50522	0.79489
54	0.72870	0.68298	-1.29455	1.37739	-0.64526	0.68655
60	0.58696	0.80788	-1.53081	1.11220	-0.76235	0.55388

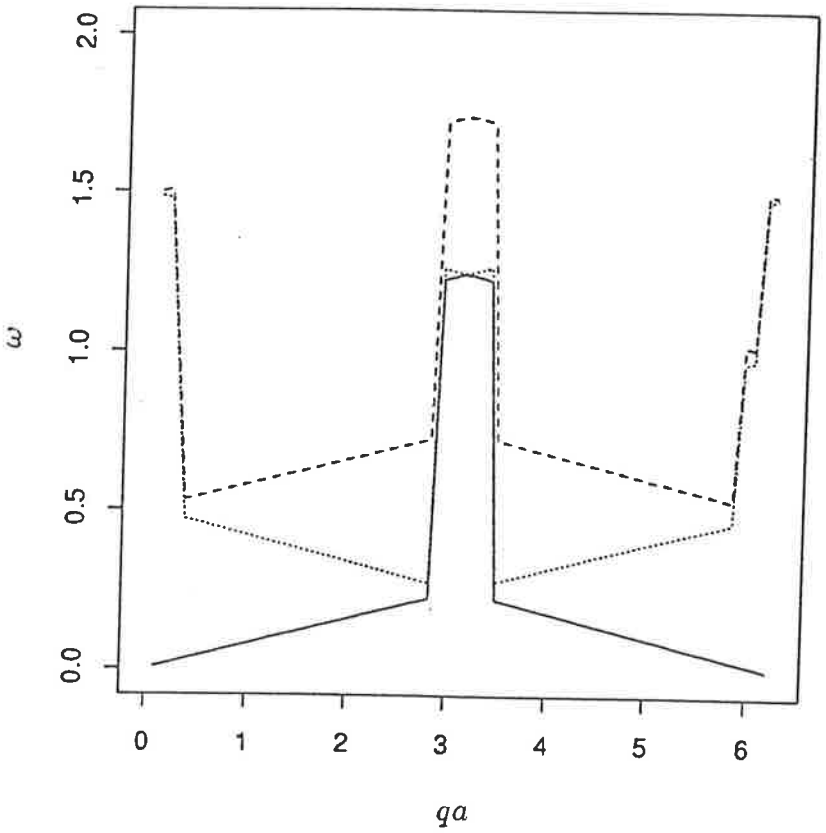

Figure 2.5
Numerical results for the first three modes
of inhomogeneous cell

CHAPTER 3

AXIALLY SYMMETRIC DEFORMATIONS

3.1 Introduction

There are two types of axially symmetric deformations of elastic materials which are considered in this chapter. The first type of deformations for which the nonzero displacement component is u_θ, are discussed by using the method of separation of variables. The second type of deformations are those for which the only non zero component is u_r. For this type of deformation, Clements et al [15] have approached the problem using the Fourier transformation. Following their technique, we employ the Laplace transformation in solving a specific axially symmetric deformation problem. The solution of a double walled cylinder and/or concentrically composite disk problem and several numerical results can be found at the end of the present chapter.

3.2 Basic equations

The basic equations relevant to the specific classes of problem considered in this chapter are provided in this section. Axially symmetric deformations refer to deformations which referred to cylindrical polar coordinate system r, θ, z are independent of θ. For axially symmetric deformations where the only nonzero displacement component is u_θ, the equilibrium equation can be written as (see for example Sokolnikoff [71])

$$\frac{\partial \sigma_{r\theta}}{\partial r} + \frac{\partial \sigma_{\theta z}}{\partial z} + \frac{2}{r}\sigma_{r\theta} = 0, \tag{3.2.1}$$

where

$$\begin{aligned}\sigma_{\theta z} &= \mu \frac{\partial u_\theta}{\partial z}, \\ \sigma_{r\theta} &= \mu \left(\frac{\partial u_\theta}{\partial r} - \frac{u_\theta}{r} \right).\end{aligned} \tag{3.2.2}$$

If we specify the inhomogeneity of the material in the form $\mu = \mu(r, z)$, then equation (3.2.1) can be rewritten as

$$\mu \left(\frac{\partial^2 u_\theta}{\partial r^2} + \frac{\partial^2 u_\theta}{\partial z^2} \right) + \frac{\partial u_\theta}{\partial r} \left(\frac{\mu}{r} + \frac{\partial \mu}{\partial r} \right) - u_\theta \left(\frac{\partial \mu}{\partial r} \frac{1}{r} + \frac{\mu}{r^2} \right) + \frac{\partial u_\theta}{\partial z} \frac{\partial \mu}{\partial z} = 0. \tag{3.2.3}$$

For the class of axially symmetric deformations where the only nonzero displacement component is in the radial direction u_r, the equation of motion can be written as (see for example Sokolnikoff [71])

$$\frac{\partial \sigma_r}{\partial r} + \frac{1}{r}(\sigma_r - \sigma_\theta) = \rho \frac{\partial^2 u_r}{\partial t^2}, \tag{3.2.4}$$

where

$$\begin{aligned}\sigma_r &= (2\mu + \lambda) \frac{\partial u_r}{\partial r} + \frac{\lambda}{r} u_r, \\ \sigma_\theta &= \lambda \frac{\partial u_r}{\partial r} + (2\mu + \lambda) \frac{u_r}{r}.\end{aligned} \tag{3.2.5}$$

By assuming λ, μ, and ρ are dependent on the radial coordinate r only, the equation (3.2.4) becomes

$$\frac{\partial^2 u_r}{\partial r^2} + A(r) \frac{\partial u_r}{\partial r} + B(r) u_r = C(r) \frac{\partial^2 u_r}{\partial t^2}, \tag{3.2.6}$$

where

$$\begin{aligned}A(r) &= \frac{d}{dr} \left[\ln(2\mu + \lambda) r \right], \\ B(r) &= \frac{1}{(2\mu + \lambda) r} \frac{d\lambda}{dr} - \frac{1}{r^2}, \\ C(r) &= \frac{\rho}{(2\mu + \lambda)}.\end{aligned} \tag{3.2.7}$$

3.3 General solution using the separation of variables method

We consider equation (3.2.3) for the axially symmetric elastostatic problem here. By performing the transformation, $u_\theta(r,z) = \mu^{-\frac{1}{2}}U(r,z)$, equation (3.2.3) becomes

$$\begin{aligned}\frac{\partial^2 U}{\partial r^2}+\frac{1}{r}\frac{\partial U}{\partial r} + \left[\frac{1}{4}\mu^{-2}\left(\frac{\partial \mu}{\partial r}\right)^2 - \frac{1}{2}\mu^{-1}\frac{\partial^2\mu}{\partial r^2} - \frac{3}{2}\mu^{-1}\frac{\partial \mu}{\partial r}\frac{1}{r} - \frac{1}{r^2}\right]U + \\ \frac{\partial^2 U}{\partial z^2} + \left[\frac{1}{4}\mu^{-2}\left(\frac{\partial \mu}{\partial z}\right)^2 - \frac{1}{2}\mu^{-1}\frac{\partial^2\mu}{\partial z^2}\right] = 0.\end{aligned} \tag{3.3.1}$$

Furthermore if we assume that U and μ take the forms

$$\begin{aligned}U(r,z) &= R(r)Z(z),\\ \mu(r,z) &= \mu_0 p(r)q(z),\end{aligned} \tag{3.3.2}$$

then by substituting equation (3.3.2) into (3.3.1) and separating the variables we obtain

$$\frac{R''}{R} + \frac{R'}{rR} - \frac{1}{r^2} + \left[\frac{1}{4}\frac{p'^2}{p} - \frac{p''}{2p} - \frac{3p'}{2rp}\right] = -\frac{Z''}{Z} - \left[\frac{1}{4}\frac{q'^2}{q} - \frac{1}{2}\frac{q''}{q}\right]. \tag{3.3.3}$$

As usual this equation should be equal to a negative constant, say $-n^2$, which gives us the two equations

$$R'' + \frac{1}{r}R' - \frac{1}{r^2}R + \left[\frac{1}{4}\left(\frac{p'}{p}\right)^2 - \frac{p''}{2p} - \frac{3p'}{2rp} + n^2\right]R = 0, \tag{3.3.4}$$

and

$$Z'' + \left[\frac{1}{4}\left(\frac{q'}{q}\right)^2 - \frac{1}{2}\frac{q''}{q} - n^2\right]Z = 0. \tag{3.3.5}$$

Here the primes denote the derivatives with respect to the relevant argument and n^2 is the separation variable constant.

Suppose $q(z)$ is an analytic function which satisfies the differential equation

$$\frac{1}{2q}\frac{d^2q}{dz^2} - \frac{1}{4}\left(\frac{1}{q}\frac{dq}{dz}\right)^2 = q_0, \tag{3.3.6}$$

where q_0 is an arbitrary constant, thus if $q(z)$ is known, q_0 can be determined. Suppose $n^2 + q_0 = \xi^2 > 0$, then equation (3.3.5) becomes

$$Z'' - \xi^2 Z = 0, \tag{3.3.7}$$

with the solution

$$Z(z) = A(\xi)e^{-\xi z} + B(\xi)e^{\xi z}. \tag{3.3.8}$$

By substitution we finally obtain

$$U(r,z) = \int_0^\infty R(\xi,r)\left[Ae^{-\xi z} + Be^{\xi z}\right] d\xi. \tag{3.3.9}$$

or

$$u_\theta(r,z) = \left[\mu_0 p(r)q(z)\right]^{-\frac{1}{2}} \int_0^\infty R(\xi,r)\left[Ae^{-\xi z} + Be^{\xi z}\right] d\xi. \tag{3.3.10}$$

Here $A(\xi)$ and $B(\xi)$ are arbitrary functions. If $p(r)$ are known, $R(r)$ can be determined from equation (3.3.4).

As an example for a particular problem, let the shear modulus take the form

$$\mu(r,z) = \mu_0 r^\alpha \exp(\beta z), \qquad \alpha \geq 0, \tag{3.3.11}$$

then equation (3.3.4) can be simplified to

$$R'' + \frac{1}{r}R' + \left[n^2 - \frac{1}{r^2}\left(\frac{\alpha}{2} + 1\right)^2\right]R = 0, \tag{3.3.12}$$

which is Bessel's equation. The solution of this differential equation can be written as

$$R(r) = AJ_{1+\frac{\alpha}{2}}(nr) + BY_{1+\frac{\alpha}{2}}(nr), \tag{3.3.13}$$

where A and B are arbitrary constants, $J_{1+\frac{\alpha}{2}}$ and $Y_{1+\frac{\alpha}{2}}$ are Bessel functions of the first and second kind respectively with order $1 + \frac{\alpha}{2}$. Since the displacements are always bounded at $r = 0$, this gives the constant $B = 0$. In addition, for the half space $z \geq 0$, $r \geq 0$ and $(r^2 + z^2)^{\frac{1}{2}} \to \infty$, the general solution may be written as

$$u_\theta(r,z) = \left[\mu_0 r^\alpha \exp(\beta z)\right]^{-\frac{1}{2}} \int_0^\infty A(\xi)e^{-\xi z} J_{1+\frac{\alpha}{2}}(nr)\, d\xi, \tag{3.3.14}$$

or

$$u_\theta(r,z) = \left[\mu_0 r^\alpha \exp(\beta z)\right]^{-\frac{1}{2}} \int_0^\infty A(\xi)e^{-\xi z} J_{1+\frac{\alpha}{2}}(r\sqrt{\xi^2 - \frac{1}{4}\beta^2})\, d\xi, \tag{3.3.15}$$

where $A(\xi)$ is an arbitrary function of ξ.

3.4 General solution using the Laplace transformation

Here we consider the equation of motion for inhomogeneous elastic materials governed by (3.2.6). By rewriting u_r as u, we have

$$\frac{\partial^2 u}{\partial r^2} + A(r)\frac{\partial u}{\partial r} + B(r)u = C(r)\frac{\partial^2 u}{\partial t^2}, \tag{3.4.1}$$

with $A(r), B(r)$ and $C(r)$ are given by (3.2.7).

By applying the Laplace transform which is defined by

$$\overline{u}(r,s) = \int_0^\infty e^{-st} u(r,t)\, dt, \tag{3.4.2}$$

with inverse

$$u(r,t) = \frac{1}{2\pi\imath}\int_{c-\imath\infty}^{c+\imath\infty} \overline{u}(r,s)e^{st}\, ds, \qquad \imath = \sqrt{-1} \tag{3.4.3}$$

to equation (3.4.1) with respect to time subject to the initial conditions $u(r,0) = 0$ and $\partial u/\partial t|_{(r,0)} = 0$ we obtain

$$\frac{\partial^2 \overline{u}}{\partial r^2} + A\frac{\partial \overline{u}}{\partial r} + \left[B - s^2 C\right]\overline{u} = 0. \tag{3.4.4}$$

According to Clements et al [15] the solution of this differential equation can be expressed in the form

$$\overline{u}(r,s) = f(r)F(q), \tag{3.4.5}$$

where $q = sg(r)$. The substitution of equation (3.4.5) into (3.4.4) yields the quadratic form

$$q^2\left[\frac{d^2F}{dq^2} - \frac{C}{g'^2}F\right] + q\left[\frac{2f'g}{fg'} + \frac{gg''}{g'^2} + \frac{Ag}{g'}\right]\frac{dF}{dq} + \frac{g^2}{fg'^2}\left[f'' + Af' + Bf\right]F = 0. \tag{3.4.6}$$

This equation is satisfied by requiring that all of the coefficients of q are equal to zero

$$\frac{d^2F}{dq^2} - \frac{C}{g'^2}F = 0, \tag{3.4.7}$$

$$\frac{2f'g}{fg'} + \frac{gg''}{g'^2} + \frac{Ag}{g'} = 0, \tag{3.4.8}$$

$$f'' + Af' + Bf = 0. \tag{3.4.9}$$

If we put

$$C = g'^2, \tag{3.4.10}$$

then equation (3.4.7) has solution

$$F = c_1(s)e^{sg(r)} + c_2(s)e^{-sg(r)}, \tag{3.4.11}$$

where $c_1(s)$ and $c_2(s)$ are arbitrary functions of s.

Substituting (3.4.11) into (3.4.5) and taking the inverse Laplace transform, we obtain

$$\begin{aligned} u(r,t) =& \frac{1}{2\pi i}\int_{c-i\infty}^{c+i\infty} f(r)\left[c_1(s)e^{sg(r)} + c_2(s)e^{-sg(r)}\right]e^{st}\,ds \\ =& \frac{f(r)}{2\pi i}\int_{c-i\infty}^{c+i\infty}\left[c_1(s)e^{s(t+g(r))} + c_2(s)e^{s(t-g(r))}\right]ds \end{aligned}$$

or

$$u(r,t) = f(r)\left[d_1(t+g(r)) + d_2(t-g(r))\right], \tag{3.4.12}$$

where d_1 and d_2 are arbitrary functions which are linear combinations of the inverse transforms of the arbitrary functions c_1 and c_2. Here $g(r)$ should satisfy equation (3.4.10), while the function $f(r)$ should satisfy either equations (3.4.8) and (3.4.9), or

$$f(r) = \int \exp\left[\int \left(\frac{2Bg'}{g'' + Ag'} - A\right)dr\right]dr. \tag{3.4.13}$$

Finally by substituting equation (3.4.13), (3.4.10) into (3.4.12) and simplifying, we obtain the general solution

$$\begin{aligned} u(r,t) = & \left[\int \exp\left\{\int \frac{4BC - AC' - 2A^2C}{C' + 2AC}\,dr\right\}dr\right] \\ & \left[d_1(t + \int C^{\frac{1}{2}}\,dr) + d_2(t - \int C^{\frac{1}{2}}\,dr)\right]. \end{aligned} \tag{3.4.14}$$

The constants here can be evaluated using the boundary conditions while the stresses can be derived by the direct substitution of (3.4.12) into (3.2.2) and (3.2.3)

$$\sigma_r(r) = \left[(2\mu+\lambda)f' + \frac{\lambda}{r}f\right][d_1+d_2] + (2\mu+\lambda)fg'[d_1'-d_2'], \tag{3.4.15}$$

$$\sigma_\theta(r) = \left[\lambda f' + \frac{2\mu+\lambda}{r}f\right][d_1+d_2] + \lambda fg'[d_1'-d_2']. \tag{3.4.16}$$

As a particular example, suppose we have the material specification in the form

$$\begin{aligned} \rho &= \rho_0 r^\alpha, \\ \mu &= \mu_0 r^\beta, \\ \lambda &= \lambda_0 r^\beta, \end{aligned} \tag{3.4.17}$$

where $\rho_0, \mu_0, \lambda_0, \alpha, \beta$ are constants. By substituting (2.4.17) into (3.2.7) we obtain

$$\begin{aligned} A &= (\beta+1)r^{-1}, \\ B &= \left(\frac{\lambda_0\beta}{2\mu_0+\lambda_0} - 1\right)r^{-2}, \\ C &= \frac{\rho_0}{2\mu_0+\lambda_0}r^{\alpha-\beta}. \end{aligned} \tag{3.4.18}$$

Also from (3.3.10) and (3.3.13), we have the relation

$$\begin{aligned} g &= \eta r^{\frac{1}{2}(\alpha-\beta)+1}, \\ f &= \frac{1}{\delta+1}r^{\delta+1}, \end{aligned} \tag{3.4.19}$$

where

$$\begin{aligned} \eta &= \left(\frac{\rho_0}{2\mu_0+\lambda_0}\right)^{\frac{1}{2}}\left[\frac{1}{2}(\alpha-\beta)+1\right]^{-1}, \\ \delta &= 4\left(\frac{\lambda_0\beta}{2\mu_0+\lambda_0} - 1\right)(\alpha+\beta+2)^{-1} - \beta + 1. \end{aligned} \tag{3.4.20}$$

Thus the solution for the displacement in (3.4.12) can be written as

$$u(r,t) = \frac{1}{\delta+1}r^{\delta+1}\left[d_1(t+\eta r^{\frac{1}{2}(\alpha-\beta)+1}) + d_2(t-\eta r^{\frac{1}{2}(\alpha-\beta)+1})\right], \tag{3.4.21}$$

while the stress in (3.4.15) and (3.4.16) can be written as

$$\begin{aligned} \sigma_r &= \tau\big[d_1+d_2\big]r^{\beta+\delta} + \kappa\big[d_1'-d_2'\big]r^{\frac{1}{2}(\alpha+\beta)+\delta+1}, \\ \sigma_\theta &= \chi\big[d_1+d_2\big]r^{\beta+\delta} + \omega\big[d_1'-d_2'\big]r^{\frac{1}{2}(\alpha+\beta)+\delta+1}, \end{aligned} \tag{3.4.22}$$

where

$$\begin{aligned}
\tau &= 2\mu_0 + \lambda_0 + \frac{\lambda_0}{\delta+1}, \\
\kappa &= \left[\rho_0(2\mu_0+\lambda_0)\right]^{\frac{1}{2}}(\delta+1)^{-1}, \\
\chi &= \lambda_0 + (2\mu_0+\lambda_0)(\delta+1)^{-1}, \\
\omega &= \left(\frac{\rho_0}{2\mu_0+\lambda_0}\right)^{\frac{1}{2}} \frac{\lambda_0}{\delta+1}.
\end{aligned} \tag{3.4.23}$$

As an application, we choose a cavity problem for an inhomegeneous cylinder made up from the material given in (3.4.17). The boundary $r = a$ of the cavity being subjected to a sudden constant pressure p. The boundary condition at $r = a$ is

$$\sigma_r(a) = pH(t), \tag{3.4.24}$$

with $H(t)$ denotes the Heaviside function. Note that, the stress expression in (3.4.12) is only valid provided that $\beta \neq \alpha+2$. For the case $\beta > \alpha+2$ the appropriate conditions for d_1 and d_2 are

$$\begin{aligned}
d_1 &= \exp\left[-\frac{\tau}{\kappa}a^{-\frac{1}{2}(\alpha-\beta)-1}\xi\right] + \frac{p}{\tau}a^{-\beta-\delta}H(\xi), \\
d_2 &= 0,
\end{aligned} \tag{3.4.25}$$

while for the case $\beta < \alpha + 2$ the appropriate conditions for the progressive wave equation are

$$\begin{aligned}
d_1 &= 0, \\
d_2 &= \exp\left[\frac{\tau}{\kappa}a^{-\frac{1}{2}(\alpha-\beta)-1}\xi\right] + \frac{p}{\tau}a^{-\beta-\delta}H(\xi),
\end{aligned} \tag{3.4.26}$$

where

$$\xi = t - |\eta|(r-a)^{\frac{1}{2}(\alpha-\beta)+1}. \tag{3.4.27}$$

The hoop stress follows immediately by substituting (3.4.25) or (3.4.26) into (3.4.22). For the case $\beta < \alpha + 2$. the hoop stress is

$$\begin{aligned}
\sigma_\theta(r) = \exp&\left[\frac{\tau}{\kappa}a^{-\frac{1}{2}(\alpha-\beta)-1}\xi\right]\left[\chi r^{\beta+\delta} - \right. \\
&\left.\frac{\omega\tau}{\kappa}r^{\frac{1}{2}(\alpha+\beta)+\delta+1}a^{-\frac{1}{2}(\alpha-\beta)-1}\right] + \frac{p\chi}{\tau}\left(\frac{r}{a}\right)^{\beta+\delta}H(\xi).
\end{aligned} \tag{3.4.28}$$

In the case $\alpha = \beta$, it simply becomes

$$\sigma_\theta(r) = \exp\left[\frac{\tau\xi}{\kappa a}\right]\left[\lambda r^{\alpha+\delta} - \frac{\omega\tau}{\kappa} r^{\alpha+\delta+1} a^{-1}\right] + \frac{p\chi}{\tau}\left(\frac{r}{a}\right)^{\alpha+\delta} H(\xi). \tag{3.4.29}$$

Another general solution in terms of Bessel functions can be obtained by choosing the coefficients of equation (3.4.6) to be

$$C = -g'^2, \tag{3.4.30}$$

$$\frac{2f'g}{fg'} + \frac{gg''}{g'^2} + \frac{Ag}{g'} = 1, \tag{3.4.31}$$

$$\frac{g^2}{fg'^2}\left[f'' + Af' + Bf\right] = -\nu^2, \tag{3.4.32}$$

so that equation (3.4.6) reduces to Bessels equation

$$q^2\frac{d^2F}{dq^2} + q\frac{dF}{dq} + (q^2 - \nu^2)F = 0. \tag{3.4.33}$$

This differential equation admits the solution

$$F(q) = c_1(s)J_\nu(q) + c_2(s)Y_\nu(q), \tag{3.4.34}$$

where c_1 and c_2 are arbitrary functions, $J_\nu(q)$ and $Y_\nu(q)$ are first and second kind of the Bessel function of order ν. The displacement can be simply obtained by using the inverse of the Laplace transform again

$$u(r,t) = \frac{f(r)}{2\pi\imath}\int_{c-\imath\infty}^{c+\imath\infty}\left[c_1(s)J_\nu(sg(r)) + c_2(s)Y_\nu(sg(r))\right]e^{st}\,ds. \tag{3.4.35}$$

3.5 Double walled thick cylinder

The inhomogeneous materials can be assumed to be made up from an n–layered homogeneous materials. In this section we consider a double walled cylinder and/or

disk made up of two layered homogeneous materials. Such as problem for example a thin disk with a circular hole and its ring (plane stress case) and/or its counterpart, a double walled cylinder (plane strain case) are of considerable practical importance. If the first homogeneous material with constants λ_1 and μ_1 is bounded by $r_0 \leq r \leq r_1$, and the second homogeneous material with constants λ_2 and μ_2 is bounded by $r_1 \leq r \leq r_2$ (see Figure 3.1), then the basic equation (3.2.4) reduces to

$$\frac{d^2u}{dr^2} + \frac{1}{r}\frac{du}{dr} - \frac{1}{r^2}u = 0. \tag{3.5.1}$$

Without any difficulty we obtain the well known solution for the displacement

$$u = cr + \frac{d}{r}, \tag{3.5.2}$$

where c and d are arbitrary constants. The stresses can be easily obtained by substituting (3.5.2) into (3.2.5)

$$\sigma_r = 2(\lambda + \mu)c - 2\mu\frac{d}{r^2}, \tag{3.5.3}$$

$$\sigma_\theta = 2(\lambda + \mu)c + 2\mu\frac{d}{r^2}. \tag{3.5.4}$$

By assuming the force at r_1 is T_1, the constants c and d can be evaluated. Using equation (3.5.3) we obtain

$$T_0 = F_1 c_1 - \frac{G_1 d_1}{r_0^2}, \tag{3.5.5}$$

and

$$T_1 = F_1 c_1 - \frac{G_1 d_1}{r_1^2}, \tag{3.5.6}$$

Thus the constants c_1 and d_1 for the first material can be specified

$$\begin{aligned} c_1 &= \frac{r_0^2 T_0 - r_1^2 T_1}{F_1(r_0^2 - r_1^2)}, \\ d_1 &= \frac{r_0^2 r_1^2 (T_0 - T_1)}{G_1(r_0^2 - r_1^2)}. \end{aligned} \tag{3.5.7}$$

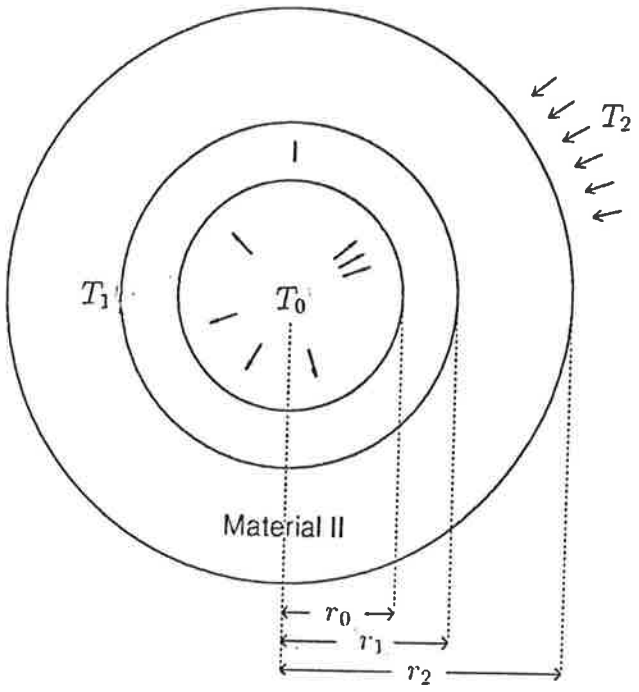

Figure 3.1
Material I with $\lambda = \lambda_1, \mu = \mu_1$ and material II with $\lambda = \lambda_2, \mu = \mu_2$

and for the second material

$$c_2 = \frac{r_1^2 T_1 - r_2^2 T_2}{F_2(r_1^2 - r_2^2)},$$
$$d_2 = \frac{r_1^2 r_2^2 (T_1 - T_2)}{G_2(r_1^2 - r_2^2)}, \tag{3.5.8}$$

where $F_1 = 2(\lambda_1 + \mu_1), F_2 = 2(\lambda_2 + \mu_2), G_1 = 2\mu_1, G_2 = 2\mu_2$. The continuity property requires that

$$u_1(r_1) = u_2(r_2). \tag{3.5.9}$$

Here the materials are assumed perfectly continuous, with u_1 and u_2 denote the displacement at the first and the second materials respectively. By using (3.5.9) we

obtain the equation

$$\frac{r_1(r_0^2T_0 - r_1^2T_1)}{F_1(r_0^2 - r_1^2)} + \frac{r_0^2r_1(T_0 - T_1)}{G_1(r_0^2 - r_1^2)} = \frac{r_1(r_1^2T_1 - r_2^2T_2)}{F_2(r_1^2 - r_2^2)} + \frac{r_1r_2^2(T_1 - T_2)}{G_2(r_1^2 - r_2^2)}. \tag{3.5.10}$$

T_1 in (3.5.10) can be written explicitly. Using this T_1 in (3.5.7) and (3.5.8) we have

$$\begin{aligned}
c_1 &= \tau\left[r_1^2r_2^2G_1T_2(F_2 + G_2) - r_0^2r_1^2G_2T_0(F_2 + G_1) + r_0^2r_2^2F_2T_0(G_2 - G_1)\right],\\
d_1 &= \tau r_0^2r_1^2\left[r_1^2G_2T_0(F_2 - F_1) - r_2^2F_2T_0(F_1 + G_2) + r_2^2F_1T_2(F_2 + G_2)\right],\\
c_2 &= \tau\left[r_1^2r_2^2G_1T_2(F_1 + G_2) - r_0^2r_1^2G_2T_0(F_1 + G_1) + r_0^2r_2^2F_1T_2(G_2 - G_1)\right],\\
d_2 &= \tau r_1^2r_2^2\left[r_1^2G_1T_2(F_2 - F_1) - r_0^2F_2T_0(F_1 + G_1) + r_0^2F_1T_2(F_2 + G_1)\right],
\end{aligned} \tag{3.5.11}$$

where

$$\begin{aligned}
\tau = \big[&r_1^2r_2^2G_1F_2(F_1 + G_2) - r_1^4G_1G_2(F_2 - F_1) +\\
&r_0^2r_2^2F_1F_2(G_2 - G_1) - r_0^2r_1^2F_1G_2(F_2 + G_1)\big]^{-1}.
\end{aligned} \tag{3.5.12}$$

Thus the displacement can be written by

$$u(r) = \begin{cases} u_1(r) = c_1r + \dfrac{d_1}{r} & \text{for} \quad r_0 \le r \le r_1,\\[2ex] u_2(r) = c_2r + \dfrac{d_2}{r} & \text{for} \quad r_1 \le r \le r_2, \end{cases} \tag{3.5.13}$$

and the stresses for plane stress case are

$$\sigma_r(r) = \begin{cases} \sigma_{r1}(r) = c_1F_1 - \dfrac{d_1G_1}{r^2} & \text{for} \quad r_0 \le r \le r_1,\\[2ex] \sigma_{r2}(r) = c_2F_2 - \dfrac{d_2G_2}{r^2} & \text{for} \quad r_1 \le r \le r_2, \end{cases} \tag{3.5.14}$$

and

$$\sigma_\theta(r) = \begin{cases} \sigma_{\theta1}(r) = c_1F_1 + \dfrac{d_1G_1}{r^2} & \text{for} \quad r_0 \le r \le r_1,\\[2ex] \sigma_{\theta2}(r) = c_2F_2 + \dfrac{d_2G_2}{r^2} & \text{for} \quad r_1 \le r \le r_2. \end{cases} \tag{3.5.15}$$

In the case of plane strain, the stresses are

$$\sigma_z(r) = \begin{cases} \sigma_{z1}(r) = \dfrac{\lambda_1}{\mu_1 + \lambda_1}c_1F_1 & \text{for} \quad r_0 \le r \le r_1,\\[2ex] \sigma_{z2}(r) = \dfrac{\lambda_2}{\mu_2 + \lambda_2}c_2F_2 & \text{for} \quad r_1 \le r \le r_2. \end{cases} \tag{3.5.16}$$

The stress intensity factor can now be determined. Suppose we choose $T_0 = 0$ and $T_2 = -T$, then equation (3.5.11) gives

$$\begin{aligned} c_1 &= -T\tau r_1^2 r_2^2 G_1(F_2 + G_2), \\ c_2 &= -T\tau r_2^2 \left[r_1^2 G_1(F_1 + G_2) + r_0^2 F_1(G_2 - G_1)\right], \\ d_1 &= -T\tau r_0^2 r_1^2 r_2^2 F_1(F_2 + G_2), \\ d_2 &= -T\tau r_1^2 r_2^2 \left[r_1^2 G_1(F_2 - F_1) + r_0^2 F_1(F_2 + G_1)\right]. \end{aligned} \tag{3.5.17}$$

The non zero stress at $r = r_0$ is

$$\sigma_\theta(r_0) = -2T\tau r_1^2 r_2^2 F_1 G_1(F_2 + G_2). \tag{3.5.18}$$

The stress intensity factor becomes

$$K = 2\tau r_1^2 r_2^2 F_1 G_1(F_2 + G_2). \tag{3.5.19}$$

For the case that a thin circular ring radius r_0 is applied along the hole of a circular disk radius r_2, or $r_0 \approx r_1 << r_2$, or $r_0/r_1 \to 1$, $r_0/r_2 \to 0$, $r_1/r_2 \to 0$ then equation (3.5.17) gives

$$\begin{aligned} c_1 &= -T\frac{G_1G_2 + G_1F_2}{G_1G_2F_2 + F_1F_2G_2}, \\ d_1 &= -T\frac{F_1F_2 + F_1G_2}{G_1G_2F_2 + F_1F_2G_2} r_0^2, \\ c_2 &= -T\frac{G_1 + F_1}{G_1F_2 + F_1F_2}, \\ d_2 &= -T\frac{G_1 - F_1}{G_1G_2 + F_1G_2} r_0^2. \end{aligned} \tag{3.5.20}$$

The stress intensity factor in this case is

$$K = 2\frac{\mu_1(\lambda_1 + \mu_1)(\lambda_2 + 2\mu_2)}{\mu_2(\lambda_2 + \mu_2)(\lambda_1 + 2\mu_1)}. \tag{3.5.21}$$

Thus if we choose the first material to be harder than the second one then the stress intensity factor becomes smaller and vice versa. For example if $\mu_1 = \frac{1}{2}\mu_2$ and

$\lambda_1 = \frac{1}{2}\lambda_2$ then the stress intensity factor becomes $K = 1$ which is smaller then the stress intensity factor ($K = 2$) obtained by using the same material for the first and second materials ($\mu_1 = \mu_2, \lambda_1 = \lambda_2$).

3.6 Numerical solutions

Problem 3.1 : Concentrically composite disk

We consider a simple plane stress problem here, which might occur for a thin circular disk with circular hole and ring around the hole, and/or in the other words, a thin circular disk concentrically made up of two kinds of the homogeneous materials as illustrate in Figure 3.1. The material I which is bounded from the circular hole to the radius $r = .7$ of the disk is chosen with non dimensionalised Lame constants of the material $\lambda_1 = .4$, $\mu_1 = .4$ and the material II which is bounded from radius $r = .7$ to $r = 1.$ of the disk with non dimensionalised Lame constants $\lambda_2 = .8$, $\mu_2 = .8$. This disk is subjected to the traction free around the circular hole and the traction $t = p$ around the exterior boundary. Using (3.5.14) and (3.5.15), we obtain the results for σ_r/p and σ_θ/p which are plotted versus radius r for several radius of the hole ($r = .1, .2, .3, .4, .5$) as in Figure 3.2 and Figure 3.3.

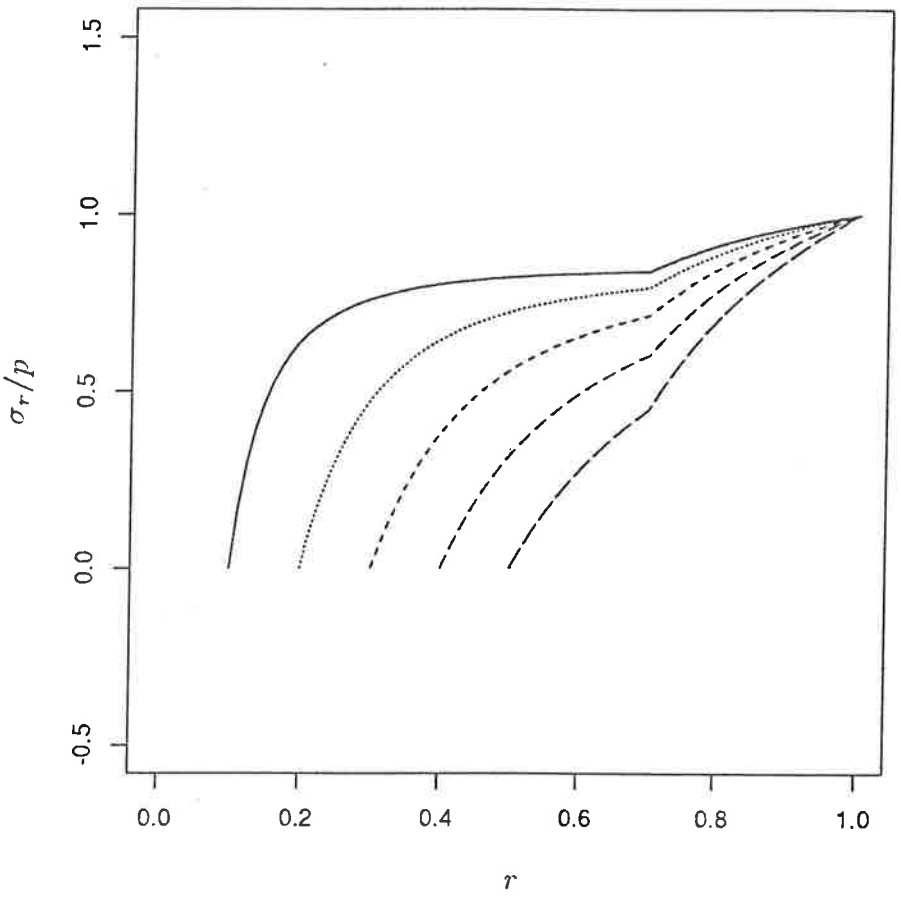

Figure 3.2
Distribution of σ_r/p for several radii of the hole

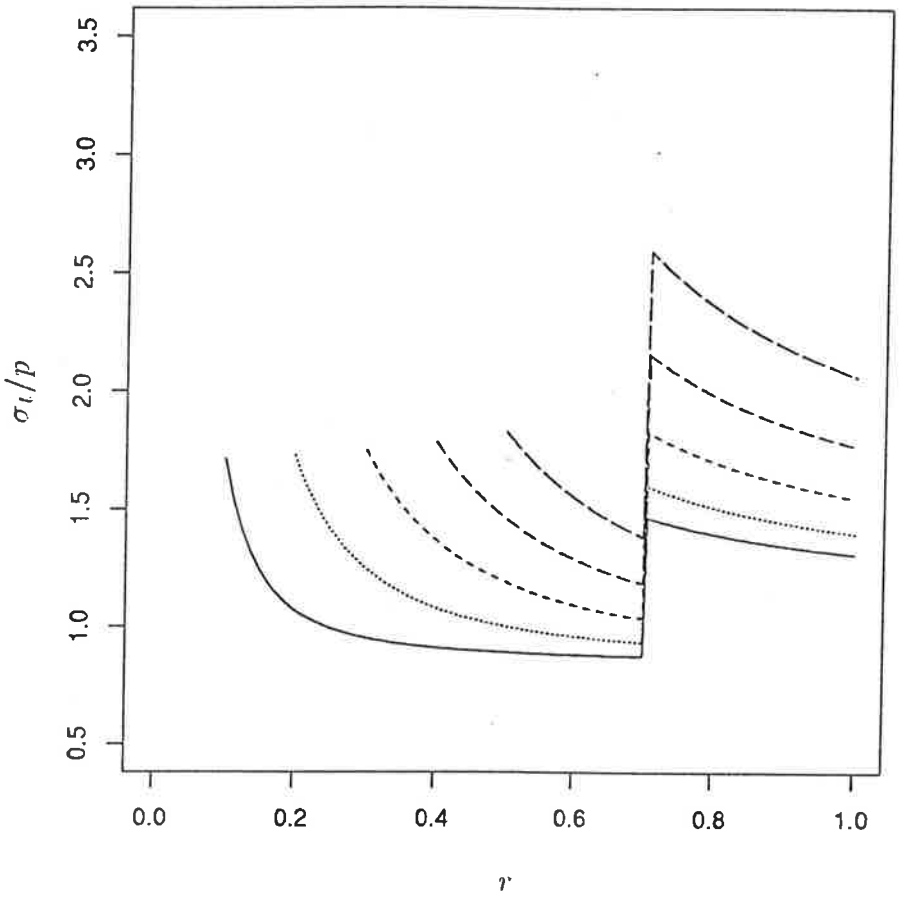

Figure 3.3
Distribution of σ_r/θ for several radii of the hole

Problem 3.2 : Inhomogeneous disk

For axially symmetric materials with the only nonzero displacement component is in the radial direction, the equilibrium equation becomes the second order differential equation with variable coefficients. Not many second order differential equation with variable coefficients can be solved analytically. Using numerical methods such as the two points boundary value method, we consider a thin circular plate with circular hole here for several materials in order to study their elastic behaviour.

If we denote material I for the material with $\lambda/\lambda_0 = 1$, $\mu/\mu_0 = r^2$, material II for the material with $\lambda/\lambda_0 = 1$, $\mu/\mu_0 = 2/(1+r)$, material III for the material with $\lambda/\lambda_0 = r^2$, $\mu/\mu_0 = 1$, material IV for the material with $\lambda/\lambda_0 = 2/(1+r)$, $\mu/\mu_0 = 1$ and material V for the homogeneous material with $\lambda/\lambda_0 = 1$, $\mu/\mu_0 = 1$, then by using the two point boundary value method as in D02GBF-NAG Fortran library routine and specifying the tolerance of error as 10^{-6}, we obtain the numerical results as given by Tables 3.1–3.5.

The plot between the displacement and radius r, the stress and radius r for these five kinds of the materials can be found through Figure 3.4 and 3.5. In Figure 3.6, we plot the stress intensity factor and the radius r for these materials. Note that from Figure 3.6, we can see that the stress intensity factor in the interior boundary can be decreased by using the material I and material III. For material I the stress intensity factor decreases at the interior boundary but increases at the exterior boundary in comparison with the homogeneous material V.

Table 3.1

Homogeneous material with $\lambda/\lambda_0 = 1$ and $\mu/\mu_0 = 1$

$\sigma_r(1) = 0$, $\sigma_r(3) = 2$ and tol=$1e^{-}6$

R	Displacement	Stress	du/dr
1.0000000	1.6874999	0.0000000	-0.5625000
1.1250000	1.6328124	0.4722222	-0.3263889
1.2500000	1.6031249	0.8100000	-0.1575000
1.3333333	1.5937499	0.9843750	-0.0703125
1.5000000	1.5937499	1.2500001	0.0625001
1.7777778	1.6328124	1.5380861	0.2065431
2.0000000	1.6874999	1.6875002	0.2812501
2.2500000	1.7656249	1.8055557	0.3402779
2.5000000	1.8562499	1.8900002	0.3825001
3.0000000	2.0625004	2.0000000	0.4375000

Table 3.2

Inhomogeneous material with $\lambda/\lambda_0 = 2/(1+r)$ and $\mu/\mu_0 = 1$

$\sigma_r(1) = 0$, $\sigma_r(3) = 2$ and tol=$1\epsilon^-6$

R	Displacement	Stress	du/dr
1.0000000	1.8078281	0.0000000	-0.6026094
1.1250000	1.7507112	0.5032808	-0.3268646
1.2500000	1.7229837	0.8588823	-0.1268136
1.5000000	1.7274417	1.3124008	0.1396781
1.7777778	1.7933257	1.5981651	0.3205398
2.0000000	1.8759508	1.7397057	0.4178958
2.2500000	1.9909116	1.8459573	0.4976073
2.5000000	2.1230629	1.9172062	0.5568635
2.7500000	2.2682095	1.9660497	0.6024294
3.0000000	2.4234848	2.0000000	0.6384343

Table 3.3

Inhomogeneous material with $\lambda/\lambda_0 = r^2$ and $\mu/\mu_0 = 1$

$\sigma_r(1) = 0$, $\sigma_r(3) = 2$ and tol=$1e^-6$

R	Displacement	Stress	du/dr
1.0000000	1.3431401	0.0000000	-0.4477134
1.0555556	1.3199862	0.1852537	-0.3879218
1.1111111	1.2998302	0.3465858	-0.3393560
1.2222222	1.2663942	0.6139988	-0.2672760
1.3333333	1.2395743	0.8269188	-0.2186065
1.5000000	1.2073099	1.0765337	-0.1728073
2.0000000	1.1370669	1.5492132	-0.1208201
2.5000000	1.0807447	1.8216841	-0.1066882
2.7500000	1.0546028	1.9192961	-0.1025738
3.0000000	1.0294197	2.0000000	-0.0989327

Table 3.4

Inhomogeneous material with $\lambda/\lambda_0 = 1$ and $\mu/\mu_0 = 2/(1+r)$

$\sigma_r(1) = 0$, $\sigma_r(3) = 2$ and tol=$1e^{-}6$

R	Displacement	Stress	du/dr
1.0000000	2.0408755	0.0000000	-0.6802918
1.0476190	2.0111892	0.2394333	-0.5689334
1.1428571	1.9661782	0.6204734	-0.3836974
1.2857143	1.9271696	1.0214819	-0.1736101
1.4000000	1.9149077	1.2456178	-0.0458150
1.6000000	1.9234848	1.5114516	0.1218350
1.7777778	1.9553014	1.6639915	0.2312027
2.0000000	2.0187078	1.7896627	0.3344181
2.5000000	2.2277223	1.9368873	0.4880393
3.0000000	2.4973229	2.0000000	0.5837795

Table 3.5

Inhomogeneous material with $\lambda/\lambda_0 = 1$ and $\mu/\mu_0 = r^2$

$\sigma_r(1) = 0$, $\sigma_r(3) = 2$ and tol=$1\epsilon^-6$

R	Displacement	Stress	du/dr
1.0000000	0.6147831	0.0000000	-0.2049277
1.0555556	0.6049697	0.0878799	-0.1503067
1.1250000	0.5964839	0.1897313	-0.0964182
1.2222222	0.5899741	0.3201864	-0.0407557
1.3333333	0.5880478	0.4558200	0.0032453
1.5000000	0.5923525	0.6399762	0.0445590
1.6000000	0.5976387	0.7425358	0.0602960
1.7777778	0.6100966	0.9149777	0.0781040
2.0000000	0.6288741	1.1191827	0.0894162
2.2500000	0.6519809	1.3410884	0.0945000
2.5000000	0.6757919	1.5599087	0.0955253
3.0000000	0.7229827	2.0000000	0.0925793

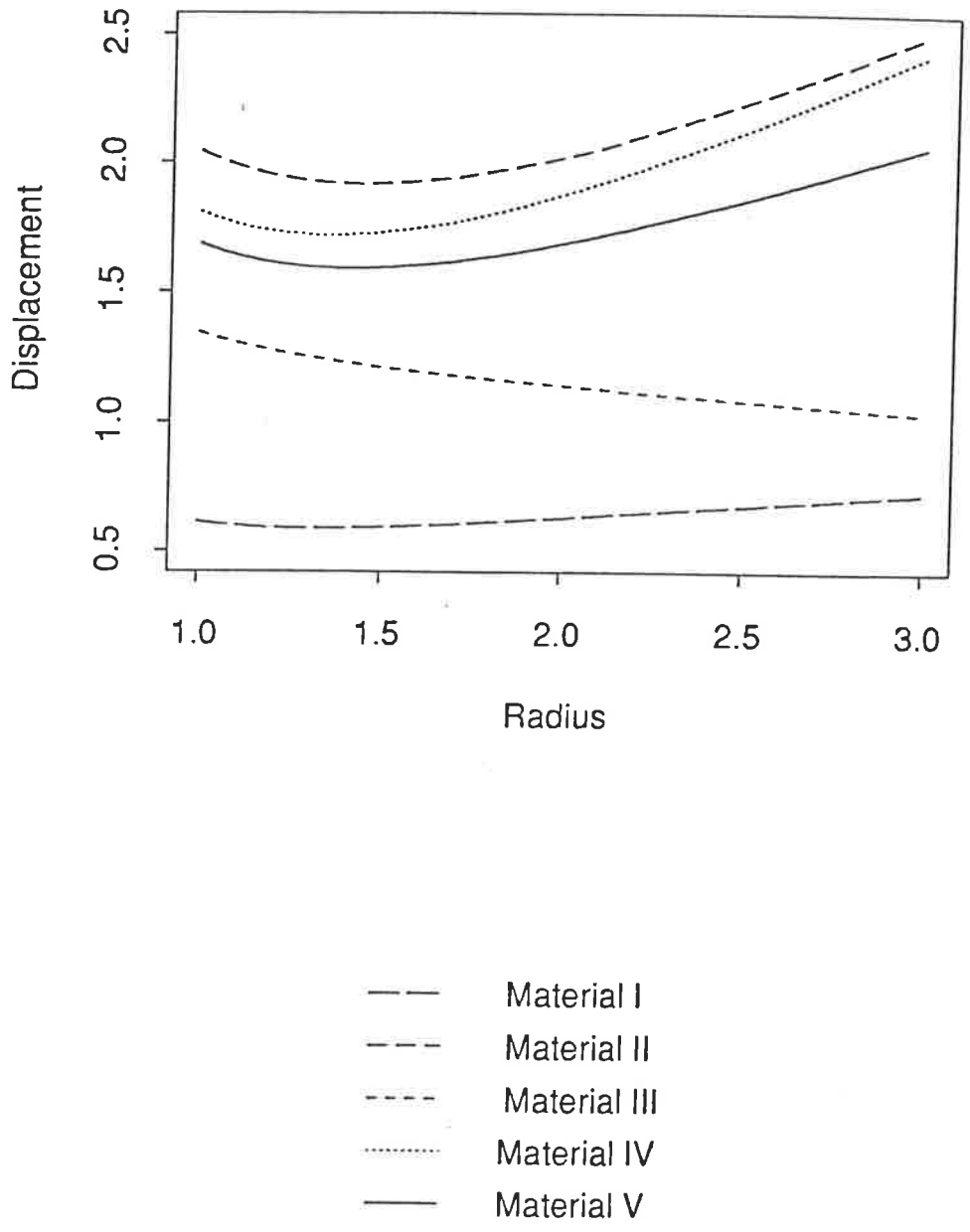

Figure 3.4
Displacement distribution for several materials

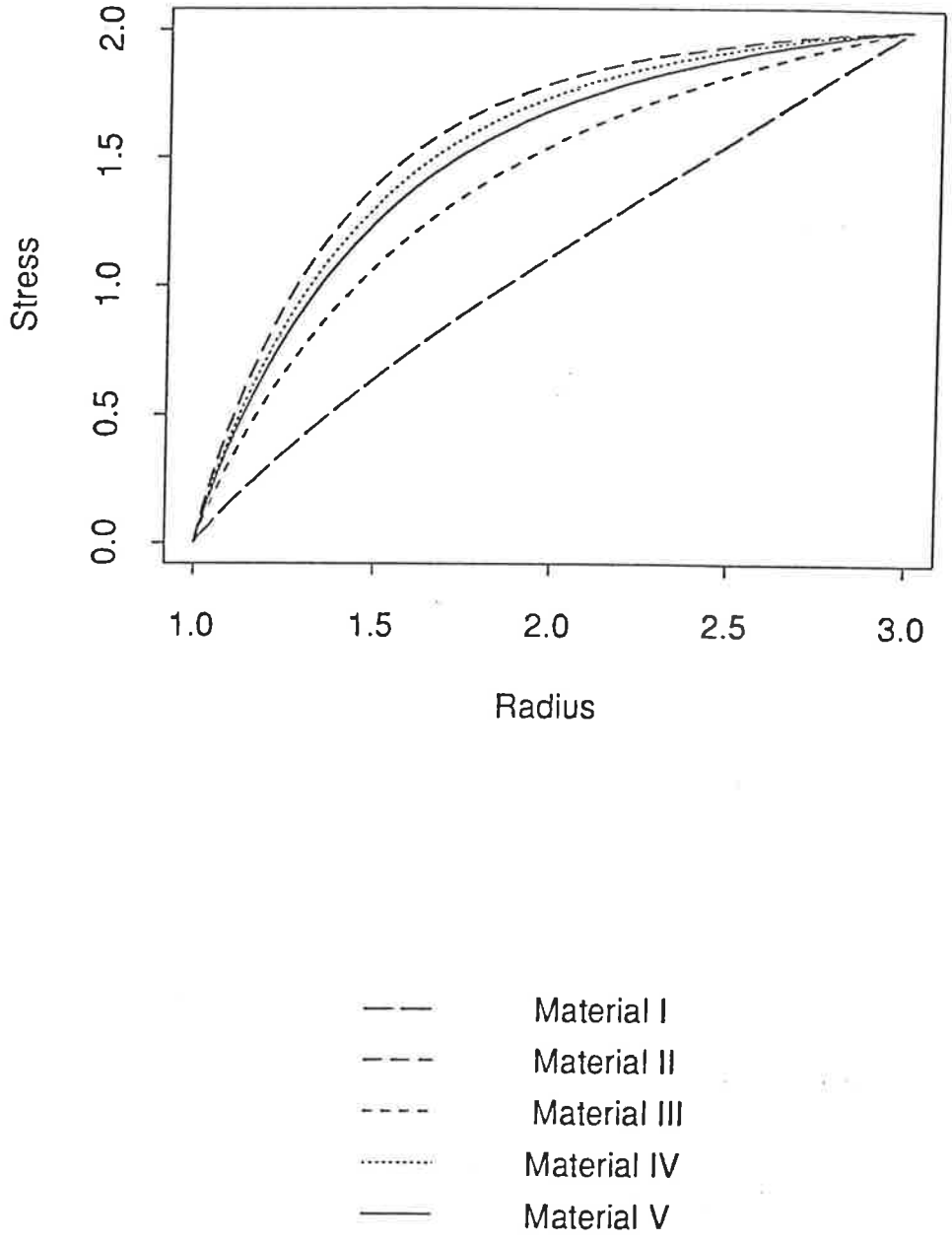

Figure 3.5
Stress distribution for several materials

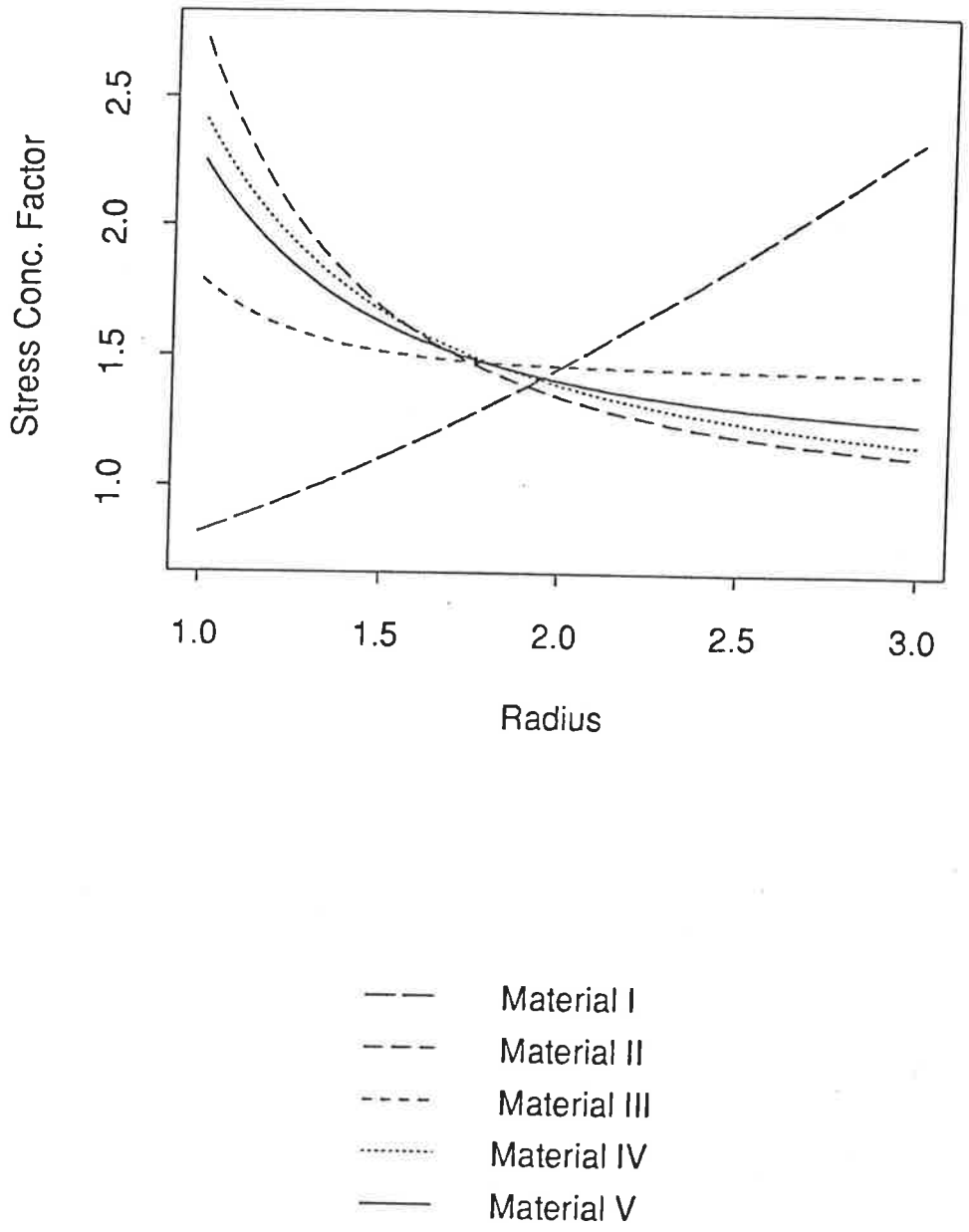

Figure 3.6
Stress concentration factor for several materials

CHAPTER 4

SPHERICALLY SYMMETRIC DEFORMATIONS

4.1 Introduction

Spherically symmetric deformations have been extensively studied in the theory of linear homogeneous isotropic elasticity, since mathematically speaking they are relatively simple to solve and have many physically important applications. Elementary solutions to static problems are given in a number of standard texts and papers by numerous authors. For example, Eason [26] has investigated dynamic problems involving spherically symmetric deformations for homogeneous materials. Solutions to spherically symmetric problems for inhomogeneous materials are less common. However in recent years a number of papers in this area have been published. For example, Clements et al [15] have considered deformations of inhomogeneous materials by employing Bäcklund transformations. These transformation reduce the governing equation into a particular elliptic equation which can then be solved using the Bergman series approach.

In the present chapter, we consider several simple static problems for spherically symmetry deformations of inhomogeneous elastic materials in which the only non zero displacement component is in the radial direction u_r. The numerical results for some simple static problems are obtained by using two point boundary value method. For the time dependent problem, we employ Bäcklund transformations so that equation of motion reduces to the simple canonical form for the wave equation.

4.2 Basic equations

For spherically symmetric problems for inhomogeneous materials in which the only nonzero displacement is in the direction of r component, and the inhomogeneity of the materials is governed by r as well, the relevant equation of motion is

$$\frac{\partial \sigma_r}{\partial r} + \frac{2}{r}(\sigma_r - \sigma_\theta) = \rho \frac{\partial^2 u}{\partial t^2}, \tag{4.2.1}$$

where

$$\begin{aligned} \sigma_r &= (\lambda + 2\mu)\frac{\partial u}{\partial r} + 2\lambda \frac{u}{r}, \\ \sigma_\theta &= \lambda \frac{\partial u}{\partial r} + 2(\mu + \lambda)\frac{u}{r}, \end{aligned} \tag{4.2.2}$$

or

$$\frac{\partial^2 u}{\partial r^2} + A(r)\frac{\partial u}{\partial r} + B(r)u = C(r)\frac{\partial^2 u}{\partial t^2}, \tag{4.2.3}$$

where

$$\begin{aligned} A(r) &= \frac{d}{dr}\left[\ln(\lambda + 2\mu)r^2\right], \\ B(r) &= \frac{2}{(\lambda + 2\mu)r}\frac{d\lambda}{dr} - \frac{2}{r^2}, \\ C(r) &= \frac{\rho}{\lambda + 2\mu}. \end{aligned} \tag{4.2.4}$$

4.3 Some simple solutions for homogeneous materials

4.3.1 Homogeneous spheres

We consider a homogeneous sphere of radius a with the material constants λ and μ here. For the case when the material is in equilibrium, the governing differential equation is

$$\frac{d^2 u}{dr^2} + \frac{2}{r}\frac{du}{dr} - \frac{2}{r^2}u = 0, \tag{4.3.1}$$

in which the well known solution can be obtained as

$$u(r) = Ar + Br^{-2}, \tag{4.3.2}$$

where A and B are constants. The stresses are

$$\begin{aligned} \sigma_r(r) &= (3\lambda + 3\mu)A - 4\mu Br^{-3}, \\ \sigma_\theta(r) &= (3\lambda + 3\mu)A + 2\mu Br^{-3}. \end{aligned} \tag{4.3.3}$$

If the pressure on the exterior of the sphere is p, then the displacement be should finite in the center of the sphere and so $B = 0$. Thus we obtain the stress pressure relation as

$$\sigma_r(r) = \sigma_\theta(r) = p, \tag{4.3.4}$$

and the displacement

$$u(r) = \frac{pr}{3\lambda + 2\mu}. \tag{4.3.5}$$

4.3.2 Spherical shells

For a homogeneous spherical shell with interior radius a and exterior radius b, the displacement and the stresses are given by equations (4.3.2) and (4.3.3) respectively. If there are two conditions are given then the constants A and B can be determined. For example if the pressure p_i is given in the interior of the shell and p_e at on the exterior of the shell then we have

$$\begin{aligned} p_i &= (3\lambda + 2\mu)A - 4\mu Ba^{-3}, \\ p_e &= (3\lambda + 2\mu)A - 4\mu Bb^{-3}, \end{aligned} \tag{4.3.6}$$

with the solution

$$\begin{aligned} A &= \frac{1}{3\lambda + 2\mu} \frac{a^3 p_i - b^3 p_e}{a^3 - b^3}, \\ B &= \frac{a^3 b^3}{4\mu} \frac{p_i - p_e}{a^3 - b^3}. \end{aligned} \tag{4.3.7}$$

By substituting (4.3.7) into (4.3.2) and (4.3.3), we obtain the displacement

$$u(r) = \frac{r}{3\lambda + 2\mu}\frac{a^3 p_i - b^3 p_e}{a^3 - b^3} + \frac{a^3 b^3}{4\mu r^2}\frac{p_i - p_e}{a^3 - b^3}, \tag{4.3.8}$$

and the stresses

$$\begin{aligned} \sigma_r(r) &= \frac{a^3 p_i - b^3 p_e}{a^3 - b^3} - \frac{a^3 b^3}{r^3}\frac{p_i - p_e}{a^3 - b^3}, \\ \sigma_\theta(r) &= \frac{a^3 p_i - b^3 p_e}{a^3 - b^3} + \frac{a^3 b^3}{2r^3}\frac{p_i - p_e}{a^3 - b^3}. \end{aligned} \tag{4.3.9}$$

4.3.3 Spheres with two layered materials

We consider the spheres with two layered homogeneous materials. Suppose the first material constants are $\lambda = \lambda_1$, $\mu = \mu_1$ with radius a and the second material constants are $\lambda = \lambda_2$ and $\mu = \mu_2$ covering the first sphere from radius a to b. If we assume at $r = a$ that there is pressure p then the displacement and the stress for the first material ($0 \le r \le a$) are

$$\begin{aligned} u_r^{(1)}(r) &= \frac{pr}{3\lambda_1 + 2\mu_1}, \\ \sigma_r^{(1)}(r) &= p. \end{aligned} \tag{4.3.10}$$

If the pressure p_e is given at the exterior of the sphere then the displacement and the stress for the second material ($a \le r \le b$) are given by

$$\begin{aligned} u_r^{(2)}(r) &= \frac{r}{3\lambda_2 + 2\mu_2}\frac{a^3 p - b^3 p_e}{a^3 - b^3} + \frac{a^3 b^3}{4\mu_2}\frac{p - p_e}{a^3 - b^3}\frac{1}{r^2}, \\ \sigma_r^{(2)}(r) &= \frac{a^3 p - b^3 p_e}{a^3 - b^3} - \frac{a^3 b^3}{r^3}\frac{p - p_e}{a^3 - b^3}. \end{aligned} \tag{4.3.11}$$

Now we determine p. Using the continuity equation

$$u_r^{(1)}(a) = u_r^{(2)}(a), \tag{4.3.12}$$

we obtain

$$p = \frac{b^3 z_1}{a^3 z_2 + b^3 z_3} p_e, \tag{4.3.13}$$

where

$$\begin{aligned} z_1 &= -18\lambda_1\mu 2 - 12\mu_1\mu_2 - 9\lambda_1\lambda_2 - 6\lambda_2\mu_1, \\ z_2 &= 8\mu_2^2 + 12\lambda_2\mu_2 - 12\lambda_1\mu_2 - 8\mu_1\mu_2, \\ z_3 &= -8\mu_2^2 - 12\lambda_2\mu_2 - 6\lambda_1\mu_2 - 4\mu_1\mu_2 - 9\lambda_1\lambda_2 - 6\lambda_2\mu_1. \end{aligned} \tag{4.3.14}$$

Thus by substituting (4.3.13) into equations (4.3.10) and (4.3.11) we obtain the displacement and stress distribution over the sphere.

4.3.4 Two layered spherical shells

Here the shell is considered to be made up from two layered materials. Suppose the interior layer is from radius a to b with material constants λ_1 and μ_1 and the exterior layer is from radius b to c with material constants λ_2 and μ_2. If the pressure p_i is applied at the interior of the shell and p_e at the exterior of the shell then by assuming the pressure is p at $r = b$, we have that the displacement and stress for $a \leq r \leq b$ are

$$\begin{aligned} u_r^{(1)}(r) &= \frac{r}{3\lambda_1 + 2\mu_1}\frac{a^3p_i - b^3p}{a^3 - b^3} + \frac{a^3b^3}{4\mu_1 r^2}\frac{p_i - p}{a^3 - b^3}, \\ \sigma_r^{(1)}(r) &= \frac{a^3p_i - b^3p}{a^3 - b^3} - \frac{a^3b^3}{r^3}\frac{p_i - p}{a^3 - b^3}, \end{aligned} \tag{4.3.15}$$

and for $b \leq r \leq c$

$$\begin{aligned} u_r^{(2)}(r) &= \frac{r}{3\lambda_2 + 2\mu_2}\frac{b^3p - c^3p_e}{b^3 - c^3} + \frac{b^3c^3}{4\mu_2 r^2}\frac{p - p_e}{b^3 - c^3}, \\ \sigma_r^{(2)}(r) &= \frac{b^3p - c^3p_e}{b^3 - c^3} - \frac{b^3c^3}{r^3}\frac{p - p_e}{b^3 - c^3}. \end{aligned} \tag{4.3.16}$$

Using the continuity equation

$$u^{(1)}(b) = u^{(2)}(b), \tag{4.3.17}$$

we obtain

$$p = \frac{a^3 p_i (b^3 - c^3) z_1 + c^3 p_e (a^3 - b^3) z_2}{a^3 b^3 z_3 + a^3 c^3 z_4 + b^3 c^3 z_5 + b^6 z_6}, \tag{4.3.18}$$

where

$$\begin{aligned}
z_1 &= 9\lambda_1\lambda_2\mu_2 + 6\lambda_1\mu_2^2 + 18\lambda_2\mu_1\mu_2 + 12\mu_1\mu_2^2, \\
z_2 &= 9\lambda_1\lambda_2\mu_1 + 18\lambda_1\mu_1\mu_2 + 6\lambda_2\mu_1^2 + 12\mu_1^2\mu_2, \\
z_3 &= 12\lambda_1\mu_1\mu_2 + 9\lambda_1\lambda_2\mu_2 + 6\lambda_1\mu_2^2 + 8\mu_1^2\mu_2 + 6\lambda_2\mu_1\mu_2 + 4\mu_1\mu_2^2, \\
z_4 &= 9\lambda_1\lambda_2\mu_1 + 6\lambda_1\mu_1\mu_2 - 9\lambda_1\lambda_2\mu_2 - 6\lambda_1\mu_2^2 + 6\lambda_2\mu_1^2 + 4\mu_1^2\mu_2 - 6\lambda_2\mu_1\mu_2 - 4\mu_1\mu_2^2, \\
z_5 &= -9\lambda_1\lambda_2\mu_1 - 6\lambda_1\mu_1\mu_2 - 6\lambda_2\mu_1^2 - 4\mu_1^2\mu_2 - 12\lambda_2\mu_1\mu_2 - 8\mu_1\mu_2^2, \\
z_6 &= -12\lambda_1\mu_1\mu_2 - 8\mu_1^2\mu_2 + 12\lambda_2\mu_1\mu_2 + 8\mu_1\mu_2^2.
\end{aligned} \tag{4.3.19}$$

Thus by doing some substitutions, we obtain the displacement and stress through equations (4.3.15) and (4.3.16). In the case that the displacement $u^{(1)}(a) = u_1$ is given instead of p_i or $u^{(2)}(c) = u_2$ is given instead of p_e then p_i or p_e can be obtained from equations (4.3.15) and (4.3.16).

4.4 Simple solutions for inhomogeneous materials

4.4.1 Bessel differential equations

We consider a shell with the inhomogeneity of the materials represented by

$$\begin{aligned}
\lambda(r) &= \frac{r^2 + \nu^2 - 2}{2r}, \\
\mu(r) &= \frac{4 - r^2 - \nu^2}{4r}.
\end{aligned} \tag{4.4.1}$$

For this case we restrict the range of the radius so that $2 < r^2 + \nu^2 < 4$. By substituting equation (4.4.1) into (4.2.3) and let the right hand side of (4.2.3) equal

to zero, we obtain

$$\begin{aligned} A(r) &= \frac{1}{r}, \\ B(r) &= 1 - \frac{\nu^2}{r^2}. \end{aligned} \tag{4.4.2}$$

Thus we have the Bessel's differential equation

$$\frac{d^2u}{dr^2} + \frac{1}{r}\frac{du}{dr} + (1 - \frac{\nu^2}{r^2})u = 0, \tag{4.4.3}$$

with solution

$$u(r) = AJ_\nu(r) + BY_\nu(r). \tag{4.4.4}$$

The stress simply becomes

$$\begin{aligned} \sigma_r(r) = A\left[\frac{1}{r}J'_\nu(r) + \frac{r^2 + \nu^2 - 2}{r^2}J_\nu(r)\right] + \\ B\left[\frac{1}{r}Y'_\nu(r) + \frac{r^2 + \nu^2 - 2}{r^2}Y_\nu(r)\right], \end{aligned} \tag{4.4.5}$$

where $J_\nu(r)$ and $Y_\nu(r)$ denote the Bessel's polynomials of the first and second kinds with order ν.

The constants A and B here can be determined if we specify two conditions involving the displacement and/or the stress. They will form a linear system with two equations and two unknowns.

For a more specific case, say with $\nu = 0$, the displacement is obtained by

$$u(r) = AJ_0(r) + BY_0(r), \tag{4.4.6}$$

and the stress by

$$\sigma_r(r) = A\left[\frac{r^2 - 2}{r^2}J_0(r) - \frac{1}{r}J_1(r)\right] + B\left[\frac{r^2 - 2}{r^2}Y_0(r) - \frac{1}{r}Y_1(r)\right]. \tag{4.4.7}$$

If we have a shell with radius from $r = 1.5$ to $r = 1.7$ and the pressure at the interior of the shell is $p_i = \sigma_r(1.5) = 2$, and at the exterior of the shell is $p_e =$

$\sigma_r(1.7) = 3$, then the constants are $A = 12.2407322$ and $B = 18.45469669$. The exact displacement at $r = 1.6$ is $u(1.6) = 13.33330683$ and stress is $\sigma_r(1.6) = 2.565725364$.

4.4.2 Some numerical results

Problem 4.1 :

Here we consider spherically shell problem for several kind of materials subjected to the given non dimensionalised radius and the boundary conditions using two point boundary value method in the D02GBF-NAG Fortran Library Routine. Table 4.1 shows the numerical results for homogeneous material using the non dimensionalised material quantities $\lambda/\lambda_0 = 1$ and $\mu/\mu_0 = 1$ by specifying the boundary conditions $\sigma_r(1) = 1$ and $\sigma_r(2) = -1$. It can be verified that the exact displacement and stress in this case are $u(r) = -\frac{9r}{35} - \frac{4}{7r^2}$ and $\sigma_r(r) = -\frac{9}{7} + \frac{16}{7r^3}$ respectively. Table 4.2 shows the numerical results for inhomogeneous material with $\lambda/\lambda_0 = (r^2 - 2)/(2r)$ and $\mu/\mu_0 = (4 - r^2)/(4r)$ by specifying the tolerance of error tol $= 10^{-5}$ and the boundary conditions $\sigma_r(1.5) = 2$ and $\sigma_r(1.7) = 3$. Tables 4.3 and 4.4 show the numerical results for inhomogeneous materials with $\lambda/\lambda_0 = 2/(r + 1)$, $\mu/\mu_0 = 1/(r + 1)$ and $\lambda/\lambda_0 = 1 + r^2$, $\mu/\mu_0 = \ln r + 2$ respectively, using the boundary conditions $u(1) = 0$, $\sigma_r(2) = -2$ for the results in Table 4.3 and $\sigma_r(1) = 1$, $\sigma_r(2) = -1$ for the results in Table 4.4 and tolerance of error is chosen to be tol $= 10^{-6}$.

Table 4.1

Homogeneous material with $\lambda/\lambda_0 = 1$ And $\mu/\mu_0 = 1$

$\sigma_r(1) = 1$, $\sigma_r(2) = -1$ and tol=$1e^-7$

R	Displacement	Stress	du/dr
1.0000000	-0.8285714	1.0000000	0.8857143
1.0500000	-0.7883025	0.6887717	0.7301001
1.0750000	-0.7709043	0.5541956	0.6628121
1.1250000	-0.7407848	0.3196159	0.5455222
1.2023810	-0.7044390	0.0291947	0.4003116
1.2500000	-0.6871428	-0.1154286	0.3280000
1.3000000	-0.6724091	-0.2453345	0.2630470
1.3750000	-0.6558146	-0.4064613	0.1824836
1.5000000	-0.6396825	-0.6084656	0.0814815
1.6666667	-0.6342857	-0.7920000	-0.0102857
1.7500000	-0.6365889	-0.8592253	-0.0438984
2.0000000	-0.6571428	-1.0000000	-0.1142857

Table 4.2

Inhomogeneous material with $\lambda/\lambda_0 = \frac{r^2-2}{2r}$ and $\mu/\mu_0 = \frac{4-r^2}{4r}$

$\sigma_r(1.5) = 2$, $\sigma_r(1.7) = 3$ and tol=$1e^-5$

R	Displacement	Stress	du/dr
1.5000000	13.3231225	2.0000000	0.7794796
1.5111111	13.3309310	2.0692399	0.6262128
1.5259259	13.3387047	2.1591103	0.4235353
1.5407407	13.3434899	2.2461570	0.2227634
1.5592593	13.3453117	2.3509615	-0.0255405
1.5814815	13.3414689	2.4708103	-0.3196301
1.6000000	13.3333060	2.5657252	-0.5614968
1.6148148	13.3235676	2.6383995	-0.7529014
1.6296296	13.3110072	2.7081731	-0.9424565
1.6592593	13.2775301	2.8390133	-1.3160399
1.6814815	13.2452177	2.9295339	-1.5914076
1.7000000	13.2136474	3.0000000	-1.8177330

Table 4.3

Inhomogeneous material with $\lambda/\lambda_0 = \frac{2}{r+1}$ and $\mu/\mu_0 = \frac{1}{r+1}$

$u(1) = 0$, $\sigma_r(2) = -2$ and tol=$1e^-6$

R	Displacement	Stress	du/dr
1.0000000	0.0000000	-2.9195925	-1.4597963
1.0555556	-0.0779744	-2.7738040	-1.3515565
1.0833333	-0.1148764	-2.7116174	-1.3062610
1.1250000	-0.1680426	-2.6292248	-1.2474045
1.2037037	-0.2626052	-2.5019871	-1.1602452
1.2592593	-0.3257159	-2.4293780	-1.1134919
1.3333333	-0.4063307	-2.3490455	-1.0655285
1.4166667	-0.4934072	-2.2756709	-1.0265971
1.5000000	-0.5777603	-2.2156206	-0.9995893
1.5833333	-0.6602538	-2.1655057	-0.9815533
1.7222222	-0.7953184	-2.0978873	-0.9659311
2.0000000	-1.0631869	-2.0000000	-0.9684065

Table 4.4

Inhomogeneous material with $\lambda/\lambda_0 = 1 + r^2$ and $\mu/\mu_0 = \ln r + 2$

$\sigma_r(1) = 1$, $\sigma_r(2) = -1$ and tol=$1\epsilon^-6$

R	Displacement	Stress	du/dr
1.0000000	-0.5768860	1.0000000	0.7880312
1.0555556	-0.5369392	0.6978468	0.6551666
1.1250000	-0.4961279	0.3925511	0.5260969
1.1666667	-0.4755394	0.2394686	0.4637919
1.2500000	-0.4412297	-0.0151009	0.3646362
1.3000000	-0.4242019	-0.1416578	0.3178288
1.3750000	-0.4025845	-0.3032011	0.2610136
1.4375000	-0.3874898	-0.4170638	0.2232856
1.5000000	-0.3745326	-0.5158999	0.1923499
1.6111111	-0.3556418	-0.6626899	0.1500319
1.7500000	-0.3375283	-0.8078512	0.1132185
2.0000000	-0.3146931	-1.0000000	0.0737805

4.5 Analytic solution for the time dependent problem

In general, equation (4.2.3) can be reduced to the canonical form of the wave equation. Following Clements et al [15], by introducing a function $v(r,t)$, the equation (4.2.3) can be written more conveniently in a matrix form

$$\Omega_r = M\Omega_t + N\Omega, \tag{4.5.1}$$

where the subscripts denote the partial derivatives and the matrices are

$$\Omega = \begin{pmatrix} u \\ v \end{pmatrix}, \qquad M = \begin{pmatrix} 0 & m_{12} \\ m_{21} & 0 \end{pmatrix}, \qquad N = \begin{pmatrix} n_{11} & 0 \\ 0 & 0 \end{pmatrix}. \tag{4.5.2}$$

Here, m_{12}, m_{21} and n_{11} are functions of r only and should satisfy the relations

$$m_{12}m_{21} = C, \tag{4.5.3}$$

$$n_{11} + \frac{d}{dr}\left[\ln m_{12}\right] = -A, \tag{4.5.4}$$

$$m_{12}\frac{d}{dr}\left[\frac{n_{11}}{m_{12}}\right] = -B. \tag{4.5.5}$$

By setting $\Phi = \exp\{-\int n_{11}\,dr\}$ or $n_{11} = -\frac{1}{\Phi}\frac{d\Phi}{dr}$, and $\mathcal{A} = \exp\{\int A\,dr\}$, equations (4.5.3) and (4.5.4) can be written as

$$m_{21} = \frac{C\mathcal{A}}{\Phi}, \tag{4.5.6}$$

and

$$m_{12} = \frac{\Phi}{\mathcal{A}}. \tag{4.5.7}$$

Thus if we set $u^*(r,t) = u(r,t)\Phi(r)$ and $v^*(r,t) = v(r,t)$, then equation (4.5.1) reduces to the form

$$\begin{pmatrix} u^* \\ v^* \end{pmatrix}_r = \begin{pmatrix} 0 & \Phi^2/\mathcal{A} \\ \mathcal{A}C/\Phi^2 & 0 \end{pmatrix}\begin{pmatrix} u^* \\ v^* \end{pmatrix}_t. \tag{4.5.8}$$

Furthermore, by introducing the new independent variables

$$r^* = \int C^{\frac{1}{2}}\, dr, \qquad t^* = t, \tag{4.5.9}$$

equation (4.5.8) reduces to

$$\begin{pmatrix} u^* \\ v^* \end{pmatrix}_{r^*} = \begin{pmatrix} 0 & K^{-\frac{1}{2}} \\ K^{\frac{1}{2}} & 0 \end{pmatrix} \begin{pmatrix} u^* \\ v^* \end{pmatrix}_{t^*}, \tag{4.5.10}$$

where

$$K = \mathcal{A}^2 \Phi^{-4} C. \tag{4.5.11}$$

Equation (4.5.10) in usual notation is

$$\frac{\partial^2}{\partial r^{*2}} u^*(r^*, t^*) = \frac{\partial^2}{\partial t^{*2}} u^*(r^*, t^*), \tag{4.5.12}$$

which is the standard wave equation. The general solution of this equation is

$$u^* = f_1(t^* + r^*) + f_2(t^* - r^*), \tag{4.5.13}$$

or

$$u(r,t) = \Phi^{-1}(r)\left[f_1(t + \int C^{\frac{1}{2}} dr) + f_2(t - \int C^{\frac{1}{2}} dr)\right], \tag{4.5.14}$$

which is a similar equation to (3.4.21).

CHAPTER 5

ANTI–PLANE DEFORMATIONS FOR ISOTROPIC MATERIALS

5.1 Introduction

Anti–plane deformations for inhomogeneous elastic materials are considered in this chapter. Several methods are employed for solving static and dynamic anti–plane problems for isotropic materials. For certain types of materials, the static problem can be solved analytically using the method of separation of variables.

Many problems involving anti–plane deformations of inhomogeneous elastic materials cannot be solved analytically. In such cases numerical methods must be employed. Finite differences, finite elements and the boundary element method are three such numerical techniques. Due to the difficulties of finding the fundamental solution, not many authors have touched on the subject of developing the boundary integral equation method for such boundary value problems. In section 5.4, the boundary element method is developed for handling the static case. This development is then applied to a seepage problem.

In section 5.5, the development of the boundary element method for certain classes of dynamic problems are discussed. The combination of the boundary element method and the perturbation technique which reduces the governing equation to the Laplace and Poisson type equations and several numerical results are given in section 5.6. Further development for the dynamic case can be found in section 5.7.

5.2 Basic equations

Elastic inhomogeneous materials are in a state of anti–plane strain if the displacements u_1, u_2 and u_3 take the form $u_1 = 0, u_2 = 0$ and $u_3 = u_3(x_1, x_2)$. In other words, the only nonzero displacement component is u_3 and it depends only on the plane coordinates x_1 and x_2.

The stress–displacement relations for inhomogeneous materials (see for example Sokolnikoff [71]), are

$$\sigma_{13} = \sigma_{31} = \mu \frac{\partial u_3}{\partial x_1} \quad \text{and} \quad \sigma_{23} = \sigma_{32} = \mu \frac{\partial u_3}{\partial x_2}, \tag{5.2.1}$$

with all other stress components zero. In (5.2.1) μ is the shear modulus which is taken to be a function of position, say $\mu = \mu(x_1, x_2)$.

The equation of motion for anti plane strain in the absence of body force may be written in the form

$$\frac{\partial \sigma_{13}}{\partial x_1} + \frac{\partial \sigma_{23}}{\partial x_2} = \rho \frac{\partial^2 u_3}{\partial t^2}, \tag{5.2.2}$$

where $\rho = \rho(x_1, x_2)$ denotes the density of the material. Using (5.2.1) in (5.2.2) and for simplicity, we change variables x_1, x_2 to x and y respectively and u_3 to u

$$\frac{\partial}{\partial x}\left[\mu \frac{\partial u}{\partial x}\right] + \frac{\partial}{\partial y}\left[\mu \frac{\partial u}{\partial y}\right] = \rho \frac{\partial^2 u}{\partial t^2}. \tag{5.2.3}$$

If the material is in equilibrium then the governing equation reduces to

$$\frac{\partial}{\partial x}\left[\mu \frac{\partial u}{\partial x}\right] + \frac{\partial}{\partial y}\left[\mu \frac{\partial u}{\partial y}\right] = 0. \tag{5.2.4}$$

5.3 Analytical solution by the method of separation of variables

A method of separation of variables is considered in this section for solving equation (5.2.4) for specific materials. By introducing a new variable

$$U(x,y) = u(x,y)\left[\mu(x,y)\right]^{\frac{1}{2}}, \tag{5.3.1}$$

to equation (5.2.4) we obtain

$$\nabla^2 U - \Lambda(x,y)U = 0. \tag{5.3.2}$$

where

$$\Lambda(x,y) = \frac{1}{2\mu}\nabla^2\mu - \frac{1}{4\mu^2}\left[\left(\frac{\partial\mu}{\partial x}\right)^2 + \left(\frac{\partial\mu}{\partial y}\right)^2\right]. \tag{5.3.3}$$

Let

$$U(x,y) = X(x)Y(y), \tag{5.3.4}$$

and assuming that μ is continuous and twice differentiable with respect to x and y, and can also be written in the form

$$\mu(x,y) = \mu_0 f(x)g(y), \tag{5.3.5}$$

where μ_0 is a constant, equation (5.3.2) now reduces into two equations

$$\begin{aligned} \frac{\partial^2 X}{\partial x^2} + \left[n^2 + \frac{1}{4}\left(\frac{1}{f}\frac{df}{dx}\right)^2 - \frac{1}{2}\left(\frac{1}{f}\frac{d^2 f}{dx^2}\right)\right]X = 0, \\ \frac{\partial^2 Y}{\partial y^2} + \left[-n^2 + \frac{1}{4}\left(\frac{1}{g}\frac{dg}{dy}\right)^2 - \frac{1}{2}\left(\frac{1}{g}\frac{d^2 g}{dy^2}\right)\right]Y = 0. \end{aligned} \tag{5.3.6}$$

Here n^2 is the separation constant. In the case that $f(x)$ satisfies the differential equation

$$\frac{1}{2f}\frac{d^2 f}{dx^2} - \frac{1}{4}\left(\frac{1}{f}\frac{df}{dx}\right)^2 = f_0, \tag{5.3.7}$$

and $g(y)$ satisfies the differential equation

$$\frac{1}{2g}\frac{d^2 g}{dy^2} - \frac{1}{4}\left(\frac{1}{g}\frac{dg}{dy}\right)^2 = g_0, \tag{5.3.8}$$

where f_0 and g_0 are constants the equation (5.3.6) reduces to

$$\begin{aligned} \frac{\partial^2 X}{\partial x^2} + k^2 X &= 0, \\ \frac{\partial^2 Y}{\partial y^2} - (f_0 + g_0 + k^2)Y &= 0, \end{aligned} \tag{5.3.9}$$

where $k^2 = n^2 - f_0$. By assuming

$$k^2 = n^2 - f_0 \geq 0, \qquad \text{and} \qquad k^2 + f_0 + g_0 \geq 0, \tag{5.3.10}$$

we find the solution for the displacement in half-plane $y \geq 0$ which satisfies the condition $u \to 0$ as $y \to \infty$ in the form

$$\begin{aligned} u(x,y) = [\mu_0 f(x) g(y)]^{-1/2} \int_0^\infty &\{A(\xi)\cos(x\xi) + B(\xi)\sin(x\xi)\} \\ &\exp\left[-(f_0 + g_0 + \xi^2)^{1/2} y\right] d\xi, \end{aligned} \tag{5.3.11}$$

where $A(\xi)$ and $B(\xi)$ are arbitrary functions of ξ.

The non zero stresses follow by using (5.3.11) in (5.2.1)

$$\begin{aligned} \sigma_{13} = &-\frac{1}{2}[\mu_0 f(x) g(y)]^{-1/2} \mu_0 \frac{df}{dx} g(y) \int_0^\infty \Big\{ A(\xi)\cos(x\xi) + \\ &B(\xi)\sin(x\xi) \Big\} \exp[-s(\xi)y]\, d\xi + [\mu_0 f(x) g(y)]^{1/2} \int_0^\infty \Big\{ B(\xi)\cos(x\xi) \\ &- A(\xi)\sin(x\xi) \Big\} \xi \exp[-s(\xi)y]\, d\xi, \end{aligned} \tag{5.3.12}$$

and

$$\begin{aligned} \sigma_{23} = &-\frac{1}{2}[\mu_0 f(x) g(y)]^{-1/2} \mu_0 f(x) \frac{dg}{dy} \int_0^\infty \Big\{ A(\xi)\cos(x\xi) + \\ &B(\xi)\sin(x\xi) \Big\} \exp[-s(\xi)y]\, d\xi - [\mu_0 f(x) g(y)]^{1/2} \int_0^\infty \Big\{ A(\xi)\cos(x\xi) \\ &+ B(\xi)\sin(x\xi) \Big\} s(\xi) \exp[-s(\xi)y]\, d\xi, \end{aligned} \tag{5.3.13}$$

where

$$s(\xi) = (a_0 + b_0 + \xi^2)^{\frac{1}{2}}. \tag{5.3.14}$$

5.4 Boundary element method for static case

The boundary element method is considered for solving boundary value problems for the static case in this section.

5.4.1 General solution in term of an arbitrary harmonic function

One of the main difficulties of solving equation (5.2.4) using the boundary element method is to find the fundamental solution. However, for certain cases, including the case when the shear modulus takes the form

$$\mu(x,y) = X(x)Y(y), \tag{5.4.1}$$

it is possible to express the solution of (5.2.4) in terms of an arbitrary harmonic function.

In the previous section. it has been shown that the simple transformation as in equation (5.3.1) reduces (5.2.4) to

$$\nabla^2 U - \Lambda(x,y)U = 0, \tag{5.4.2}$$

where $\Lambda(x,y)$ is given by (5.3.3). For some specific cases, for example $\mu(x,y) = (\mu_1 xy + \mu_2 x + \mu_3 y + \mu_4)^2$ where μ_1, μ_2, μ_3 and μ_4 are constants, or in more general for the case that the shear modulus satisfy $\nabla^2 \mu^{\frac{1}{2}} = 0$, we obtain $\Lambda(x,y) = 0$ so that equation (5.4.2) simply reduces to the Laplace equation in which the general solution can be well expressed in terms of harmonic functions.

For the case when the shear modulus is given by (5.4.1), equation (5.4.2) can be written as

$$\nabla^2 U - \big[\Lambda_1(x) + \Lambda_2(y)\big]U = 0, \tag{5.4.3}$$

with

$$\Lambda_1(x) = \frac{d}{dx}\left[\left(\frac{dX}{dx}\right)^2 \Big/ 4X\right] \Big/ \left(\frac{dX}{dx}\right),$$
$$\Lambda_2(y) = \frac{d}{dy}\left[\left(\frac{dY}{dy}\right)^2 \Big/ 4Y\right] \Big/ \left(\frac{dY}{dy}\right). \tag{5.4.4}$$

The general solution now is sought in the form of the double series

$$U = \sum_{n=0}^{\infty}\sum_{m=0}^{\infty} f_n(x) g_m(y) F_n^m(x,y), \tag{5.4.5}$$

where F_n^m satisfy the two-dimensional Laplace's equation.

By substituting (5.4.5) into (5.4.3), we obtain

$$\sum_{n=0}^{\infty}\sum_{m=0}^{\infty}\Bigg\{ g_m(y)\left[2\frac{df_n}{dx}\frac{\partial F_n^m}{\partial x} + F_n^m\frac{d^2 f_n}{dx^2}\right] + f_n(x)\left[2\frac{dg_m}{dy}\frac{\partial F_n^m}{\partial y} + F_n^m\frac{d^2 g_m}{dy^2}\right] - \big(\Lambda_1(x)+\Lambda_2(y)\big) f_n(x) g_m(y) F_n^m \Bigg\} = 0. \tag{5.4.6}$$

Now (5.4.5) is a solution of (5.4.3) if we choose $f_n(x)$, $g_m(y)$ and F_n^m to satisfy

$$\frac{\partial F_n^m}{\partial x} = F_{n-1}^m \qquad \text{for} \quad m \geq 0 \quad \text{and} \quad n \geq 1, \tag{5.4.7}$$

$$\frac{\partial F_n^m}{\partial y} = F_n^{m-1} \qquad \text{for} \quad m \geq 1 \quad \text{and} \quad n \geq 0, \tag{5.4.8}$$

and

$$2\frac{df_{n+1}}{dx} + \frac{d^2 f_n}{dx^2} - \Lambda_1(x) f_n = 0,$$
$$2\frac{dg_{m+1}}{dy} + \frac{d^2 g_m}{dy^2} - \Lambda_2(y) g_m = 0, \tag{5.4.9}$$

for $n \geq 0$ and $m \geq 0$ with f_0 and g_0 being constants.

If $\Phi_0(z)$ ($z = x + iy$) is an analytic function of z in the domain of interest, define $\Phi_n(z)$ to be analytic functions of z given by the recurrence relation

$$\Phi_n(z) = \int_0^z \Phi_{n-1}(t)\, dt \qquad \text{for} \qquad n = 1, 2, 3, \cdots \tag{5.4.10}$$

Letting

$$F_n^m(x,y) = \Re\Big\{(-i)^m \Phi_{m+n}(z)\Big\}, \tag{5.4.11}$$

we find that, after using (5.4.10), equations (5.4.7) and (5.4.8) are satisfied. Therefore, the choice of F_n^m as given in (5.4.11) is a suitable one.

Proceeding further as in Clements [10], we obtain

$$\Phi_n(z) = \frac{1}{(n-1)!}\int_0^z (z-t)^{n-1}\Phi_0(t)\,dt \quad \text{for} \quad n \geq 1, \tag{5.4.12}$$

and hence

$$F_n^m(x,y) = \frac{1}{(n+m-1)!}\Re\left\{(-\imath)^m \int_0^z (z-t)^{n+m-1}\Phi_0(t)\,dt\right\}, \tag{5.4.13}$$

for $n+m = 1,2,3,\cdots$.

Thus, a solution of (5.2.4) with (5.4.1) may be expressed in the series form

$$\begin{aligned} u(x,y) = {} & \left[\mu(x,y)\right]^{-\frac{1}{2}}\Re\Bigg\{f_0 g_0 \Phi_0(z) + \\ & \sum_{\substack{n=0 \\ m+n\neq 0}}^{\infty}\sum_{m=0}^{\infty} \frac{(-\imath)^m f_n(x) g_m(y)}{(n+m-1)!}\int_0^z (z-t)^{n+m-1}\Phi_0(t)\,dt\Bigg\}. \end{aligned} \tag{5.4.14}$$

The validity of this solution depends on the convergence properties of the infinite series. The convergence of the series will depend on $f_n(x)$ and $g_m(y)$ which are, of course, related to the coefficient of the shear modulus $\mu(x,y)$ through the equations (5.4.1) and (5.4.7)–(5.4.9).

Here the question of the convergence of the series in general case will not be examined in detail. It will be sufficient to note that the series may be truncated after a finite number of terms for certain $\mu(x,y)$. The validity of (5.4.14) as a solution of (5.2.4) in such cases is assured. Specifically let

$$\mu(x,y) = (\alpha x + \beta)^n(\delta y + \eta)^q, \tag{5.4.15}$$

then equation (5.4.9) gives

$$\begin{aligned} f_n(x) &= \frac{(-\alpha)^n p(p-2n)}{2^{3n}n!}\prod_{r=1}^{n-1}\left[p^2-(2r)^2\right](\alpha x+\beta)^{-n} f_0 \qquad n \geq 1 \\ g_m(y) &= \frac{(-\delta)^m q(q-2m)}{2^{3m}m!}\prod_{r=1}^{m-1}\left[q^2-(2r)^2\right](\delta y+\eta)^{-m} g_0 \qquad m \geq 1. \end{aligned} \tag{5.4.16}$$

It is clear that for $p = 0, \pm 2, \pm 4, \cdots$ and $q = 0, \pm 2, \pm 4, \cdots$ the series is truncated after several terms and thus converges uniformly and absolutely.

5.4.2 Boundary integral equation

Consider a region $\mathcal{R}$ bounded by a simple closed curve C. For a point $(a, b) \in C$, define a small semi circle segment Γ centre at the point (a, b) with radius ϵ (Figure 5.1). If u and u' are two solutions of (5.2.4) valid in $\mathcal{R}$ then it can be verified that (see Appendix A, theorem 1 by putting $\omega = 0$)

$$\int_{C+\Gamma} \mu(x, y) \left[\frac{\partial u}{\partial n} u' - \frac{\partial u'}{\partial n} u \right] dS = 0. \tag{5.4.17}$$

Let u' be given by (5.4.14) with $f_0 = g_0 = 1$ and

$$\Phi_0 = \gamma \log(z - z_0), \tag{5.4.18}$$

with γ a constant, $z = x + \imath y$ and $z_0 = a + \imath b$. Thus on Γ

$$x = a + \epsilon \cos\theta, \qquad y = b + \epsilon \sin\theta, \qquad z = z_0 + \epsilon \exp(\imath\theta), \tag{5.4.19}$$

so that

$$\begin{aligned} u' = & \frac{\gamma}{\left[\mu(a + \epsilon\cos\theta, b + \epsilon\sin\theta)\right]^{\frac{1}{2}}} \Bigg\{ \log\epsilon + \\ & \sum_{\substack{n=0 \\ m+n\neq 0}}^{\infty} \sum_{m=0}^{\infty} \frac{(-\imath)^m f_n(a + \epsilon\cos\theta) g_m(b + \epsilon\sin\theta)}{(n + m - 1)!} \\ & \int_0^{z_0 + \epsilon\exp(\imath\theta)} \left[z_0 + \epsilon\exp(\imath\theta) - t \right]^{n+m-1} \log(t - z_0)\, dt \Bigg\}. \end{aligned} \tag{5.4.20}$$

It may be readily verified that by letting $\epsilon \to 0$ we obtain

$$u' = \frac{\gamma}{\left[\mu(a, b)\right]^{\frac{1}{2}}} \log\epsilon + O(1) + O(\epsilon\log\epsilon) \tag{5.4.21}$$

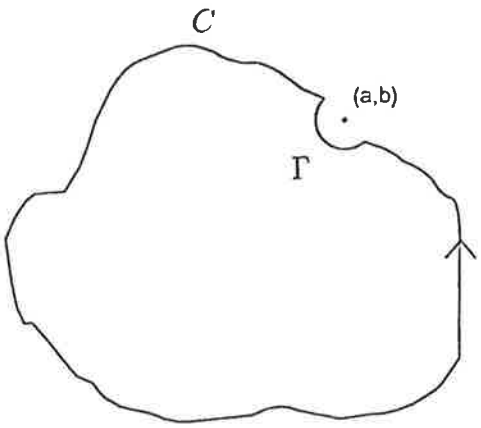

Figure 5.1
Simple closed curve C

$$\frac{\partial u'}{\partial n} = \frac{-\gamma}{\left[\mu(a,b)\right]^{\frac{1}{2}}}\frac{1}{\epsilon} + O(1) + O(\log\epsilon) \tag{5.4.22}$$

Hence for small ϵ

$$\begin{aligned}\int_\Gamma \mu\frac{\partial u'}{\partial n}u\,dS &= \frac{-\gamma}{\left[\mu(a,b)\right]^{\frac{1}{2}}}\int_\alpha^{\alpha+\pi}\mu(a+\epsilon\cos\theta, b+\epsilon\sin\theta)u(a+\epsilon\cos\theta, b+\epsilon\sin\theta)\,d\theta \\ &\quad + O(\epsilon) + O(\epsilon\log\epsilon) \\ &= -\pi\gamma\left[\mu(a,b)\right]^{\frac{1}{2}}u(a,b) + O(\epsilon) + O(\epsilon\log\epsilon)\end{aligned} \tag{5.4.23}$$

and

$$\int_\Gamma \mu(x,y)\frac{\partial u}{\partial n}u'\,dS = O(\epsilon) + O(\epsilon\log\epsilon). \tag{5.4.24}$$

In the above it has been assumed that Γ is a semicircle so that the limits on the integral on (5.4.23) are α and $\alpha+\pi$ where α is the appropriate angle. If the geometry is such that Γ is not a semicircle then it is necessary to make an appropriate adjustment to the limits on the integral in (5.4.23). Also, note that, for each $z_0 \in C$, the branch cut of the complex logarithmic function in (5.4.18) is selected in such a way that the function is single-valued throughout $\mathcal{R}$. This is to ensure that u' and its partial derivatives are all single-valued throughout the entire domain.

Using (5.4.17), (5.4.23) and (5.4.24), it now follows that in the limit as $\epsilon \to 0$

$$u(a,b) = \frac{-1}{\pi\gamma\left[\mu(a,b)\right]^{\frac{1}{2}}} \int_C \mu(x,y)\left[\frac{\partial u}{\partial n}u' - \frac{\partial u'}{\partial n}u\right] dS \qquad \text{for} \qquad (a,b) \in C \quad (5.4.25)$$

The arbitrary constant γ here cancels out with the γ in u' and $\partial u'/\partial n$.

5.4.3 Integral equation for interior points

If $\Phi_0 = \gamma \log(z - z_0)$ and u' is given by (5.4.14) then in the case $z_0 \in \mathcal{R}$ it is not possible for both u' and $\partial u'/\partial n$ to be single-valued throughout $\mathcal{R}$. Thus the standard boundary integral equation for an interior point $(a,b) \in \mathcal{R}$ which expresses $u(a,b)$ in terms of an integral round the boundary C of $\mathcal{R}$ cannot be used. Instead it is convenient to proceed as follows. The domain $\mathcal{R}$ is divided up as shown in Figure 5.2. Note that $C = C_1 \cup C_2$. Both u and $\partial u/\partial n$ are known on C_1 and C_2 through calculation using (5.4.25).

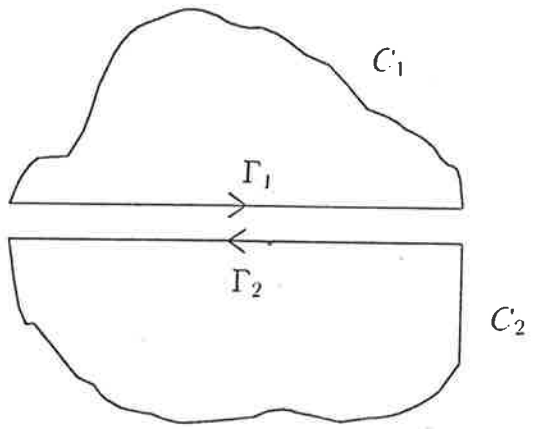

Figure 5.2
Simple closed curves C_1 and C_2

Now

$$u(a,b) = \frac{-1}{\pi\gamma\left[\mu(a,b)\right]^{\frac{1}{2}}} \int_{\Gamma_1} \mu(x,y)\left[\frac{\partial u}{\partial n}u' - \frac{\partial u'}{\partial n}u\right] dS + I_1 \qquad \text{for} \qquad (a,b) \in \Gamma_1 \tag{5.4.26}$$

and

$$u(a,b) = \frac{-1}{\pi\gamma\left[\mu(a,b)\right]^{\frac{1}{2}}} \int_{\Gamma_2} \mu(x,y)\left[\frac{\partial u}{\partial n}u' - \frac{\partial u'}{\partial n}u\right] dS + I_2 \qquad \text{for} \qquad (a,b) \in \Gamma_2 \tag{5.4.27}$$

where

$$I_r = \frac{-1}{\pi\gamma\left[\mu(a,b)\right]^{\frac{1}{2}}} \int_{C_r} \mu(x,y)\left[\frac{\partial u}{\partial n}u' - \frac{\partial u'}{\partial n}u\right] dS \qquad \text{for} \qquad r = 1,2 \tag{5.4.28}$$

and since u and $\partial u/\partial n$ are known on C_1 and C_2 both I_1 and I_2 can be readily calculated.

The integral in equations (5.2.26) and (5.2.27) can be discretised to provide a system of linear algebraic equations for the unknown u and $\partial u/\partial n$ on Γ_1 and Γ_2. Continuity conditions on u and $\partial u/\partial n$ on the interface of Γ_1 and Γ_2 can then be applied to complete the linear system of equations so that the system can be solved for u and $\partial u/\partial n$.

5.4.4 Numerical examples

Problem 5.1 :

To demonstrate the accuracy of the method, consider the following boundary value problem.

Find a solution to

$$\frac{\partial}{\partial x}\left[(xy)^{-2}\frac{\partial u}{\partial x}\right] + \frac{\partial}{\partial y}\left[(xy)^{-2}\frac{\partial u}{\partial y}\right] = 0, \tag{5.4.29}$$

which is valid in the square $1 < x < 2$, $1 < y < 2$ and is subject to the boundary conditions

$$\begin{aligned}
u &= \frac{1}{2}(1-x^2)\arctan(x^{-1}) + \frac{1}{2}x && \text{on} \quad y = 1 \\
u &= \frac{1}{2}(y^2-4)\arctan(\frac{1}{2}y) + y && \text{on} \quad x = 2 \\
\frac{\partial u}{\partial n} &= 2\arctan(2x^{-1}) + \frac{1}{2}\frac{x(4-x^2)}{x^2+4} + \frac{1}{2}x && \text{on} \quad y = 2 \\
\frac{\partial u}{\partial n} &= \arctan(y) + \frac{1}{2}\frac{y(y^2-1)}{1+y^2} - \frac{1}{2}y && \text{on} \quad x = 1
\end{aligned} \tag{5.4.30}$$

This problem admits an analytical solution in the form

$$u = \frac{1}{2}(y^2 - x^2)\arctan(y/x) + \frac{1}{2}xy. \tag{5.4.31}$$

According to equation (5.4.25), the integral equation corresponding to (5.4.29) can be written as

$$u(a,b) = \frac{ab}{\pi}\int_C (xy)^{-2}\left[\frac{\partial u'}{\partial n}u - \frac{\partial u}{\partial n}u'\right] dS \tag{5.4.32}$$

with u' is given by (5.4.14) or

$$u' = xy\left[F_0^0 - \frac{1}{x}F_1^0 - \frac{1}{y}F_0^1 + \frac{1}{xy}F_1^1\right], \tag{5.4.33}$$

where

$$\begin{aligned}
F_0^0 &= \Re\Big\{\log(z - z_0)\Big\}, \\
F_1^0 &= \Re\Big\{(z - z_0)\log(z - z_0) + z_0\log(-z_0) - z\Big\}, \\
F_0^1 &= \Re\Big\{-\imath(z - z_0)\log(z - z_0) - \imath z_0\log(-z_0) + \imath z\Big\}, \\
F_1^1 &= \Re\Big\{\frac{1}{2}\imath(z - z_0)^2\log(z - z_0) - \frac{1}{2}\imath z_0^2\log(-z_0) - \frac{1}{4}\imath(z - z_0)^2 + \frac{1}{4}\imath {z_0}^2\Big\}.
\end{aligned} \tag{5.4.34}$$

To ensure that u' and its normal derivative $\partial u'/\partial n$ are single valued throughout the entirely square boundary, it is necessary to consider the branch cut of the complex logarithmic function in (5.4.34). The adjustment might be done by writing the logarithmic function in the form

$$\log(z - z_0) = \log(r) + \imath\theta, \qquad r = \left[(x-a)^2 + (y-b)^2\right]^{\frac{1}{2}}. \tag{5.4.35}$$

The imaginary part of the complex logarithmic function in (5.4.35), θ is determined by the following procedure

Step1. Determine $\overline{\theta} = \arctan\left(\dfrac{y-b}{x-a}\right)$ so that $0 \leq \overline{\theta} < 2\pi$.

Step2. If $n_1 > 0$ then $\theta = \overline{\theta}$.

If $n_1 = 0$ and $n_2 > 0$ then $\theta = \overline{\theta}$;

In the case $\theta = 0$, it should be replaced by $\theta = 2\pi$.

If $n_1 = 0$ and $n_2 < 0$ then $\theta = \overline{\theta}$. (5.4.36)

If $n_1 < 0$ and $n_2 \geq 0$ then $\theta = \overline{\theta}$;

In the case $\theta > \pi$, it should be replaced by $\theta = \overline{\theta} - 2\pi$.

If $n_1 < 0$ and $n_2 < 0$ then $\theta = \overline{\theta}$;

In the case $\theta > \dfrac{3}{2}\pi$, it should be replaced by $\theta = \overline{\theta} - 2\pi$,

where n_1 and n_2 denote the outward normal components at point z_0. Now, equation (5.4.32) can be employed using the standard boundary element procedure. By using five segments on each side of the square boundary, a comparison of the numerical results using the boundary element technique and the analytical results on the boundary for the $\partial u/\partial n$ can be found in the Table 5.1, while the results for u are in the Table 5.2. Numerical results and analytical results for u and its normal derivative at certain interior points are compared in Table 5.3. From Tables 5.1–5.3, we find that numerical results to be in reasonable agreement with the analytical results.

Table 5.1

Comparison of analytical and numerical results

$\partial u/\partial n$ at boundary points

Boundary point	$\partial u/\partial n$(BEM)	$\partial u/\partial n$(ANAL.)
(1.10,1.00)	-1.3000	-1.235553
(1.30,1.00)	-1.0946	-1.138967
(1.50,1.00)	-1.0356	-1.049541
(1.70,1.00)	-0.9423	-0.968742
(1.90,1.00)	-0.9607	-0.896625
(2.00,1.10)	-0.0475	-0.161157
(2.00,1.30)	-0.1738	-0.238866
(2.00,1.50)	-0.3025	-0.327002
(2.00,1.70)	-0.3984	-0.422051
(2.00,1.90)	-0.5601	-0.520840

Table 5.2

Comparison of analytical and numerical results

for u at boundary points

Boundary point	u (BEM)	u (ANAL.)
(1.90,2.00)	2.0465	2.058152
(1.70,2.00)	2.1924	2.180798
(1.50,2.00)	2.3269	2.311383
(1.30,2.00)	2.4606	2.448556
(1.10,2.00)	2.5724	2.589795
(1.00,1.90)	2.3422	2.367646
(1.00,1.70)	1.8157	1.831923
(1.00,1.50)	1.3500	1.364246
(1.00,1.30)	0.9513	0.965710
(1.00,1.10)	0.6198	0.637463

Table 5.3

Comparison of analytical and numerical results

for u and its normal derivative at interior points

Interior point	u(BEM)	u(ANAL.)	$\partial u/\partial y$ (BEM)	$\partial u/\partial y$(ANAL.)
(1.10,1.40)	1.1287	1.10931	2.0646	1.94688
(1.30,1.40)	1.0361	1.02103	1.7738	1.84947
(1.50,1.40)	0.9518	0.94112	1.7184	1.74964
(1.70,1.40)	0.8759	0.86965	1.5901	1.65150
(1.90,1.40)	0.8081	0.80610	1.6943	1.55762

Problem 5.2 :

In the beginning of this chapter, it is mentioned that the development of boundary element method can be directly applied to the seepage problem. For flow of ground water that obeys Darcy's law, the governing equation can be written as

$$\frac{\partial}{\partial x}\left[K\frac{\partial H}{\partial x}\right]+\frac{\partial}{\partial y}\left[K\frac{\partial H}{\partial y}\right]=0. \tag{5.4.36}$$

where $K=K(x,y)$ is hydraulic conductivity, H is piezometric head, which is corresponding to equation (5.2.4) simply by replacing u by H and μ by K. Of the practical interest here, the permeability is chosen as the square of the bilinear function

$$K(x,y)=(k_1xy+k_2x+k_3y+k_4)^2, \tag{5.4.37}$$

since it is easy to use this to fit $K(x,y)$ to a wide range of field permeability data. The numerical results for the seepage in a square box bounded by $0\leq x\leq 1$ and $0\leq y\leq 1$ with the boundary conditions $H=0$ along $x=0$ and $H=1000$ along $x=1$ and $\partial H/\partial n=0$ along $y=0$ and $y=1$ which are presented in equipotential lines can be found in Figure 5.3. Here, the computation is carried out by discretising the boundary over 32 equal segments and the permeabilities are chosen as $K=(1.073xy-0.684x-0.553y+1)^2$ for Figure 5.3 (a) and $K=(0.89949xy-0.45228x-y+1)^2$ for Figure 5.3 (b). Note that, similar results in Figure 5.3 (a) have been obtained by Rangogni [59] using a different method.

5.5 Boundary element method for dynamic case

In this section a class of dynamic problems are considered. Specifically we consider problems for which the displacement can be written as

$$u(x,y,t)=v(x,y)e^{-i\omega t}, \tag{5.5.1}$$

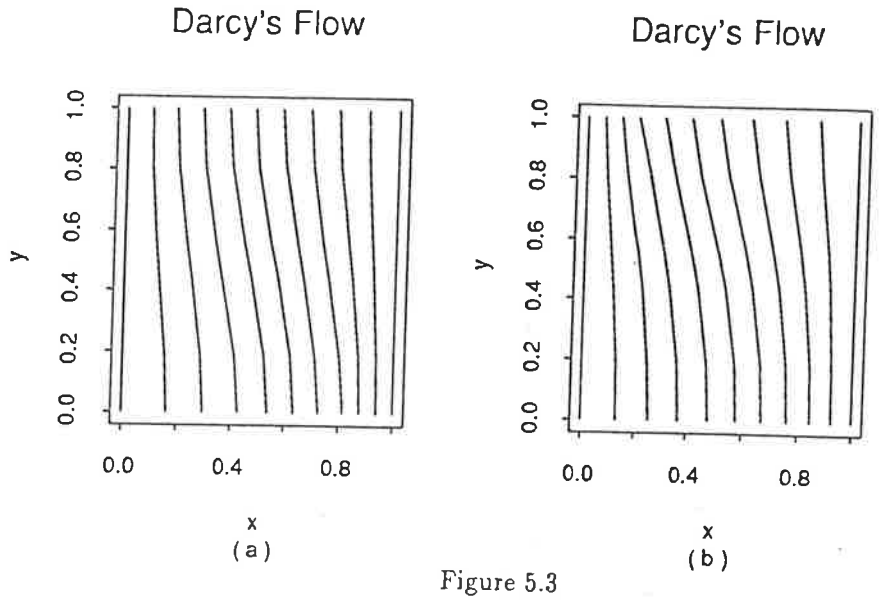

Figure 5.3
Darcy's flow

so that from (5.2.3) $v(x,y)$ must satisfy the equation

$$\frac{\partial}{\partial x}\left[\mu\frac{\partial v}{\partial x}\right]+\frac{\partial}{\partial y}\left[\mu\frac{\partial v}{\partial y}\right]+\rho\omega^2 v=0. \tag{5.5.2}$$

Furthermore, let

$$v(x,y)=\mu^{-\frac{1}{2}}U, \tag{5.5.3}$$

then equation (5.5.2) will be satisfied if

$$\nabla^2 U-\Lambda(x,y)U=0, \tag{5.5.4}$$

where

$$\Lambda(x,y)=\frac{1}{2\mu}\nabla^2\mu-\frac{1}{4\mu^2}\left[\left(\frac{\partial\mu}{\partial x}\right)^2+\left(\frac{\partial\mu}{\partial y}\right)^2\right]-\frac{\rho\omega^2}{\mu}. \tag{5.5.5}$$

Suppose

$$\rho(x,y)=k\mu(x,y), \tag{5.5.6}$$

where k is a constant and the shear modulus satisfies

$$\nabla^2\mu^{\frac{1}{2}}=0, \tag{5.5.7}$$

then equation (5.5.4) simply reduces to the Helmholtz equation

$$\nabla^2 U + k\omega^2 U = 0. \tag{5.5.8}$$

5.5.1 Boundary integral equation

The reciprocal relation corresponding to equation (5.5.2) subject to the region $\mathcal{R}$ which is bounded by the contour C is (see Appendix A, theorem 1 by replacing u with v, u' with v')

$$\int_C \mu \left[\frac{\partial v}{\partial n} v' - \frac{\partial v'}{\partial n} v \right] dS = 0, \tag{5.5.9}$$

where v' and v are the solution to equation (5.5.2). It can be verified that the fundamental solution of (5.5.8) takes the form (see for example Coleman [20])

$$U = \frac{1}{4} Y_0(\nu r), \tag{5.5.10}$$

where $\nu = \omega\sqrt{k}$, $r = [(x-a)^2 + (y-b)^2]^{\frac{1}{2}}$ with $(a,b) \in \mathcal{R}$, and Y_0 denotes the second Bessel function of order zero so that the solution for (5.5.2) with the shear modulus given by (5.5.7) can be chosen as

$$v' = \frac{1}{4} \mu^{-\frac{1}{2}} Y_0(\nu r). \tag{5.5.11}$$

To obtain the integral equation corresponding to (5.5.2), it is necessary to exclude a point (a,b) and surrounding it by a small circle Γ of radius ϵ. The equation (5.5.9) yields

$$\int_{C+\Gamma} \mu \left[\frac{\partial v}{\partial n} v' - \frac{\partial v'}{\partial n} v \right] dS = 0. \tag{5.5.12}$$

It may be verified that

$$\lim_{\epsilon \to 0} \int_\Gamma \mu \left[\frac{\partial v}{\partial n} v' - \frac{\partial v'}{\partial n} v \right] dS = \left[\mu(a,b) \right]^{\frac{1}{2}} v(a,b). \tag{5.5.13}$$

Thus the integral equation

$$\lambda v(a,b)\left[\mu(a,b)\right]^{\frac{1}{2}} = \int_C \mu\left[\frac{\partial v'}{\partial n}v - \frac{\partial v}{\partial n}v'\right] dS, \tag{5.5.14}$$

where λ is a constant with $0 < \lambda < 1$. If C has a continuously turning tangent then $\lambda = \frac{1}{2}$.

5.5.2 Numerical technique

The numerical technique here directly employs equation (5.5.14) by discretising the boundary C into N segments so that for $\mu(x,y) = (\mu_1 xy + \mu_2 x + \mu_3 y + \mu_4)^2$, where $\mu_1, \mu_2, \mu_3, \mu_4$ are constants, the equation (5.5.14) is approximated by

$$\lambda(\mu_1 ab + \mu_2 a + \mu_3 b + \mu_4)v_k(a,b) = \sum_{m=1}^{N} v_m T_{mk} - w_m S_{mk}, \tag{5.5.15}$$

where v_m denotes value of v on segment m, w_m denotes $\partial v/\partial n$ on segment m and

$$T_{mk} = \int_{C_m} \mu \frac{\partial v'}{\partial n}\, dS \qquad \text{and} \qquad S_{mk} = \int_{C_m} \mu v'\, dS. \tag{5.5.16}$$

When $m \neq k$ the integrals in (5.5.16) can be evaluated using standard numerical integration techniques (For example the Romberg integration technique). When $m = k$, the first integral in (5.5.16) may be written as

$$\begin{aligned} T_{mk} = &-\frac{1}{4}r\left\{Y_0(\nu r) + \frac{\pi}{2}\left[\mathcal{H}_0(\nu r)Y_1(\nu r) - \mathcal{H}_1(\nu r)Y_0(\nu r)\right]\right\} \\ &\{(\mu_1 y_h + \mu_2)n_1 + (\mu_1 x_h + \mu_3)n_2 + (\mu_1 y_l + \mu_2)n_1 + (\mu_1 x_l + \mu_3)n_2\} + \\ &\int_{C_k} \frac{1}{4}\left\{Y_0(\nu r) + \frac{\pi}{2}\left[\mathcal{H}_0(\nu r)Y_1(\nu r) - \mathcal{H}_1 Y_0(\nu r)\right]\right\} - \\ &\frac{1}{4}(\mu_1 xy + \mu_2 x + \mu_3 y + \mu_4)\frac{\nu}{r}Y_1(\nu r)\left\{(x-a)n_1 + (y-b)n_2\right\} dS \end{aligned} \tag{5.5.17}$$

and the second integral by

$$
\begin{aligned}
S_{mk} = &-\frac{1}{4}r\left\{Y_0(\nu r)+\frac{\pi}{2}\left[\mathcal{H}_0(\nu r)Y_1(\nu r)-\mathcal{H}_1(\nu r)Y_0(\nu r)\right]\right\} \\
&\{\mu_1(x_h y_h + x_l y_l)+\mu_2(x_h+x_l)+\mu_3(y_h+y_l)+2\mu_4\}- \\
&\int_{C_k}\frac{1}{4}\left\{Y_0(\nu r)+\frac{\pi}{2}\left[\mathcal{H}_0(\nu r)Y_1(\nu r)-\mathcal{H}_1 Y_0(\nu r)\right]\right\} \\
&\{(\mu_1 y+\mu_2)(x-a)+(\mu_1 x+\mu_3)(y-b)\}\, dS
\end{aligned}
\tag{5.5.18}
$$

where r denotes half length of segment k, (x_h, y_h) and (x_l, y_l) denote the coordinates of end points of segment k, $\mathcal{H}_0$ and $\mathcal{H}_1$ denote the Struve functions of order zero and one respectively. Both n_1 and n_2 denote the outward normal components with respect to spatial variables x and y.

The integrals in (5.5.17) and (5.5.18) can be evaluated numerically so that (5.5.15) will form a set of linear algebraic equations. Once this set of equations is solved, the values of v_m and w_m are obtained all over the boundary. The numerical evaluation for interior points are then carried out by employing equation (5.5.15) again.

5.5.3 Another shear moduli

If the shear modulus $\mu(x, y)$ takes the form

$$\mu(x, y) = \exp(\mu_1 x + \mu_2 y), \tag{5.5.19}$$

where μ_1 and μ_2 are constants and the density is given by (5.5.6), then (5.5.5) gives

$$\Lambda(x, y) = \frac{1}{4}(\mu_1^2 + \mu_2^2) - k\omega^2. \tag{5.5.20}$$

To obtain the general solution for (5.5.2) with the shear modulus given by (5.5.19), it is necessary to consider three separate cases. The first case is the case where the frequency satisfies

$$\omega^2 > \frac{\mu_1^2 + \mu_2^2}{4k}, \tag{5.5.21}$$

then the fundamental solution for (5.5.2) is

$$v' = \frac{1}{4}\exp\left[-(\mu_1 x + \mu_2 y)/2\right] Y_0(\nu r). \tag{5.5.22}$$

The second case is the case with the frequency satisfies

$$\omega^2 = \frac{\mu_1^2 + \mu_2^2}{4k}, \tag{5.5.23}$$

then the fundamental solution is

$$v' = \frac{1}{2\pi}\exp\left[-(\mu_1 x + \mu_2 y)/2\right] \log(r). \tag{5.5.24}$$

The third case is the case with the frequency satisfies

$$\omega^2 < \frac{\mu_1^2 + \mu_2^2}{4k}, \tag{5.5.25}$$

then the fundamental solution is

$$v' = -\frac{1}{2\pi}\exp\left[-(\mu_1 x + \mu_2 y)/2\right] K_0(\nu r), \tag{5.5.26}$$

where K_0 denotes the modified second Bessel function of zeroth order. The numerical solution for this kind of shear modulus can be computed directly by employing the integral equation as in (5.5.14) with the fundamental solutions v' given in (5.5.22), (5.5.24) and (5.5.26).

5.5.4 Numerical examples

Problem 5.3 : A test problem for shear modulus $\mu(x, y) = (\mu_1 xy + \mu_2 x + \mu_3 y + \mu_4)^2$.

The test problem here is considered by solving the partial differential equation

$$\frac{\partial}{\partial x}\left[(xy)^2 \frac{\partial v}{\partial x}\right] + \frac{\partial}{\partial y}\left[(xy)^2 \frac{\partial v}{\partial y}\right] + (xy)^2 v = 0, \tag{5.5.27}$$

subject to the square region $\mathcal{R}$ with $1 < x < 2$ and $1 < y < 2$. Here the non-dimensionalised shear modulus constants are taken to be $\mu_1 = 1$, $\mu_2 = \mu_3 = \mu_4 = 0$ and $\nu = 1$. By specifying $v = J_0(\nu R)/(xy)$ on all over the boundary, where J_0 denotes the first Bessel function of order zero and $R = \sqrt{x^2 + y^2}$ then discretising the boundary of each side of the square into five equal segments we obtain the numerical results at some boundary points for $\partial v/\partial n$ as in Table 5.4. The analytical results in Table 5.4 are given by

$$\frac{\partial v}{\partial n} = -\left(\frac{J_0(R)}{x^2 y} + \frac{J_1(R)}{yR}\right)n_1 - \left(\frac{J_0(R)}{xy^2} + \frac{J_1(R)}{xR}\right)n_2, \tag{5.5.28}$$

where n_1 and n_2 denote the outward normal components and J_1 denotes the first Bessel function of order one. From Table 5.4, we can see that the numerical results and the analytical results are reasonable compared.

Problem 5.4 : A test problem for shear modulus $\mu(x, y) = \exp(\mu_1 x + \mu_2 y)$

By specifying the material constants $\mu_1 = .2$, $\mu_2 = .1$ and $k = .3125$ or using the material with the non-dimensionalised shear modulus $\mu(x, y)/\mu_0 = \exp(.2x + .1y)$ and the density $\rho/\rho_0 = .3125\exp(.2x + .1y)$, the frequencies $\omega = .4$, $\omega = .2$ and $\omega = .1$ then are applied. The comparison between numerical solutions and the analytical solutions for $\partial v/\partial n$ on the boundary are in Table 5.5. Similar comparisons for v at interior points are in Table 5.6. Note that, the numerical results in Table 5.5 and Table 5.6 are obtained using the similar domain and discretisation points as in problem 5.3 and specifying v all over the boundary by

$$\begin{aligned} v &= \exp\big[-.1x - .05y\big]\, J_0(.19365\sqrt{x^2 + y^2}) \qquad \text{for} \qquad \omega = .4 \\ v &= \exp\big[-.1x - .05y\big] \qquad\qquad\qquad\qquad\quad \text{for} \qquad \omega = .2 \\ v &= \exp\big[-.1x - .05y\big]\, I_0(.09682\sqrt{x^2 + y^2}) \qquad \text{for} \qquad \omega = .1 \end{aligned} \tag{5.5.29}$$

where J_0 and I_0 denote the first Bessel function and modified Bessel function of zeroth order respectively.

Table 5.4

Comparison of analytical and numerical results

$\partial v/\partial n$ at boundary points

Boundary point	$\partial v/\partial n$(BEM)	$\partial v/\partial n$(ANAL.)
(1.30,1.00)	0.5886	0.601661
(1.70,1.00)	0.3120	0.313602
(2.00,1.30)	-0.1680	-0.170697
(2.00,1.70)	-0.0868	-0.087995
(1.70,2.00)	-0.0867	-0.087995
(1.30,2.00)	-0.1681	-0.170697
(1.00,1.70)	0.3120	0.313602
(1.00,1.30)	0.5887	0.601661

Table 5.5

Comparison of analytical and numerical results

$\partial v/\partial n$ at boundary points

	$\omega = .4$		$\omega = .2$		$\omega = .1$	
Boundary point	BEM	ANAL.	BEM	ANAL.	BEM	ANAL.
(1.30,1.00)	0.0551	0.0562	0.0409	0.0418	0.0373	0.0381
(1.70,1.00)	0.0532	0.0535	0.0399	0.0401	0.0365	0.0361
(2.00,1.30)	-0.0995	-0.1007	-0.0759	-0.0767	-0.0697	-0.0705
(2.00,1.70)	-0.0962	-0.0977	-0.0741	-0.0752	-0.0683	-0.0693
(1.70,2.00)	-0.0622	-0.0635	-0.0374	-0.0382	-0.0309	-0.0316
(1.30,2.00)	-0.0661	-0.0666	-0.0395	-0.0397	-0.0326	-0.0328
(1.00,1.70)	0.0945	0.0954	0.0822	0.0831	0.0790	0.0800
(1.00,1.30)	0.0969	0.0984	0.0835	0.0848	0.0801	0.0813

Table 5.6

Comparison of analytical and numerical results

at interior points of v

	$\omega = .4$		$\omega = .2$		$\omega = .1$	
Interior point	BEM	ANAL.	BEM	ANAL.	BEM	ANAL.
(1.30,1.30)	0.7970	0.7970	0.8228	0.8228	0.8294	0.8294
(1.50,1.50)	0.7652	0.7652	0.7985	0.7985	0.8070	0.8070
(1.70,1.70)	0.7335	0.7335	0.7749	0.7749	0.7855	0.7854

5.6 Boundary element method and perturbation technique

5.6.1 Perturbation technique

The coupling of the boundary element method and the perturbation technique is investigated here. Using the same transformation as in (5.5.1) and (5.5.3) and assuming that the density of the materials are proportional to the shear modulus as given in (5.5.6), the equation (5.2.3) is then transformed into

$$\nabla^2 U + \Lambda(x,y)U + \nu^2 U = 0, \tag{5.6.1}$$

where

$$\Lambda(x,y) = \frac{1}{4}\mu^{-2}\left[\left(\frac{\partial \mu}{\partial x}\right)^2 + \left(\frac{\partial \mu}{\partial y}\right)^2\right] - \frac{1}{2}\mu^{-1}\nabla^2\mu, \tag{5.6.2}$$

and $\nu^2 = k\omega^2$.

Instead of equation (5.6.1) here, we consider the equation

$$\nabla^2 U + \left[\epsilon\Lambda(x,y) + \nu^2\right]U = 0, \qquad 0 \le \epsilon \le 1 \tag{5.6.3}$$

or, in other words, equation (5.6.3) is thought of as a perturbation of equation (5.6.1). For $\epsilon = 0$, equation (5.6.3) simply reduces to the Helmholtz equation, while for $\epsilon = 1$, we obtain equation (5.6.1). If $\nu = 0$ then equation (5.6.3) simply reduces to the static problem.

The solution of (5.6.3) is sought in the form

$$U = \sum_{i=0}^{\infty} \epsilon^i U_i. \tag{5.6.4}$$

Using (5.6.4) in (5.6.3) and ordering the powers of epsilon yields

$$\left[\nabla^2 U_0 + \nu^2 U_0\right] + \epsilon\left[\nabla^2 U_1 + \nu^2 U_1 + \Lambda U_0\right] + \epsilon^2\left[\nabla^2 U_2 + \nu^2 U_2 + \Lambda U_1\right] + \cdots = 0. \tag{5.6.5}$$

This equation is then solved for

$$\nabla^2 U_0 + \nu^2 U_0 = 0, \tag{5.6.6}$$

which is a Helmholtz equation (or Laplace equation if $\nu = 0$), subject to the given boundary conditions. Once this equation is solved, it provides the first right hand side of the recursive form of

$$\nabla^2 U_i + \nu^2 U_i = -\Lambda(x,y) U_{i-1} \qquad i = 1, 2, \cdots \tag{5.6.7}$$

These equations then can be solved subject to specified zero boundary conditions. Here it is assumed that the boundary conditions for $U_0, U_1, \cdots$ are imposed. The given boundary conditions are used for U_0, so that the remaining boundary conditions for $U_1, U_2, \cdots$ are zero.

5.6.2 Boundary element method

The boundary element method for solving the Helmholtz equation or Laplace's equation is well established (see for example Cruse [22], Rizzo [61]). Without any difficulty, this boundary element method can be extended to solve equations of the type (5.6.7).

Without going into detail, the corresponding boundary integral equations for equation (5.6.6) and (5.6.7) are

$$\begin{aligned} &\int_C U_0 \frac{\partial G}{\partial n} - G \frac{\partial U_0}{\partial n}\, dS = \lambda U_0(a,b) \\ &\int_C U_i \frac{\partial G}{\partial n} - G \frac{\partial U_i}{\partial n}\, dS = \lambda U_i(a,b) + \int_R G \Lambda U_{i-1}\, dR \qquad i \geq 1 \end{aligned} \tag{5.6.8}$$

where λ is a constant with $0 < \lambda < 1$. If C has a continuously turning tangent then $\lambda = \frac{1}{2}$. The Green function or the fundamental solution here is given by

$$G = \begin{cases} \dfrac{1}{2\pi} \log r & \text{for} \quad \nu = 0, \\ -\dfrac{i}{4} H_0(\nu r) & \text{for} \quad \nu \neq 0, \end{cases} \tag{5.6.9}$$

with $\imath = \sqrt{-1}$, $r = \sqrt{(x-a)^2 + (y-b)^2}$ and H_0 denotes the Hankel function or the third Bessel function of zeroth order.

5.6.3 Numerical results

Problem 5.5 : A test problem (comparison with problem 5.1)

We consider the problem 5.1 again using this coupling of the boundary element and perturbation technique. Using five segments on each side of the boundary and discretising the domain $\mathcal{R}$ into 36 subdomains, and using three terms of the perturbation series, the numerical results for $\partial\phi/\partial n$ and for ϕ on the boundary are obtained as in Table 5.7 and Table 5.8. The results of the numerical computation for some u and $\partial u/\partial y$ in the interior points are in Table 5.9.

Although the comparison between Table 5.1, Table 5.2 and Table 5.7, Table 5.8 show that the coupling between the boundary element method and the perturbation technique is less accurate, it provides the solution for a more general shear modulus.

Table 5.7

Comparison of analytical and numerical results

$\partial u/\partial n$ at boundary points

Boundary point	$\partial u/\partial n$(BEM)	$\partial u/\partial n$(ANAL.)
(1.10,1.00)	-1.1820	-1.235553
(1.30,1.00)	-1.0919	-1.138967
(1.50,1.00)	-1.1035	-1.049541
(1.70,1.00)	-1.0633	-0.968742
(1.90,1.00)	-1.0399	-0.896625
(2.00,1.10)	-0.1916	-0.161157
(2.00,1.30)	-0.3317	-0.238866
(2.00,1.50)	-0.3589	-0.327002
(2.00,1.70)	-0.3524	-0.422051
(2.00,1.90)	-0.3680	-0.520840

Table 5.8

Comparison of analytical and numerical results

for u at boundary points

Boundary point	u(NUM.)	u (ANAL.)
(1.90,2.00)	2.0175	2.058152
(1.70,2.00)	2.1213	2.180798
(1.50,2.00)	2.2052	2.311383
(1.30,2.00)	2.2836	2.448556
(1.10,2.00)	2.3536	2.589795
(1.00,1.90)	2.1495	2.367646
(1.00,1.70)	1.6685	1.831923
(1.00,1.50)	1.2599	1.364246
(1.00,1.30)	0.9111	0.965710
(1.00,1.10)	0.6144	0.637463

Table 5.9

Comparison of analytical and numerical results

for u and $\partial u/\partial y$ at interior points

Interior point	u(NUM.)	u(ANAL.)	$\partial u/\partial y$ (NUM.)	$\partial u/\partial y$ (ANAL.)
(1.0833,1.4167)	1.1279	1.14992	1.9578	1.98409
(1.2500,1.4167)	1.0614	1.07388	1.7974	1.90395
(1.4167,1.4167)	1.0118	1.00352	1.7616	1.82102
(1.5833,1.4167)	0.9672	0.93912	1.7306	1.73807
(1.7500,1.4167)	0.9224	0.88047	1.6995	1.65694
(1.9167,1.4167)	0.8751	0.82726	1.7633	1.57892

5.7 Further technique for the dynamic case

In the section 5.4 we have considered the anti plane deformation for the static case including the case that the shear modulus takes the form

$$\mu(x,y) = X(x)Y(y). \tag{5.7.1}$$

Here, we extend the boundary element method for such materials to the dynamic case.

In section 5.5, we have seen that by using the simple transformation as given in (5.5.1) equation (5.2.3) becomes

$$\frac{\partial}{\partial x}\left[\mu\frac{\partial v}{\partial x}\right] + \frac{\partial}{\partial y}\left[\mu\frac{\partial v}{\partial y}\right] + \rho\omega^2 v = 0. \tag{5.7.2}$$

and by using (5.5.3) we can reduce the equation (5.2.3) into

$$\nabla^2 U - \Lambda(x,y)U = 0, \tag{5.7.3}$$

where $\Lambda(x,y)$ is given by (5.5.5). In the case that the shear modulus is given by (5.7.1), then equation (5.7.2) can be written as

$$\nabla^2 U - \left[\Lambda_1(x) + \Lambda_2(y) - \rho\omega^2(XY)^{-1}\right]U = 0, \tag{5.7.4}$$

where $\Lambda_1(x)$ and $\Lambda_2(y)$ are given by (5.4.4).

5.7.1 General solution

For the case when the density of the materials satisfies

$$\rho(x,y) = k\mu(x,y), \tag{5.7.5}$$

the general solution of (5.7.3) can be sought in term of the double series form

$$U = \sum_{n=0}^{\infty} \sum_{m=0}^{\infty} f_n(x) g_m(y) G_n^m(x, y), \tag{5.7.6}$$

with G_n^m satisfying the two dimensional Helmholtz equation

$$\nabla^2 G_n^m + \nu^2 G_n^m = 0, \qquad \nu^2 = k\omega^2. \tag{5.7.7}$$

Substituting (5.7.5) into (5.7.3) yields

$$\begin{aligned} \sum_{n=0}^{\infty} \sum_{m=0}^{\infty} \Bigg\{ & g_m(y) \left[2 \frac{df_n}{dx} \frac{\partial G_n^m}{\partial x} + G_n^m \frac{d^2 f_n}{dx^2} \right] + f_n(x) \left[2 \frac{dg_m}{dy} \frac{\partial G_n^m}{\partial y} + G_n^m \frac{d^2 g_m}{dy^2} \right] \\ & - (\Lambda_1(x) + \Lambda_2(y)) f_n(x) g_m(y) G_n^m \Bigg\} = 0. \end{aligned} \tag{5.7.8}$$

If we choose

$$\frac{\partial G_n^m}{\partial x} = G_{n-1}^m \qquad \text{for} \quad m \geq 0 \quad \text{and} \quad n \geq 1, \tag{5.7.9}$$

$$\frac{\partial G_n^m}{\partial y} = G_n^{m-1} \qquad \text{for} \quad m \geq 1 \quad \text{and} \quad n \geq 0, \tag{5.7.10}$$

then equation (5.7.7) will vanish if and only if f_n and g_m satisfy

$$\begin{aligned} 2 \frac{df_{n+1}}{dx} + \frac{d^2 f_n}{dx^2} - \Lambda_1(x) f_n = 0, \\ 2 \frac{dg_{m+1}}{dy} + \frac{d^2 g_m}{dy^2} - \Lambda_2(y) g_m = 0, \end{aligned} \tag{5.7.11}$$

for $n \geq 0$ and $m \geq 0$ with f_0 and g_0 being constants. Thus the solution of (5.7.2) may be expressed in the form

$$v = [\mu(x, y)]^{-\frac{1}{2}} \sum_{n=0}^{\infty} \sum_{m=0}^{\infty} f_n(x) g_m(y) G_n^m(x, y). \tag{5.7.12}$$

5.7.2 Boundary integral equation

It has been shown in the previous section that by choosing specific materials the series can be truncated thus convergence is assured uniformly and absolutely. Here we discuss a more specific case in which the shear modulus is given by

$$\mu(x) = (\alpha x + \beta)^{-2}. \tag{5.7.13}$$

Using (5.7.13) in (5.5.14), the integral equation can be written as

$$\lambda v(a,b)(\alpha a+\beta)^{-1}=\int_C(\alpha x+\beta)^{-2}\left[\frac{\partial v'}{\partial n}v-\frac{\partial v}{\partial n}v'\right]dS, \tag{5.7.14}$$

where

$$v'=(\alpha x+\beta)G_0-\alpha G_1, \tag{5.7.15}$$

with

$$G_0=\frac{1}{4}Y_0(\nu r),\qquad r=\left[(x-a)^2+(y-b)^2\right]^{\frac{1}{2}}, \tag{5.7.16}$$

and

$$G_1=\frac{1}{4}\int_a^x Y_0(\nu\bar{r})\,dt,\qquad \bar{r}=\left[(t-a)^2+(y-b)^2\right]^{\frac{1}{2}}. \tag{5.7.17}$$

5.7.3 Numerical results

In order to evaluate the integral equation (5.7.14), it is necessary to obtain the functions v' and $\partial v'/\partial n$ and/or the function G_0, G_1 and their normal derivatives. The evaluation of G_0 or equivalently the Bessel function and its normal derivative can be easily obtained (see Abramowitz and Stegun [2]). However it is more difficult to evaluate G_1 and $\partial G_1/\partial y$ since these functions are multi valued. By expanding the Bessel function Y_0 in (5.7.17) in an infinite series in the form

$$\begin{aligned}Y_0(\nu r)=\frac{2}{\pi}\ln(\frac{\nu}{2}r)\left\{1-a_1r^2\nu^2+a_2r^4\nu^4-a_3r^6\nu^6+a_4r^8\nu^8-a_5r^{10}\nu^{10}\right\}\\ +\frac{2}{\pi}\gamma+\frac{2}{\pi}r^2\nu^2\left\{b_1-b_2r^2\nu^2+b_3r^4\nu^4-b_4r^6\nu^6+b_5r^8\nu^8\right\},\end{aligned} \tag{5.7.18}$$

where

$$\begin{aligned}a_1&=\frac{1}{4} & b_1&=\frac{1}{4}(-\gamma+1)\\ a_2&=\frac{1}{64} & b_2&=\frac{1}{64}(-\gamma+1+\frac{1}{2})\\ a_3&=\frac{1}{2304} & b_3&=\frac{1}{2304}(-\gamma+1+\frac{1}{2}+\frac{1}{3})\\ a_4&=\frac{1}{147456} & b_4&=\frac{1}{147456}(-\gamma+1+\frac{1}{2}+\frac{1}{3}+\frac{1}{4})\\ a_5&=\frac{1}{14745600} & a_5&=\frac{1}{14745600}(-\gamma+1+\frac{1}{2}+\frac{1}{3}+\frac{1}{4}+\frac{1}{5})\end{aligned} \tag{5.7.19}$$

and $\gamma = .57721566490153$ is the Euler constant, the evaluation of the integral can be carried out and the value of the arctan function can be adjusted to make the functions single valued (Graphs Illustration of these multivalueness for G_1 and $\partial G_1/\partial y$ can be found in Appendix B). For example, if Y_0 is approximated as in (5.7.18) then

$$
\begin{aligned}
G_1 = \frac{1}{2\pi}\Big\{ & (\gamma-1)\dot{x} + \nu^2\dot{x}^3\Big(\frac{b_1}{3}+\frac{a_1}{9}\Big) + \nu^2\dot{x}\dot{y}^2\Big(b_1+\frac{2a_1}{3}\Big) - \nu^4\dot{x}^5\Big(\frac{b_2}{5}+\frac{a_2}{25}\Big) - \\
& \nu^4\dot{x}^3\dot{y}^2\Big(\frac{2b_2}{3}+\frac{7a_2}{45}\Big) - \nu^4\dot{x}\dot{y}^4\Big(b_2+\frac{8a_2}{15}\Big) + \nu^6\dot{x}^7\Big(\frac{b_3}{7}+\frac{a_3}{49}\Big) + \nu^6\dot{x}^5\dot{y}^2\Big(\frac{3b_3}{5}+ \\
& \frac{16a_3}{175}\Big) + \nu^6\dot{x}^3\dot{y}^4\Big(b_3+\frac{19a_3}{105}\Big) + \nu^6\dot{x}\dot{y}^6\Big(b_3+\frac{16a_3}{35}\Big) - \nu^8\dot{x}^9\Big(\frac{b_4}{9}+\frac{a_4}{81}\Big) - \\
& \nu^8\dot{x}^7\dot{y}^2\Big(\frac{4b_4}{7}+\frac{29a_4}{441}\Big) - \nu^8\dot{x}^5\dot{y}^4\Big(\frac{6b_4}{5}+\frac{233a_4}{1575}\Big) - \nu^8\dot{x}^3\dot{y}^6\Big(\frac{4b_4}{3}+\frac{187a_4}{945}\Big) - \\
& \nu^8\dot{x}\dot{y}^8\Big(b_4+\frac{128a_4}{315}\Big) + \overset{*}{\theta}\Big(\dot{y} - \frac{2}{3}\nu^2a_1\dot{y}^3 + \frac{8}{15}\nu^4a_2\dot{y}^5 - \frac{16}{35}\nu^6a_3\dot{y}^7 + \frac{128}{315}\nu^8a_4\dot{y}^9\Big) \\
& + \ln\Big(\frac{\nu}{2}r\Big)\Big[\dot{x}\big(1-\nu^2a_1r^2+\nu^4a_2r^4-\nu^6a_3r^6+\nu^8a_4r^8\big) + \dot{x}^3\Big(\frac{2}{3}\nu^2a_1 - \\
& \frac{4}{3}\nu^4r^2 + 2\nu^6a_3r^4 - \frac{8}{3}\nu^8a_4r^6\Big) + \dot{x}^5\Big(\frac{8}{15}\nu^4a_2 - \frac{8}{5}\nu^6a_3r^2 + \frac{48}{15}\nu^8a_4r^4\Big) \\
& + \dot{x}^7\Big(\frac{16}{35}\nu^6a_3 - \frac{192}{105}\nu^8a_4r^2\Big) + \frac{384}{945}\dot{x}^9\nu^8a_4\Big]\Big\},
\end{aligned}
\tag{5.7.20}
$$

$$
\begin{aligned}
\frac{\partial G_1}{\partial y} = \frac{1}{2\pi}\Big\{ & 2\nu^2\dot{x}\dot{y}\Big(b_1+\frac{2a_1}{3}\Big) - 2\nu^4\dot{x}^3\dot{y}\Big(\frac{2b_2}{3}+\frac{7a_2}{45}\Big) - 4\nu^4\dot{x}\dot{y}^3\Big(b_2+\frac{8a_2}{15}\Big) + \\
& 2\nu^6\dot{x}^5\dot{y}\Big(\frac{3b_3}{5}+\frac{16a_3}{175}\Big) + 4\nu^6\dot{x}^3\dot{y}^3\Big(b_3+\frac{19a_3}{105}\Big) + 6\nu^6\dot{x}\dot{y}^5\Big(b_3+\frac{16a_3}{35}\Big) - \\
& 2\nu^8\dot{x}^7\dot{y}\Big(\frac{4b_4}{7}+\frac{29a_4}{441}\Big) - 4\nu^8\dot{x}^5\dot{y}^3\Big(\frac{6b_4}{5}+\frac{233a_4}{1575}\Big) - 6\nu^8\dot{x}^3\dot{y}^5\Big(\frac{4b_4}{3}+\frac{187a_4}{945}\Big) \\
& - 8\nu^8\dot{x}\dot{y}^7\Big(b_4+\frac{128a_4}{315}\Big) - \frac{\dot{x}}{r^2}\Big(\dot{y} - \frac{2}{3}\nu^2a_1\dot{y}^3 + \frac{8}{15}\nu^4a_2\dot{y}^5 - \frac{16}{35}\nu^6a_3\dot{y}^7 \\
& + \frac{128}{315}\nu^8a_4\dot{y}^9\Big) + \overset{*}{\theta}\Big(1 - 2\nu^2a_1\dot{y}^2 + \frac{8}{3}\nu^4a_2\dot{y}^4 - \frac{16}{5}\nu^6a_3\dot{y}^6 + \frac{128}{35}\nu^8a_4\dot{y}^8\Big) \\
& + \frac{\dot{y}}{r^2}\Big(\dot{x}\big(1-\nu^2a_1r^2+\nu^4a_2r^4-\nu^6a_3r^6+\nu^8a_4r^8\big) + \dot{x}^3\Big(\frac{2}{3}\nu^2a_1 - \\
& \frac{4}{3}\nu^4a_2r^2 + 2\nu^6a_3r^4 - \frac{8}{3}\nu^8a_4r^6\Big) + \dot{x}^5\Big(\frac{8}{15}\nu^4a_2 - \frac{8}{5}\nu^6a_3r^2 + \frac{48}{15}\nu^8a_4r^4\Big) \\
& + \dot{x}^7\Big(\frac{16}{35}\nu^6a_3 - \frac{192}{105}\nu^8a_4r^2\Big) + \frac{384}{945}\nu^8a_4\dot{x}^9\Big) + \ln\Big(\frac{\nu}{2}r\Big)\Big(\dot{x}\dot{y}(-2\nu^2a_1 + \\
& 4\nu^4a_2r^2 - 6\nu^6a_3r^4 + 8\nu^8a_4r^6\big) + \dot{x}^3\dot{y}\Big(-\frac{8}{3}\nu^4a_2 + 8\nu^6a_3r^2 - 16\nu^8a_4r^4\Big)
\end{aligned}
$$

$$+\dot{x}^5\dot{y}(-\frac{16}{5}\nu^6 a_3+\frac{192}{15}\nu^8 a_4 r^2)+\dot{x}^7\dot{y}(-\frac{384}{105}\nu^8 a_4)\Big)\Big\}, \tag{5.7.21}$$

where

$$\begin{aligned}\dot{x}&=x-a,\\ \dot{y}&=y-b,\\ r&=\left[(x-a)^2+(y-b)^2\right]^{\frac{1}{2}},\\ \overset{*}{\theta}&=\arctan\left(\frac{x-a}{y-b}\right).\end{aligned} \tag{5.7.22}$$

Here $\overset{*}{\theta}$ is given by

$$\overset{*}{\theta}=\frac{\pi}{2}-\theta, \tag{5.7.23}$$

where $\theta=\arctan((y-b)/(x-a))$ obtained by the procedure as in (5.4.36). To this end, we note that ν should be sufficiently small to ensure the series in equations (5.7.18), (5.7.20) and (5.7.21) are converge.

Problem 5.6 : A test problem for dynamic case with shear modulus $\mu(x)=(\alpha x+\beta)^{-2}$

Here, we try to find the solution of the partial differential equation given by

$$\frac{\partial}{\partial x}\left[x^{-2}\frac{\partial v}{\partial x}\right]+\frac{\partial}{\partial y}\left[x^{-2}\frac{\partial v}{\partial y}\right]+x^{-2}v=0, \tag{5.7.24}$$

subject to domain $1<x<2$, $1<y<2$ and the boundary condition

$$v=(x-1)e^x\cos(\sqrt{2}y), \tag{5.7.25}$$

which is specified all over the boundary.

Using the boundary element method and discretising the boundary into twenty equal segments, the numerical results for $\partial v/\partial n$ as well as the analytical results for two sides of the boundary are given by Table 5.10 below. From their comparison we can see a good agreement between the numerical and the analytical solutions.

Table 5.10

Comparison of analytical and numerical results

$\partial v/\partial n$ at boundary points

Boundary point	$\partial v/\partial n$(BEM)	$\partial v/\partial n$(ANAL.)
(1.10,1.00)	0.6247	0.419656
(1.30,1.00)	1.5785	1.537705
(1.50,1.00)	3.1366	3.130263
(1.70,1.00)	5.2354	5.352636
(1.90,1.00)	9.4378	8.405645
(2.00,1.10)	0.1422	0.224048
(2.00,1.30)	-4.0062	-3.908752
(2.00,1.50)	-7.7295	-7.730931
(2.00,1.70)	-10.7404	-10.938748
(2.00,1.90)	-14.1359	-13.277284

CHAPTER 6

ANTI–PLANE DEFORMATIONS FOR ANISOTROPIC MATERIALS

6.1 Introduction

In the previous chapter, we have considered anti plane deformations for isotropic inhomogeneous materials. In the present chapter, the boundary element method is developed to solve the more general problem of anti plane problems for inhomogeneous anisotropic materials.

In section 6.3, the boundary element method is developed for handling a specific static case in which the elastic parameter varies in one spatial direction only. The general solution for this specific material is obtained by modifying the solution given by Clements and Rogers [19]. Numerical approximation as well as a test problem for justifying the accuracy of the procedure are discussed. For the dynamic case, the fundamental solution of a specific material is obtained through several transformations. A numerical example as a test problem can also be found in section 6.4.

6.2 Basic equations

The governing equation for the dynamic case of anti–plane deformations for the inhomogeneous materials considered in the present chapter is given by

$$\frac{\partial}{\partial x_i}\left[\mu_{ij}\frac{\partial u}{\partial x_j}\right] = \rho\frac{\partial^2 u}{\partial t^2}, \tag{6.2.1}$$

where the repeated suffix summation convention (summing from 1 to 2) is employed, t is the time coordinate, ρ is the density of the materials, and the shear modulus $\mu_{12} = \mu_{21}$ satisfies the ellipticity condition

$$\mu_{12}^2 - \mu_{11}\mu_{22} < 0. \tag{6.2.2}$$

Note that if $\partial^2 u/\partial t^2 = 0$ then (6.2.1) reduces to the equilibrium equation

$$\frac{\partial}{\partial x_i}\left[\mu_{ij}\frac{\partial u}{\partial x_j}\right] = 0. \tag{6.2.3}$$

6.3 Boundary element method for static case

In general, to obtain the analytical solution of (6.2.3) is difficult. However, for certain materials for which the shear modulus is a function of one spatial coordinate only, it is possible to obtain the solution of (6.2.3) in terms of analytic functions.

6.3.1 General analytical solution

The shear modulus is considered here to be a function of x_2 only. Following Clements and Rogers [19], let the displacement u take the form

$$u = \sum_{n=0}^{\infty} T_n(x_2)E_n(x_1 + S(x_2)), \qquad T_0 \neq 0, \tag{6.3.1}$$

and E_n satisfy the recurrence relations

$$E_n' = E_{n-1} \qquad \text{for} \quad n = 1, 2, \cdots \tag{6.3.2}$$

where the prime denotes the derivative with respect to the argument in question. Then by substitution of (6.3.1) into (6.2.3) yields

$$\sum_{n=0}^{\infty}\Big\{T_n E_n''\left[\mu_{11} + 2\mu_{12}S' + \mu_{22}S'^2\right] + E_n'\left[\mu_{22}'S'T_n + \right.$$
$$\left. 2\mu_{21}T_n' + 2\mu_{22}S'T_n' + \mu_{22}S''T_n + \mu_{21}'T_n\right] + E_n\left[\mu_{22}'T_n' + \mu_{22}T_n''\right]\Big\} = 0,$$

or in another form

$$\sum_{n=0}^{\infty}\Big\{T_nE_n''(\mu_{11}+2\mu_{12}S'+\mu_{22}S'^2)+ \\ 2E_n'(\mu_{12}+\mu_{22}S')^{\frac{1}{2}}\frac{d}{dx_2}\left[(\mu_{12}+\mu_{22}S')^{\frac{1}{2}}T_n\right]+E_n\frac{d}{dx_2}\left[\mu_{22}T_n'\right]\Big\}=0. \tag{6.3.3}$$

The first term in (6.3.3) will vanish for all n if

$$S'=\mu_{22}^{-1}\left[-\mu_{12}\pm(\mu_{12}^2-\mu_{11}\mu_{22})^{\frac{1}{2}}\right]. \tag{6.3.4}$$

The use of the second term together with the third term provides

$$T_0=C\left[\mu_{12}+\mu_{22}S'\right]^{-\frac{1}{2}}, \tag{6.3.5}$$

where C is an arbitrary constant and

$$T_n=-\frac{1}{2}\left[\mu_{12}+\mu_{22}S'\right]^{-\frac{1}{2}}\int\left[\frac{\frac{d}{dx_2}\{\mu_{22}T_{n-1}'\}}{\left[\mu_{12}+\mu_{22}S'\right]^{\frac{1}{2}}}\right]dx_2, \qquad \text{for} \quad n=1,2,\cdots \tag{6.3.6}$$

In view of (6.2.2) it follows that (6.3.4) yields a complex conjugate $\tau(x_2)$ and $\overline{\tau}(x_2)$ where $\tau(x_2)$ is obtained from (6.3.4) by taking the positive sign. The corresponding T_n obtained from (6.3.5) and (6.3.6) will be denoted by T_n and $\overline{T}_n$ respectively. Hence a real function u which satisfies (6.2.3) may be written in the form

$$u=\sum_{n=0}^{\infty}\Big[T_n(x_2)E_n(x_1+\tau(x_2))+\overline{T}_n(x_2)\overline{E}_n(x_1+\overline{\tau}(x_2))\Big], \tag{6.3.7}$$

where

$$T_n=C\imath^{n-\frac{1}{2}}h_n, \\ \overline{T}_n=C(-\imath)^{n-\frac{1}{2}}h_n, \tag{6.3.8}$$

and

$$h_0=\left[\mu_{11}\mu_{22}-\mu_{12}^2\right]^{-\frac{1}{4}}, \\ h_n=\frac{1}{2}\left[\mu_{11}\mu_{22}-\mu_{12}^2\right]^{-\frac{1}{4}}\int\left[\mu_{11}\mu_{22}-\mu_{12}^2\right]^{-\frac{1}{4}}\frac{d}{dx_2}\{\mu_{22}T_{n-1}'\}\,dx_2. \tag{6.3.9}$$

Let $z = x_1 + \tau(x_2)$ so that from (6.3.2)

$$E_n(z) = \int_0^z E_{n-1}(t)\,dt \qquad \text{for} \quad n = 1, 2, \cdots. \tag{6.3.10}$$

Hence

$$E_n(z) = \frac{1}{(n-1)!}\int_0^z (z-t)^{n-1} E_0(t)\,dt \qquad \text{for} \quad n \geq 1 \tag{6.3.11}$$

Furthermore, if we choose

$$E_n = \frac{1}{2} i^{\frac{1}{2}} \Phi_n(z), \tag{6.3.12}$$

we obtain the general solution for equation (6.2.3) as

$$\begin{aligned} u = C\Big\{ & h_0(x_2)\Re\{\Phi_0(z)\} + \\ & \sum_{n=1}^{\infty}(-1)^n \Big[h_{2n-1}(x_2)\Im\{\Phi_{2n-1}(z)\} + h_{2n}(x_2)\Re\{\Phi_{2n}(z)\} \Big] \Big\}, \end{aligned} \tag{6.3.13}$$

where $\Re$ and $\Im$ denote the real and imaginary parts of the argument of the complex function respectively.

Equation (6.3.13) provides the required solution to (6.2.3) in any domain in which the infinite series converges uniformly. The uniform converge of the series may be investigated after the manner of Bergman, but here it will be sufficient to note that for certain inhomogeneities the series (6.3.13) truncates after a finite number of terms. For this class of problems where the shear modulus μ_{ij} takes the form

$$\mu_{ij} = \lambda_{ij}(\alpha x_2 + \beta)^p, \tag{6.3.14}$$

with $\lambda_{ij}, \alpha, \beta, p$ are constants, we obtain

$$\begin{aligned} h_0 &= \Lambda(\alpha x_2 + \beta)^{-\frac{p}{2}}. \qquad \Lambda = (\lambda_{11}\lambda_{22} - \lambda_{12}^2)^{-\frac{1}{4}} \\ h_n &= \frac{(\alpha\lambda_{22})^n \Lambda^{2n+1}}{2^{3n} n!} p(p-2n) \prod_{r=1}^{n-1} \left[p^2 - (2r)^2\right](\alpha x_2 + \beta)^{-\frac{p}{2}-n}. \end{aligned} \tag{6.3.15}$$

It is clear that for certain number of p or for $p = \pm 2, \pm 4, \cdots$ the h_n vanish thus the series converges uniformly.

6.3.2 Boundary integral equation

We consider a region $\mathcal{R}$ bounded by a simple closed curved C. For a point (a, b) on C, define a small semi circle segment Γ centre at the point (a, b) with radius ϵ. Let u denotes a required solution to the boundary value problem governed by the partial differential equation (6.2.3) and u' be another solution to (6.2.3) given by (6.3.13) with

$$\Phi_0(z) = \log(z - z_0), \tag{6.3.16}$$

where $z = x_1 + \tau(x_2)$, $z_0 = a + \tau(b)$. Hence

$$\begin{aligned} u' = {} & Ch_0(x_2)\Re\{\log(z - z_0)\} + \\ & C\sum_{n=1}^{\infty}(-1)^n\Big[h_{2n-1}(x_2)\Im\{\Phi_{2n-1}(z)\} + h_{2n}(x_2)\Re\{\Phi_{2n}(z)\}\Big], \end{aligned} \tag{6.3.17}$$

where

$$\begin{aligned} \Phi_n(z) = {} & \sum_{r=0}^{n-1}\frac{(-1)^r(z - z_0)^{n-1-r}}{(r+1)!(n-1-r)!}\Big\{(z - z_0)^{r+1}\log(z - z_0) - \\ & (-z_0)^{r+1}\log(-z_0) - \frac{(z - z_0)^{r+1}}{r+1} + \frac{(-z_0)^{r+1}}{r+1}\Big\}. \end{aligned} \tag{6.3.18}$$

Here the logarithmic function in (6.3.16) should be selected in such a way so that the functions u' and its partial derivatives are all single valued throughout the entire domain. The reciprocal relation corresponding to equation (6.2.3) is (see Appendix A, theorem 2 by putting $\omega = 0$)

$$\int_{C+\Gamma}\left[\mu_{ij}\frac{\partial u}{\partial x_j}n_i u' - \mu_{ij}\frac{\partial u'}{\partial x_j}n_i u\right]dS = 0. \tag{6.3.19}$$

Now, on Γ

$$\begin{aligned} x_1 &= a + \epsilon\cos\theta, \qquad x_2 = b + \epsilon\sin\theta, \\ z_0 &= a + \tau(b), \\ z &= x_1 + \tau(x_2) \\ &= a + \epsilon\cos\theta + \tau(b + \epsilon\sin\theta) \\ &= a + \epsilon\cos\theta + \tau(b) + \epsilon\sin\theta\tau'(b) + O(\epsilon^2), \\ z - z_0 &= \epsilon\big[\cos\theta + \tau'(b)\sin\theta\big] + O(\epsilon^2). \end{aligned}$$

So that

$$u' = Ch_0(b+\epsilon\sin\theta)\Re\Big\{\log\big[\epsilon(\cos\theta+\tau'(b)\sin\theta)+O(\epsilon^2)\big]\Big\}+$$
$$C\sum_{n=1}^{\infty}(-1)^n\Big[h_{2n-1}(b+\epsilon\sin\theta)\Im\Big\{\Phi_{2n-1}\Big\}+h_{2n}(b+\epsilon\sin\theta)\Re\Big\{\Phi_{2n}\Big\}\Big], \tag{6.3.20}$$

where

$$\Phi_n = \sum_{r=0}^{n-1}\frac{(-1)^r}{(r+1)!(n-1-r)!}\big[\epsilon(\cos\theta+\tau'(b)\sin\theta)+O(\epsilon^2)\big]^{n-1-r}$$
$$\Big\{\big[\epsilon(\cos\theta+\tau'(b)\sin\theta)+O(\epsilon^2)\big]\log\big[\epsilon(\cos\theta+\tau'(b)\sin\theta)+O(\epsilon^2)\big]-$$
$$\big[-(a+\tau(b))\big]^{r+1}\log\big[-(a+\tau(b))\big]-\frac{\big[\epsilon(\cos\theta+\tau'(b)\sin\theta)+O(\epsilon^2)\big]^{r+1}}{r+1}+$$
$$\frac{\big[-(a+\tau(b))\big]^{r+1}}{r+1}\Big\} \tag{6.3.21}$$

Hence for small ϵ

$$\begin{aligned}
u' &= Ch_0(b)\Re\big\{\log\epsilon\big\}+O(1)+O(\epsilon\log\epsilon),\\
\frac{\partial u'}{\partial x_1} &= Ch_0(b)\Re\Big\{\frac{1}{\epsilon(\cos\theta+\tau'(b)\sin\theta)}\Big\}+O(1)+O(\log\epsilon),\\
\frac{\partial u'}{\partial x_2} &= Ch_0(b)\Re\Big\{\frac{\tau'}{\epsilon(\cos\theta+\tau'(b)\sin\theta)}\Big\}+O(1)+O(\log\epsilon),
\end{aligned} \tag{6.3.22}$$

Thus for small ϵ

$$\begin{aligned}
&\int_\Gamma \mu_{ij}\frac{\partial u'}{\partial x_j}um_i\,dS\\
&= C\int_\alpha^{\alpha+\pi}\Re\Big\{\frac{h_0(b)\big[\mu_{11}(b)n_1+\mu_{21}(b)n_2+(\mu_{12}(b)n_1+\mu_{22}(b)n_2)\tau'(b)\big]}{\cos\theta+\tau'(b)\sin\theta}\Big\}u(a,b)\,d\theta\\
&\quad+O(\epsilon)+O(\epsilon\log\epsilon)\\
&= -K(b)Cu(a,b)+O(\epsilon)+O(\epsilon\log\epsilon),
\end{aligned} \tag{6.3.23}$$

where

$$K(b)=\int_\alpha^{\alpha+\pi}\Re\Big\{\frac{h_0(b)\big[\mu_{11}(b)+\mu_{12}(b)\tau'(b)\big]\cos\theta}{\cos\theta+\tau'(b)\sin\theta}+\frac{h_0(b)\big[\mu_{21}(b)+\mu_{22}(b)\tau'(b)\big]\sin\theta}{\cos\theta+\tau'(b)\sin\theta}\Big\}\,d\theta \tag{6.3.24}$$

since $n_1 = -\cos\theta$ and $n_2 = -\sin\theta$ and α denotes the appropriate angle of the boundary.

Now from physical consideration the parameter $\mu_{ij}(x_2)$ are bounded in $\mathcal{R}$, so that if the derivatives $\partial u/\partial x_1$ and $\partial u/\partial x_2$ are required to be bounded in $\mathcal{R}$ then it follows that for small ϵ

$$\int_\Gamma \mu_{ij}\frac{\partial u}{\partial x_j}n_i u'\,dS = O(\epsilon\log\epsilon). \tag{6.3.25}$$

Hence

$$\lim_{\epsilon\to 0}\int_\Gamma\left[\mu_{ij}\frac{\partial u}{\partial x_j}n_i u' - \mu_{ij}\frac{\partial u'}{\partial x_j}n_i u\right]dS = CK(b)u(a,b). \tag{6.3.26}$$

Thus (6.3.19) yields

$$\int_C\left[\mu_{ij}\frac{\partial u}{\partial x_j}n_i u' - \mu_{ij}\frac{\partial u'}{\partial x_j}n_i u\right]dS = -CK(b)u(a,b). \tag{6.3.27}$$

Since $u = 1$ is the solution of (6.2.3) it should satisfy (6.3.27), so we obtain the relation

$$\int_C\left[\mu_{ij}\frac{\partial u'}{\partial x_j}n_i\right]dS = CK(b). \tag{6.3.28}$$

Using (6.3.28) in (6.3.27), we finally obtain the integral equation for equation (6.2.3) as

$$u(a,b)\int_C\left[\mu_{ij}\frac{\partial u'}{\partial x_j}n_i\right]dS = \int_C\left[\mu_{ij}\frac{\partial u'}{\partial x_j}n_i u - \mu_{ij}\frac{\partial u}{\partial x_j}n_i u'\right]dS. \tag{6.3.29}$$

6.3.3 Numerical approximations

The boundary element method employs (6.3.29) by discretising the boundary C over N segments and by assuming u and $\mu_{ij}\partial u/\partial x_j n_i$ are constants over the boundary C, (6.3.29) gives

$$\begin{aligned} u(a,b)\sum_{m=1}^{N}\int_{C_m}\left[\mu_{ij}\frac{\partial u'}{\partial x_j}n_i\right]dS = \sum_{m=1}^{N}u_m\int_{C_m}\left[\mu_{ij}\frac{\partial u'}{\partial x_j}n_i\right]dS - \\ \left[\mu_{ij}\frac{\partial u}{\partial x_j}n_i\right]_m\int_{C_m}u'\,dS. \end{aligned} \tag{6.3.30}$$

By specifying $\mu_{ij}\partial u/\partial x_j n_i$ over the boundary C, equation (6.3.30) forms a set of linear algebraic equations for u over the boundary. Similarly, if u is given over the boundary C then (6.3.30) forms a set of linear algebraic equations for $\mu_{ij}\partial u/\partial x_j n_i$. Thus we can solve this linear algebraic set to obtain $\mu_{ij}\partial u/\partial x_j n_i$ and u all over the boundary C. The mixed boundary data here can be handled in the similar manner.

In order to obtain the solution numerically, it is necessary to evaluate

$$\int_{C_m}\left[\mu_{ij}\frac{\partial u'}{\partial x_j}n_i\right]dS \qquad \text{and} \qquad \int_{C_m} u'\,dS. \tag{6.3.31}$$

By putting $C = 1$ in (6.3.17), the second integral in (6.3.31) can be easily evaluated for $m = k$ using numerical integration technique.

For a class of problem where μ_{ij} is given by (6.3.14) the evaluation of the second integral in (6.3.31) for $m = k$ is given by

$$\begin{aligned}\int_{C_k} u'\,dS = {} & r(\log r - 1)\big[h_0(x_2|_h) + h_0(x_2|_l)\big] - \int_{C_k}(x_2 - b)h_0'(\log r - 1)\,dS + \\ & \int_{C_k} h_0 \log\Big\{\cos^2\theta + \frac{\lambda_{11}}{\lambda_{22}}\sin^2\theta - \frac{2\lambda_{12}}{\lambda_{22}}\sin\theta\cos\theta\Big\}^{\frac{1}{2}}\,dS + \\ & \int_{C_k}\sum_{n=1}^{\infty}(-1)^n\Big[h_{2n-1}(x_2)\Im\big\{\Phi_{2n-1}(z)\big\} + h_{2n}(x_2)\Re\big\{\Phi_{2n}(z)\big\}\Big]\,dS,\end{aligned} \tag{6.3.32}$$

where $h_0(x_2|_h)$ and $h_0(x_2|_l)$ denote the value of h_0 at the upper end and the lower end of the segment C_k, r denotes the distance from the singular point to the end of the segment (here we assume that the singular point (a, b) is located at middle of the segment), θ denotes the angle of the segment according to Cartesian coordinates system centre at point (a, b) $(0 \le \theta < 2\pi)$ and h_0' denotes the derivative of h_0.

The evaluation of the first integral in (6.3.31) is carried out in the similar manner. For the singular point we obtain

$$\int_{C_k} \mu_{ij}\frac{\partial u'}{\partial x_j}n_i\,dS = C_2 r(\log r - 1)\Big[(\alpha x_2|_h + \beta)^p\{h_0'(x_2|_h) - \delta h_1(x_2|_h)\}+$$

$$(\alpha x_2|_l + \beta)^p\{h_0'(x_2|_l) - \delta h_1(x_2|_l)\}\Big]-$$

$$\int_{C_k} C_2(x_2 - b)(\log r - 1)\Big[\alpha p(\alpha x_2 + \beta)^{p-1}(h_0' - \delta h_1)+$$

$$(\alpha x_2 + \beta)^p(h_0'' - \delta h_1')\Big]\,dS+$$

$$\int_{C_k} C_2(\alpha x_2 + \beta)^p\Big[(h_0' - \delta h_1)\log(\cos^2\theta + \frac{\lambda_{11}}{\lambda_{22}}\sin^2\theta-$$

$$\frac{2\lambda_{12}}{\lambda_{22}}\sin\theta\cos\theta)^{\frac{1}{2}} - \gamma h_1\Im\{\Phi_0\}\Big]\,dS+$$

$$\int_{C_k} C_1(\alpha x_2 + \beta)^p\Big\{h_0\Re\{\Phi_{-1}\} - h_1\Im\{\Phi_0\} - h_2\Re\{\Phi_1\}+$$

$$\sum_{n=1}^{\infty}(-1)^{n+1}\Big[h_{2n+1}\Im\{\Phi_{2n}\} + h_{2n+2}\Re\{\Phi_{2n+1}\}\Big]\Big\}+$$

$$C_2(\alpha x_2 + \beta)^p\Big\{h_0\Re\{\tau'\Phi_{-1}\} - h_1'\Im\{\Phi_1\} - h_2'\Re\{\Phi_2\}-$$

$$h_2\Re\{\tau'\Phi_1\} + \sum_{n=1}^{\infty}(-1)^{n+1}\Big[h_{2n+1}'\Im\{\Phi_{2n+1}\} + h_{2n+2}'\Re\{\Phi_{2n+2}\}$$

$$+ h_{2n+1}\Im\{\tau'\Phi_{2n}\} + h_{2n+2}\Re\{\tau'\Phi_{2n+1}\}\Big]\Big\}\,dS, \tag{6.3.33}$$

where

$$\begin{aligned} C_1 &= \lambda_{11}n_1 + \lambda_{21}n_2,\\ C_2 &= \lambda_{12}n_1 + \lambda_{22}n_2,\\ \gamma &= \frac{-\lambda_{12}}{\lambda_{22}},\\ \delta &= \frac{(\lambda_{11}\lambda_{22} - \lambda_{12}^2)^{\frac{1}{2}}}{\lambda_{22}}\\ \tau' &= \gamma + \delta i,\\ \Phi_{-1} &= 1/(z - z_0). \end{aligned} \tag{6.3.34}$$

Once we obtain u and $\mu_{ij}\partial u/\partial x_j n_i$ all over the boundary, the evaluation of u and their derivatives in the interior domain $\mathcal{R}$ is carried out in a straight forward

way using (6.3.30).

6.3.4 Numerical example

Problem 6.1 : A test problem

To demonstrate the accuracy of the procedure, consider the following partial differential equation

$$\frac{\partial}{\partial x_1}\left[2x_2^{-2}\frac{\partial u}{\partial x_1}\right]+\frac{\partial}{\partial x_1}\left[x_2^{-2}\frac{\partial u}{\partial x_2}\right]+\frac{\partial}{\partial x_2}\left[x_2^{-2}\frac{\partial u}{\partial x_1}\right]+\frac{\partial}{\partial x_2}\left[4x_2^{-2}\frac{\partial u}{\partial x_2}\right]=0, \quad (6.3.35)$$

which is valid in the square region $1 < x_1 < 2$, $1 < x_2 < 2$ and subject to the boundary conditions

$$\begin{aligned}
\frac{\partial u}{\partial x_1}+4\frac{\partial u}{\partial x_2} &= 0 \qquad \text{on} \qquad x_2 = 1\\
u &= 8-x_2 \qquad \text{on} \qquad x_1 = 2\\
\frac{\partial u}{\partial x_1}+4\frac{\partial u}{\partial x_2} &= 0 \qquad \text{on} \qquad x_2 = 2\\
u &= 4-x_2 \qquad \text{on} \qquad x_1 = 1.
\end{aligned} \quad (6.3.36)$$

Note that equation (6.3.35) corresponds to equation (6.2.3) with the shear modulus given by (6.3.14) using the non dimensionalised shear modulus constants $\lambda_{11} = 2$, $\lambda_{12} = \lambda_{21} = 1$, $\lambda_{22} = 4$, $\alpha = 1$, $\beta = 0$, $p = -2$. The integral equation for this problem is

$$u(a,b)\int_C\left[\lambda_{ij}x_2^{-2}\frac{\partial u'}{\partial x_j}n_i\right]dS=\int_C\left[\lambda_{ij}x_2^{-2}\frac{\partial u'}{\partial x_j}n_iu-\lambda_{ij}x_2^{-2}\frac{\partial u}{\partial x_j}n_iu'\right]dS. \quad (6.3.37)$$

where

$$u' = 7^{-\frac{1}{4}} x_2 \Re\Big\{\log(z - z_0)\Big\} - 4.7^{-\frac{3}{4}} \Im\Big\{(z - z_0)\log(z - z_0) + z_0 \log(-z_0) - z\Big\},$$

$$\lambda_{ij} x_2^{-2} \frac{\partial u'}{\partial x_j} n_i = (2n_1 + n_2) x_2^{-2} \left[7^{-\frac{1}{4}} x_2 \Re\left\{\frac{1}{z - z_0}\right\} - 4.7^{-\frac{3}{4}} \Im\Big\{\log(z - z_0)\Big\}\right] +$$
$$(n_1 + 4n_2) x_2^{-2} \left[7^{-\frac{1}{4}} \Re\Big\{\log(z - z_0) + 7^{-\frac{1}{4}} x_2 \Re\left\{\frac{-\frac{1}{4} + 7^{\frac{1}{2}} i}{z - z_0}\right\} -$$
$$4.7^{-\frac{3}{4}} \Im\Big\{(-\frac{1}{4} + 7^{\frac{1}{2}}) i \log(z - z_0)\Big\}\right]. \tag{6.3.38}$$

Here the logarithmic function in (6.3.38) might be evaluated by writing the logarithmic function in the form

$$\log(z - z_0) = \log \overset{*}{r} + i\overset{*}{\theta}, \tag{6.3.39}$$

where

$$\overset{*}{r} = \left[(x_1 - a)^2 - \frac{2\lambda_{12}}{\lambda_{22}}(x_1 - a)(x_2 - b) + \frac{\lambda_{11}}{\lambda_{22}}(x_2 - b)^2\right]^{\frac{1}{2}}. \tag{6.3.40}$$

The imaginary part of the complex logarithmic function in (6.3.39) $\overset{*}{\theta}$ is determined by procedure

Step1. Determine $\overline{\theta} = \arctan\left(\dfrac{(x_2 - b)\sqrt{\lambda_{11}\lambda_{22} - \lambda_{12}^2}/\lambda_{22}}{(x_1 - a) - (x_2 - b)\lambda_{12}/\lambda_{22}}\right)$ so that $0 \le \overline{\theta} < 2\pi$.

Step2. If $n_1 > 0$ then $\overset{*}{\theta} = \overline{\theta}$.

If $n_1 = 0$ and $n_2 > 0$ then $\overset{*}{\theta} = \overline{\theta}$;

In the case $\overset{*}{\theta} = 0$, it should be replaced by $\overset{*}{\theta} = 2\pi$.

If $n_1 = 0$ and $n_2 < 0$ then $\overset{*}{\theta} = \overline{\theta}$.

If $n_1 < 0$ and $n_2 \ge 0$ then $\overset{*}{\theta} = \overline{\theta}$;

In the case $\overset{*}{\theta} > \pi$, it should be replaced by $\overset{*}{\theta} = \overline{\theta} - 2\pi$.

If $n_1 < 0$ and $n_2 < 0$ then $\overset{*}{\theta} = \overline{\theta}$;

In the case $\overset{*}{\theta} > \dfrac{3}{2}\pi$, it should be replaced by $\overset{*}{\theta} = \overline{\theta} - 2\pi$,

(6.3.41)

where n_1 and n_2 denote the outward normal components at point (a, b). By discretising the boundary into five segments on each side of the square, we obtain the numerical results for u and $\mu_{ij}\partial u/\partial x_j n_i$ on the boundary as in Tables 6.1 and 6.2 respectively. The analytical results for the comparison in Tables 6.1 and 6.2 are obtained by $u = 4x_1 - x_2$ and $\mu_{ij}\partial u/\partial x_j n_i = 7x_2^{-2}n_1$. For the interior points, a similar modification as in section 5.4.3 is carried out. Numerical evaluation for u, $\partial u/\partial x_1$, and $\partial u/\partial x_2$ at some interior points can be found in Table 6.3.

Table 6.1

Comparison of analytical and numerical results

u on boundary

Boundary point	u(BEM)	u(ANAL.)
(1.10,1.00)	3.3779	3.4000
(1.30,1.00)	4.1999	4.2000
(1.50,1.00)	5.0159	5.0000
(1.70,1.00)	5.8308	5.8000
(1.90,1.00)	6.6386	6.6000
(1.90,2.00)	5.5889	5.6000
(1.70,2.00)	4.7772	4.8000
(1.50,2.00)	3.9740	4.0000
(1.30,2.00)	3.1718	3.2000
(1.10,2.00)	2.3651	2.4000

Table 6.2

Comparison of analytical and numerical results

$\mu_{ij}\partial u/\partial x_j n_i$ at boundary points

	$\mu_{ij}\partial u/\partial x_j n_i$	
Boundary point	BEM	Analytic
(2.00,1.10)	5.9847	5.7851
(2.00,1.30)	4.5407	4.1420
(2.00,1.50)	3.0610	3.1111
(2.00,1.70)	2.2477	2.4221
(2.00,1.90)	2.0881	1.9391
(1.00,1.90)	-2.1128	-1.9391
(1.00,1.70)	-2.2820	-2.4221
(1.00,1.50)	-3.0683	-3.1111
(1.00,1.30)	-3.9528	-4.1420
(1.00,1.10)	-6.4996	-5.7851

Table 6.3

Comparison of analytical and numerical results

u, $\partial u/\partial x_1$, $\partial u/\partial x_2$ at some interior points

	BEM			Analytical		
Interior point	u	$\partial u/\partial x_1$	$\partial u/\partial x_2$	u	$\partial u/\partial x_1$	$\partial u/\partial x_2$
(1.30,1.30)	3.8899	4.0047	-0.9918	3.9000	4.0000	-1.0000
(1.50,1.50)	4.4956	4.0176	-1.0059	4.5000	4.0000	-1.0000
(1.80,1.80)	5.4084	4.0113	-0.9495	5.4000	4.0000	-1.0000

6.4 Boundary element method for dynamic case

6.4.1 General analytical solution

In this section, we consider equation (6.2.1) for a specific material in which the shear modulus takes the form

$$\mu_{ij} = \lambda_{ij}(\alpha_1 x_1 + \alpha_2 x_2 + \alpha_3)^2, \tag{6.4.1}$$

and the density

$$\rho = \rho_0(\alpha_1 x_1 + \alpha_2 x_2 + \alpha_3)^2, \tag{6.4.2}$$

where $\lambda_{ij} = \lambda_{ji}$, $\alpha_1, \alpha_2, \alpha_3$ and ρ_1 are constants.

By assuming that the displacement can be written in the form

$$u = v(x_1, x_2)e^{i\omega t}, \tag{6.4.3}$$

then (6.2.1) becomes

$$\frac{\partial}{\partial x_i}\left[\lambda_{ij}(\alpha_1 x_1 + \alpha_2 x_2 + \alpha_3)^2 \frac{\partial v}{\partial x_j}\right] + \rho_0\omega^2(\alpha_1 x_1 + \alpha_2 x_2 + \alpha_3)^2 v = 0. \tag{6.4.4}$$

Let

$$v = (\alpha_1 x_1 + \alpha_2 x_2 + \alpha_3)^{-1}\psi(x_1, x_2), \tag{6.4.5}$$

then (6.4.4) becomes

$$\lambda_{ij}\frac{\partial^2 \psi}{\partial x_i \partial x_j} + \nu^2\psi = 0, \tag{6.4.6}$$

where $\nu^2 = \rho_0\omega^2$. Let τ be a complex number with positive imaginary part and $\overline{\tau}$ is it conjugate pair of quadratic equation

$$\lambda_{11} + 2\lambda_{12}\tau + \lambda_{22}\tau^2 = 0, \tag{6.4.7}$$

and

$$\begin{aligned} z &= x_1 + \tau x_2 \\ \overline{z} &= x_1 + \overline{\tau} x_2 \end{aligned} \tag{6.4.8}$$

where $\overline{z}$ denotes the conjugate pair of z, then (6.4.6) is ready to be transformed into

$$2\left[\lambda_{11}+\lambda_{12}(\tau+\overline{\tau})+\lambda_{22}\tau\overline{\tau})\right]\frac{\partial^2\psi}{\partial z\partial\overline{z}}+\nu^2\psi=0. \tag{6.4.9}$$

Furthermore, if we transform (6.4.9) into a new independent variables

$$\begin{aligned}\overline{x}_1 &= \frac{1}{2}z+\frac{1}{2}\overline{z},\\ \overline{x}_2 &= \frac{1}{2i}z-\frac{1}{2i}\overline{z},\end{aligned} \tag{6.4.10}$$

then (6.4.9) becomes

$$\frac{\partial^2\psi}{\partial\overline{x}_1{}^2}+\frac{\partial^2\psi}{\partial\overline{x}_2{}^2}+\overline{\nu}^2\psi=0, \tag{6.4.11}$$

which is the Helmholtz equation with

$$\overline{\nu}^2=\frac{\rho_0\lambda_{22}\omega^2}{\lambda_{11}\lambda_{22}-\lambda_{12}^2}. \tag{6.4.12}$$

The solution of (6.4.11) is the well known as the Hankel function. Let (a,b) is the source of vibration then the solution of (6.4.6) will be

$$\psi=cH_0(\overline{\nu}\,\overline{r}), \tag{6.4.13}$$

where c is a constant and

$$\overline{r}=\left[(x_1-a)^2+\frac{\lambda_{11}}{\lambda_{22}}(x_2-b)^2-2\frac{\lambda_{12}}{\lambda_{22}}(x_1-a)(x_2-b)\right]^{\frac{1}{2}}. \tag{6.4.14}$$

Thus the general solution of (6.4.4) can be written as

$$v=c(a_1x_1+a_2x_2+a_3)^{-1}H_0(\overline{\nu}\,\overline{r}). \tag{6.4.15}$$

6.4.2 Integral equation

To derive the integral equation, it is necessary to exclude a point (a,b) in $\mathcal{R}$ and surrounding it with a small circle Γ of radius ϵ. Using the reciprocal relation theorem as in appendix A (theorem 2) yields

$$\int_{C+\Gamma}\left[\mu_{ij}\frac{\partial v}{\partial x_j}v'n_i-\mu_{ij}\frac{\partial v'}{\partial x_j}vn_i\right]dS=0. \tag{6.4.16}$$

If we choose v' as given by (6.4.15) with $c = -\imath/4$ then on Γ

$$\begin{aligned} x_1 &= a + \epsilon\cos\theta, \\ x_2 &= b + \epsilon\sin\theta, \end{aligned} \tag{6.4.17}$$

$$v' = -\frac{\imath}{4}\big[\alpha_1(a+\epsilon\cos\theta) + \alpha_2(b+\epsilon\sin\theta) + \alpha_3\big]^{-1} H_0(\overline{\nu}\,\overline{r}), \tag{6.4.18}$$

$$\begin{aligned} \frac{\partial v'}{\partial x_1} = {} & \frac{\imath\overline{\nu}}{4}\big[\alpha_1(a+\epsilon\cos\theta) + \alpha_2(b+\epsilon\sin\theta) + \alpha_3\big]^{-1} H_1(\overline{\nu}\,\overline{r}) \\ & \frac{\cos\theta - \frac{\lambda_{12}}{\lambda_{22}}\sin\theta}{\big[\cos^2\theta + \frac{\lambda_{11}}{\lambda_{22}}\sin^2\theta - \frac{2\lambda_{11}}{\lambda_{22}}\cos\theta\sin\theta\big]^{\frac{1}{2}}} + \\ & \frac{\alpha_1\imath}{4}\big[\alpha_1(a+\epsilon\cos\theta) + \alpha_2(b+\epsilon\sin\theta) + \alpha_3\big]^{-2} H_0(\overline{\nu}\,\overline{r}), \\ \frac{\partial v'}{\partial x_2} = {} & \frac{\imath\overline{\nu}}{4}\big[\alpha_1(a+\epsilon\cos\theta) + \alpha_2(b+\epsilon\sin\theta) + \alpha_3\big]^{-1} H_1(\overline{\nu}\,\overline{r}) \\ & \frac{\frac{\lambda_{11}}{\lambda_{22}}\sin\theta - \frac{\lambda_{12}}{\lambda_{22}}\cos\theta}{\big[\cos^2\theta + \frac{\lambda_{11}}{\lambda_{22}}\sin^2\theta - \frac{2\lambda_{11}}{\lambda_{22}}\cos\theta\sin\theta\big]^{\frac{1}{2}}} + \\ & \frac{\alpha_2\imath}{4}\big[\alpha_1(a+\epsilon\cos\theta) + \alpha_2(b+\epsilon\sin\theta) + \alpha_3\big]^{-2} H_0(\overline{\nu}\,\overline{r}), \end{aligned} \tag{6.4.19}$$

where

$$\overline{r} = \epsilon\big[\cos^2\theta + \frac{\lambda_{11}}{\lambda_{22}}\sin^2\theta - \frac{2\lambda_{11}}{\lambda_{22}}\cos\theta\sin\theta\big]^{\frac{1}{2}}. \tag{6.4.20}$$

Since for fixed $\overline{\nu}$, and $\overline{r} \to 0$

$$\begin{aligned} -\frac{\imath}{4}H_0(\overline{\nu}\,\overline{r}) &\sim \frac{1}{2\pi}\log(\overline{\nu}\,\overline{r}), \\ \frac{\imath}{4}H_1(\overline{\nu}\,\overline{r}) &\sim \frac{1}{\overline{\nu}\,\overline{r}}. \end{aligned} \tag{6.4.21}$$

It follows for $\epsilon \to 0$

$$\int_\Gamma \mu_{ij}\frac{\partial v}{\partial x_j}v' n_i\, dS = O(\epsilon\log\epsilon), \tag{6.4.22}$$

$$\int_\Gamma \mu_{ij}\frac{\partial v'}{\partial x_j}v n_i\, dS = -K(a,b)v(a,b) + O(\epsilon\log\epsilon), \tag{6.4.23}$$

where

$$K(a,b) = \frac{1}{2\pi}(\alpha_1 a + \alpha_2 b + \alpha_3)\int_{\theta_1}^{\theta_2} \frac{\lambda_{11}\lambda_{22} - \lambda_{12}^2}{\lambda_{22}\cos^2\theta - 2\lambda_{12}\sin\theta\cos\theta + \lambda_{11}\sin^2\theta}\, d\theta. \tag{6.4.24}$$

Thus (6.4.16) gives

$$\int_C \left[\mu_{ij} \frac{\partial v}{\partial x_j} v' n_i - \mu_{ij} \frac{\partial v'}{\partial x_j} v n_i \right] dS + K(a,b)v(a,b) = 0, \tag{6.4.25}$$

or

$$K(a,b)v(a,b) = \int_C \left[\mu_{ij} \frac{\partial v'}{\partial x_j} v n_i - \mu_{ij} \frac{\partial v}{\partial x_j} v' n_i \right] dS. \tag{6.4.26}$$

Note that $K(a,b)$ in (6.2.24) depends on the position in the given domain, the angles θ_1 and θ_2 as well as the shear modulus of the material.

6.4.3 Numerical example

Problem 6.2 : A test problem

The accuracy of the numerical procedure is tested by considering the partial differential equation given by (6.4.4) and specifying $\lambda_{11} = 1, \lambda_{12} = \lambda_{21} = 1, \lambda_{22} = 3, \alpha_1 = 0, \alpha_2 = 1, \alpha_3 = 0, \rho_0 = \frac{2}{3}, \omega = 1$, or

$$\begin{aligned} \frac{\partial}{\partial x_1}\left[x_2^2 \frac{\partial v}{\partial x_1} \right] + \frac{\partial}{\partial x_1}\left[x_2^2 \frac{\partial v}{\partial x_2} \right] + \frac{\partial}{\partial x_2}\left[x_2^2 \frac{\partial v}{\partial x_1} \right] + \\ \frac{\partial}{\partial x_2}\left[3x_2^2 \frac{\partial v}{\partial x_2} \right] + \frac{2}{3} x_2^2 v = 0, \end{aligned} \tag{6.4.27}$$

which is valid in the square region $1 < x_1 < 2, 1 < x_2 < 2$, and subject to the source of the vibration at point $(3.5, 5)$ and the boundary condition

$$v = x_2^{-1} H_0(r), \tag{6.4.28}$$

which is specified all over the boundary. Here H_0 denotes the Hankel function of order zero and

$$r = \left[(x_1 - 3.5)^2 + \frac{1}{3}(x_2 - 5)^2 - \frac{2}{3}(x_1 - 3.5)(x_2 - 5) \right]^{\frac{1}{2}}. \tag{6.4.29}$$

The numerical procedure is used to calculate

$$\mu_{ij} \frac{\partial v}{\partial x_j} n_i = x_2^2 \frac{\partial v}{\partial x_1}(n_1 + n_2) + x_2^2 \frac{\partial v}{\partial x_2}(n_1 + 3n_2), \tag{6.4.30}$$

and without any difficulty we obtain the analytical solution as

$$\mu_{ij}\frac{\partial v}{\partial x_j}n_i = -(n_1+3n_2)H_0(r) - x_2 H_1(r)\Big[(n_1+n_2)\frac{(x_1-3.5)-\frac{1}{3}(x_2-5)}{r} + (n_1+3n_2)\frac{(x_2-5)-(x_1-3.5)}{3r}\Big]. \tag{6.4.31}$$

Using boundary element method and specify ten segments on each side of the square boundary, the numerical evaluation of $\mu_{ij}\partial v/\partial x_j n_i$ as well as the analytical solution for some boundary points can be found in Table 6.4, while the evaluation of v and $\partial v/\partial x_1, \partial v/\partial x_2$ for some interior points are in Table 6.5 and Table 6.6 respectively.

6.4.4 Two inhomogeneous anisotropic materials

Consider the case when the material is made up of two kinds of inhomogeneous anisotropic materials with an interface boundary (see illustration in Chapter 7, Figure 7.1) and the function v satisfies the differential equation

$$\frac{\partial}{\partial x_i}\left[\lambda_{ij}^{(\Omega)}(\alpha_1^{(\Omega)}x_1+\alpha_2^{(\Omega)}x_2+\alpha_3^{(\Omega)})^2\frac{\partial v^{(\Omega)}}{\partial x_j}\right]+\rho_0^{(\Omega)}\omega^2(\alpha_1^{(\Omega)}x_1+\alpha_2^{(\Omega)}x_2+\alpha_3^{(\Omega)})^2 v^{(\Omega)}=0, \tag{6.4.32}$$

where the superscript $(\Omega)=(1)$ denotes the governing differential equation in the first material and $(\Omega)=(2)$ denotes the governing differential equation in the second material. In this case the integral equation may be written as

$$K^{(\Omega)}(a,b)v^{(\Omega)}(a,b) = \int_C\Big[\lambda_{ij}^{(\Omega)}(\alpha_1^{(\Omega)}x_1+\alpha_2^{(\Omega)}x_2+\alpha_3^{(\Omega)})^2\frac{\partial v'^{(\Omega)}}{\partial x_j}v^{(\Omega)}n_i - \lambda_{ij}^{(\Omega)}(\alpha_1^{(\Omega)}x_1+\alpha_2^{(\Omega)}x_2+\alpha_3^{(\Omega)})^2\frac{\partial v^{(\Omega)}}{\partial x_j}v'^{(\Omega)}n_i\Big]\,dS, \tag{6.4.33}$$

Table 6.4

Comparison of analytical and numerical results

$\mu_{ij}\partial v/\partial x_j n_i$ on some boundary points

	BEM		Analytical	
Boundary point	Real	Imaginary	Real	Imaginary
(1.15,1.00)	-0.2678	1.6336	-0.27340	1.59602
(1.45,1.00)	-0.1115	1.6862	-0.11894	1.66510
(1.75,1.00)	0.0279	1.7616	-0.00995	1.70706
(2.00,1.25)	0.0276	-0.7142	0.05844	-0.63687
(2.00,1.55)	0.0964	-0.7815	0.11711	-0.72766
(2.00,1.75)	0.1262	-0.8747	0.16437	-0.80786
(1.65,2.00)	0.1961	-2.0635	0.11197	-2.07692
(1.55,2.00)	0.2450	-2.0015	0.16942	-2.02237
(1.35,2.00)	0.3726	-1.8435	0.29651	-1.90797
(1.00,1.55)	-0.5557	0.5170	-0.53394	0.57308
(1.00,1.35)	-0.4656	0.5010	-0.44989	0.54807
(1.00,1.15)	-0.3841	0.4632	-0.37080	0.52632

Table 6.5

Comparison of analytical and numerical results

v at some interior points

	BEM		Analytical	
Interior point	Real	Imaginary	Real	Imaginary
(1.30,1.30)	0.1723	0.3862	0.1748	0.3921
(1.50,1.50)	0.2049	0.3204	0.2079	0.3250
(1.80,1.80)	0.2377	0.2366	0.2416	0.2403

Table 6.6

Comparison of analytical and numerical results

$\partial v/\partial x_1$ and $\partial v/\partial x_2$ at some interior points

	BEM				Analytical			
	$\partial v/\partial x_1$		$\partial v/\partial x_2$		$\partial v/\partial x_1$		$\partial v/\partial x_2$	
Point	Real	Imag	Real	Imag	Real	Imag	Real	Imag
(1.3,1.3)	0.2110	-0.0374	-0.0298	-0.3161	0.2152	-0.0411	-0.0232	-0.3229
(1.5,1.5)	0.1705	-0.0579	-0.0393	-0.2455	0.1749	-0.0585	-0.0337	-0.2518
(1.8,1.8)	0.1203	-0.0727	-0.0423	-0.1814	0.1232	-0.0698	-0.0369	-0.1886

for $\Omega = 1, 2$, where

$$
\begin{aligned}
v'^{(\Omega)} &= -\frac{i}{4}\left(\alpha_1^{(\Omega)}x_1 + \alpha_2^{(\Omega)}x_2 + \alpha_3^{(\Omega)}\right)^{-1} H_0\left(\overline{\nu}^{(\Omega)}\overline{r}^{(\Omega)}\right), \\
\overline{\nu}^{2(\Omega)} &= \frac{\rho_0^{(\Omega)}\omega^2\lambda_{22}^{(\Omega)}}{\lambda_{11}^{(\Omega)}\lambda_{22}^{(\Omega)} - \lambda_{12}^{2\ (\Omega)}}, \\
\overline{r}^{(\Omega)} &= \left[(x_1 - a)^2 + \frac{\lambda_{11}^{(\Omega)}}{\lambda_{22}^{(\Omega)}}(x_2 - b)^2 - 2\frac{\lambda_{12}^{(\Omega)}}{\lambda_{22}^{(\Omega)}}(x_1 - a)(x_2 - b)\right]^{\frac{1}{2}}.
\end{aligned}
\tag{6.4.34}
$$

The function $K^{(\Omega)}(a, b)$ in (6.4.33) may be evaluated with by the help of a solution of (6.4.32)

$$
w^{(\Omega)} = -\frac{i}{4}\left(\alpha_1^{(\Omega)}x_1 + \alpha_2^{(\Omega)}x_2 + \alpha_3^{(\Omega)}\right)^{-1} H_0\left(\overline{\nu}^{(\Omega)}\overline{s}^{(\Omega)}\right), \tag{6.4.35}
$$

where

$$
\overline{s}^{(\Omega)} = \left[x_1^2 + \frac{\lambda_{11}^{(\Omega)}}{\lambda_{22}^{(\Omega)}}x_2^2 - 2\frac{\lambda_{12}^{(\Omega)}}{\lambda_{22}^{(\Omega)}}x_1x_2\right]^{\frac{1}{2}}. \tag{6.4.36}
$$

Since (6.4.35) satisfies (6.4.32), it should also satisfy the integral equation (6.4.33) thus we obtain

$$
\begin{aligned}
K^{(\Omega)}(a, b) = \left[w^{(\Omega)}(a, b)\right]^{-1} \int_C \Bigg[& \lambda_{ij}^{(\Omega)}\left(\alpha_1^{(\Omega)}x_1 + \alpha_2^{(\Omega)}x_2 + \alpha_3^{(\Omega)}\right)^2 \frac{\partial v'^{(\Omega)}}{\partial x_j} w^{(\Omega)} n_i - \\
& \lambda_{ij}^{(\Omega)}\left(\alpha_1^{(\Omega)}x_1 + \alpha_2^{(\Omega)}x_2 + \alpha_3^{(\Omega)}\right)^2 \frac{\partial w^{(\Omega)}}{\partial x_j} v'^{(\Omega)} n_i \Bigg] dS.
\end{aligned}
\tag{6.4.37}
$$

By applying the continuity equations

$$
\begin{aligned}
v^{(1)} &= v^{(2)}, \\
\lambda_{ij}^{(1)}\left(\alpha_1^{(1)}x_1 + \alpha_2^{(1)}x_2 + \alpha_3^{(1)}\right)^2 \frac{\partial v^{(1)}}{\partial x_j} n_i &= \lambda_{ij}^{(2)}\left(\alpha_1^{(2)}x_1 + \alpha_2^{(2)}x_2 + \alpha_3^{(2)}\right)^2 \frac{\partial v^{(2)}}{\partial x_j} n_i,
\end{aligned}
\tag{6.4.38}
$$

across the interface boundary, and using the boundary element procedure, we obtain a set of linear algebra equation. Once $v^{(\Omega)}$ and/or $\lambda_{ij}^{(\Omega)}\left(\alpha_1^{(\Omega)}x_1 + \alpha_2^{(\Omega)}x_2 + \alpha_3^{(\Omega)}\right)^2 \frac{\partial v^{(\Omega)}}{\partial x_j} n_i$ are specified on the boundary we obtain $v^{(\Omega)}$ and $\lambda_{ij}^{(\Omega)}\left(\alpha_1^{(\Omega)}x_1 + \alpha_2^{(\Omega)}x_2 + \alpha_3^{(\Omega)}\right)^2 \frac{\partial v^{(\Omega)}}{\partial x_j} n_i$ in the whole domain through equation (6.4.33).

6.4.5 Numerical example

Problem 6.3 : A test problem

The accuracy of the procedure is tested by considering the partial differential equation given by (6.4.32) and specifying $\lambda_{11}^{(1)} = \lambda_{11}^{(2)} = 1$, $\lambda_{12}^{(1)} = \lambda_{12}^{(2)} = 1$, $\lambda_{22}^{(1)} = \lambda_{22}^{(2)} = 3$, $\alpha_1^{(1)} = \alpha_1^{(2)} = 0$, $\alpha_2^{(1)} = \alpha_2^{(2)} = 1$, $\alpha_3^{(1)} = \alpha_3^{(2)} = 0$, $\rho_0^{(1)} = \rho_0^{(2)} = \frac{2}{3}$, $\omega = 1$ or

$$\begin{aligned} &\frac{\partial}{\partial x_1}\left[x_2^2 \frac{\partial v^{(\Omega)}}{\partial x_1}\right] + \frac{\partial}{\partial x_1}\left[x_2^2 \frac{\partial v^{(\Omega)}}{\partial x_2}\right] + \frac{\partial}{\partial x_2}\left[x_2^2 \frac{\partial v^{(\Omega)}}{\partial x_1}\right] + \\ &\frac{\partial}{\partial x_2}\left[3x_2^2 \frac{\partial v^{(\Omega)}}{\partial x_2}\right] + \frac{2}{3}x_2^2 v^{(\Omega)} = 0, \qquad \Omega = 1, 2 \end{aligned} \tag{6.4.39}$$

subject to triangle region with vertices $(1,1)$, $(2,1)$, $(2,2)$ for the first material and $(1,1)$, $(1,2)$, $(2,2)$ for the second material. By specifying the source of the vibration at point $(3.5, 5)$ and the boundary condition as in (6.4.28) on all over the boundary, we obtain the numerical results as in Tables 6.7, 6.8 and 6.9. Here, we discretise the boundary with 10 segments on each side of the square and 30 segments on the interface boundary. From the tables we can see that the numerical results are in reasonable accuracy.

Table 6.7

Comparison of analytical and numerical results

$\lambda_{ij}(a_1x_1 + a_2x_2 + a_3)^2 \partial v/\partial x_j n_i$ on some boundary points

	BEM		Analytical	
Boundary point	Real	Imaginary	Real	Imaginary
(1.15,1.00)	-0.2735	1.5874	-0.27340	1.59602
(1.25,1.00)	-0.2192	1.6192	-0.21767	1.62241
(1.35,1.00)	-0.1692	1.6427	-0.16600	1.64536
(2.00,1.35)	0.0801	-0.6604	0.07632	-0.66346
(2.00,1.45)	0.0988	-0.6902	0.09589	-0.69365
(2.00,1.55)	0.1194	-0.7236	0.11711	-0.72766
(1.75,2.00)	0.0687	-2.1262	0.05937	-2.12937
(1.65,2.00)	0.1207	-2.0717	0.11197	-2.07692
(1.55,2.00)	0.1769	-2.0152	0.16942	-2.02237
(1.00,1.65)	-0.5756	0.5767	-0.57754	0.58638
(1.00,1.55)	-0.5325	0.5653	-0.53394	0.57308
(1.00,1.45)	-0.4898	0.5534	-0.49135	0.56025

Table 6.8

Comparison of analytical and numerical results

v at some interior points

	BEM		Analytical	
Interior point	Real	Imaginary	Real	Imaginary
(1.50,1.30)	0.2143	0.3828	0.2144	0.3828
(1.30,1.50)	0.1697	0.3360	0.1698	0.3359
(1.80,1.50)	0.2522	0.3077	0.2522	0.3075
(1.70,1.20)	0.2495	0.4096	0.2498	0.4095
(1.20,1.80)	0.1409	0.2802	0.1409	0.2801

Table 6.9

Comparison of analytical and numerical results

$\partial v/\partial x_1$ and $\partial v/\partial x_2$ at some interior points

	BEM				Analytical			
	$\partial v/\partial x_1$		$\partial v/\partial x_2$		$\partial v/\partial x_1$		$\partial v/\partial x_2$	
Point	Real	Imag	Real	Imag	Real	Imag	Real	Imag
(1.5,1.3)	0.1764	-0.0542	-0.0376	-0.3274	0.1798	-0.0499	-0.0320	-0.3314
(1.3,1.5)	0.2012	-0.0437	-0.0309	-0.2410	0.2051	-0.0486	-0.0272	-0.2443
(1.8,1.5)	0.1207	-0.0567	-0.0424	-0.2635	0.1188	-0.0541	-0.0345	-0.2659
(1.7,1.2)	0.1395	-0.0455	-0.0444	-0.3957	0.1383	-0.0434	-0.0353	-0.3955
(1.2,1.8)	0.1995	-0.0452	-0.0312	-0.1615	0.2037	-0.0479	-0.0287	-0.1673

CHAPTER 7

PLANE DEFORMATIONS

7.1 Introduction

There are two general types of plane problems which may be defined by setting down certain restriction and assumptions on the stress and the displacement fields. Plane stress is relevant in the case where one physical dimension is obviously much smaller than the other two, such as a thin sheet or diaphragm loaded in the plane perpendicular to the small dimension. Plane strain is relevant where one dimension is much greater than the others two, such as a long pressurised pipe, or perhaps a dam between massive end walls. Plane strain and plane stress problems for homogeneous isotropic materials have been widely investigated (see for example Ang [4], Clements and Rizzo [16], England [27], Rizzo [61]), however for inhomogeneous materials solutions to particular problems are less common. In general, solving plane deformations problem involving inhomogeneous materials is difficult. For inhomogeneous material involving the join of two kinds of homogeneous materials with interface boundary, some progress can be made. In the present chapter, we develop the boundary element method for such materials. The kernel of the integral equation here is obtained via the complex function approach. For the problem with continuous small variation of the material coefficients, the solution is obtained by combining the boundary element method with the perturbation technique. Some stress intensity factor problems which were previously discussed in chapter three are considered again using the boundary element method. Both numerical results obtained using the two point boundary value method and the boundary element method are compared in order to verify the accuracy of the procedure. Several others numerical results can be found at the end of this chapter.

7.2 Governing differential equation and the fundamental singular solution

Consider a system of differential equations

$$(\lambda + \mu)u_{j,ij} + \mu u_{i,jj} = 0, \tag{7.2.1}$$

for a body $\mathcal{R}$ bounded by a single smooth contour C, where the λ and μ are constants. Using standard techniques (see for example Sokolnikoff [71]), this system can be reduced to the biharmonic equation

$$u_{i,jjkk} = 0, \qquad i,j,k = 1,2. \tag{7.2.2}$$

Here the usual index notation of Cartesian tensors is adopted. The subscript denotes the Cartesian tensor component while the comma denotes the partial derivative for the relevant arguments.

By assuming $u_{i,jj} = P_1(x_1, x_2)$ the analytic function

$$F(z) = P_1 + \imath P_2, \tag{7.2.3}$$

can be constructed through the Cauchy–Rieman equations and P_2 is obtained by integrating

$$\begin{aligned} dP_2 &= P_{2,1}dx_1 + P_{2,2}dx_2 \\ &= -P_{1,2}dx_1 + P_{1,1}dx_2, \end{aligned}$$

or

$$P_2 = \int_{c_0}^{c_1} -P_{1,2}dx_1 + P_{1,1}dx_2. \tag{7.2.4}$$

Consider a harmonic function $\Omega(z)$ which satisfies

$$\Omega(z) = p_1 + \imath p_2 = \frac{1}{4}\int F(z)dz, \tag{7.2.5}$$

therefore

$$\Omega' = p_{1,1} + \imath p_{2,1} = \frac{1}{4}(P_1 + \imath P_2), \tag{7.2.6}$$

and from the Cauchy-Riemann equations

$$\begin{aligned} p_{1,1} =& p_{2,2} = \frac{1}{4}P_1, \\ p_{1,2} =& -p_{2,1} = -\frac{1}{4}P_2. \end{aligned} \tag{7.2.7}$$

Hence from (7.2.2) and (7.2.7) we obtain

$$(u_i - p_1 x_1 - p_2 x_2)_{,kk} = 0, \tag{7.2.8}$$

since p_1 and p_2 are harmonic in R, u_i can be written as

$$u_i = p_1 x_1 + p_2 x_2 + q_1(x_1, x_2), \tag{7.2.9}$$

where $q_1(x_1, x_2)$ is harmonic also in R. Now, if $\omega(z) = q_1 + \imath q_2$ is an analytic function of z, then equation (7.2.9) can be written as

$$u_i = \Re\left\{\overline{z}\Omega(z) + \omega(z)\right\},$$

or

$$u_i = \frac{1}{2}\left\{\overline{z}\Omega(z) + z\overline{\Omega(z)} + \omega(z) + \overline{\omega(z)}\right\}, \tag{7.2.10}$$

where $\overline{z}, \overline{\Omega(z)}$ and $\overline{\omega(z)}$ denote the conjugate of $z, \Omega(z)$ and $\omega(z)$ respectively.

If the right hand side of equation (7.2.1) is a delta function say

$$(\lambda + \mu)u_{j,ij} + \mu u_{i,jj} = K_i \delta(\vec{x} - \vec{x_0}), \tag{7.2.11}$$

where δ denotes the Dirac delta function, K_i are real constants and $\vec{x} = (x_1, x_2)$ and $\vec{x_0} = (\xi_1, \xi_2)$ is a point in R then it may be readily verified that a suitable choice of $\Omega(z)$ and $\omega(z)$ in (7.2.10) in order to satisfy (7.2.11) is

$$\begin{aligned} \Omega(z) =& -\psi \ln(z - z_0), \\ \omega(z) =& \kappa\overline{\psi}\ln(z - z_0) + \frac{\psi\overline{z_0}}{z - z_0}, \end{aligned} \tag{7.2.12}$$

where $z = x_1 + \imath x_2, z_0 = \xi_1 + \imath\xi_2, \kappa = (\lambda + 3\mu)$ while ψ is a complex constant corresponding to K_i.

7.3 General second order elliptic system for anisotropic media and the fundamental singular solution

Consider a general system of second order differential equation given by

$$c_{ijkl}u_{k,jl} = 0, \qquad j,l = 1,2;\ i,k = 1,2,\cdots,n \tag{7.3.1}$$

where u_k are functions of the dependent variables x_j, c_{ijkl} are real constants which satisfies

$$c_{ijkl} = c_{klij}. \tag{7.3.2}$$

and equation (7.3.1) satisfy the elliptic condition,

$$c_{ijkl}u_{i,j}u_{k,l} \geq 0. \tag{7.3.3}$$

By assuming u_k are analytic. and the solution of equation (7.3.1) can be written as

$$u_k = A_k f(x_1 + px_2), \tag{7.3.4}$$

where A_k are constants and f is an arbitrary analytic function, then substitution of equation (7.3.4) into (7.3.1) form a set of linear algebra system

$$(c_{i1k1} + c_{i1k2} + c_{i2k1} + c_{i2k2})A_k = 0. \tag{7.3.5}$$

This system only have a nontrivial solution if

$$|c_{i1k1} + c_{i1k2}p + c_{i2k1}p + c_{i2k2}p^2| = 0, \tag{7.3.6}$$

which is a polynomial of degree $2n$ in p.

By assuming a complex p_α and its conjugate $\overline{p}_\alpha$, $(\alpha = 1,2,\cdots,n)$ are the solution of equation (7.3.6) (this condition are guaranteed by equation (7.3.3) see Clements and Rizzo [16]) then equation (7.3.4) can be written as

$$u_k = \sum_{\alpha=1}^{n} A_{k\alpha} f_\alpha(x + p_\alpha x_2) + \sum_{\alpha=1}^{n} \overline{A}_{k\alpha} \overline{f}_\alpha(x + \overline{p}_\alpha x_2). \tag{7.3.7}$$

If the right hand side of equation (7.3.1) is a delta function

$$c_{ijkl} u_{k,jl} = K_i \delta(\vec{x} - \vec{x_0}), \tag{7.3.8}$$

where $\vec{x} = (x_1, x_2), \vec{x_0} = (\xi_1, \xi_2)$ and K_i are constants, then by choosing

$$f_\alpha(z_\alpha) = \frac{1}{2\pi i} D_\alpha \ln(z_\alpha - \xi_\alpha), \tag{7.3.8}$$

with $\xi_\alpha = \xi_1 + p_\alpha \xi_2$ and D_α are constant, the equation (7.3.7) becomes

$$u_k = \frac{1}{2\pi i} \left\{ \sum_{\alpha=1}^{n} A_{k\alpha} D_\alpha \ln(z_\alpha - \xi_\alpha) - \sum_{\alpha=1}^{n} \overline{A}_{k\alpha} \overline{D}_\alpha \ln(\overline{z}_\alpha - \overline{\xi}_\alpha) \right\}. \tag{7.3.9}$$

The the fundamental singular solution can be obtained now by determining the constants which satisfy the appropriate conditions.

7.4 Boundary integral equation

7.4.1 Perturbation technique

The equilibrium equation in terms of the displacements in the absence of body forces for plane elasticity problems for inhomogeneous materials is

$$\left[\lambda \delta_{ij} u_{k,k} + \mu(u_{i,j} + u_{j,i})\right]_{,j} = 0. \tag{7.4.1}$$

Here δ_{ij} denotes the kronecker δ, u_i denotes the displacement with respect to the relevant coordinates system, and λ and μ denote the elastic parameters.

By taking λ and μ as a function of position, say

$$\begin{aligned}\lambda(x_1, x_2) &= \lambda_0 + \epsilon\lambda_1(x_1, x_2),\\ \mu(x_1, x_2) &= \mu_0 + \epsilon\mu_1(x_1, x_2),\end{aligned} \tag{7.4.2}$$

where λ_0 and μ_0 are constants, ϵ is a small perturbation constant, the equation (7.4.1) becomes

$$\begin{aligned}(\lambda_0 + \mu_0)u_{j,ij} + \mu_0 u_{i,jj} + \epsilon\mu_1(u_{j,ij} + u_{i,jj}) + \epsilon\mu_{1,j}(u_{i,j} + u_{j,i})\\ +\epsilon\lambda_1 u_{k,kj} + \epsilon\lambda_{1,j}\delta_{ij}u_{k,k} = 0.\end{aligned} \tag{7.4.3}$$

Let the displacement take the form

$$u_i = u_i^{(0)} + \epsilon u_i^{(1)} + \epsilon^2 u_i^{(2)} + \cdots \tag{7.4.4}$$

Substitution into (7.4.3) and by equating the power of ϵ yields

$$\begin{aligned}(\lambda_0 + \mu_0)u_{j,ij}^{(0)} + \mu_0 u_{i,jj}^{(0)} &= 0,\\ (\lambda_0 + \mu_0)u_{j,ij}^{(n)} + \mu_0 u_{i,jj}^{(n)} &= -f_{ij,j}^{(n)} \qquad (n \geq 1),\end{aligned} \tag{7.4.5}$$

where

$$f_{ij}^{(n)} = \lambda_1\delta_{ij}u_{k,k}^{(n-1)} + \mu_1(u_{i,j}^{(n-1)} + u_{j,i}^{(n-1)}). \tag{7.4.6}$$

If we write the stress as

$$\sigma_{ij} = \sigma_{ij}^{(0)} + \epsilon\sigma_{ij}^{(1)} + \epsilon^2\sigma_{ij}^{(2)} + \cdots, \tag{7.4.7}$$

then we obtain the relation

$$\begin{aligned}\sigma_{ij}^{(0)} &= \lambda_0\delta_{ij}u_{k,k}^{(0)} + \mu_0(u_{i,j}^{(0)} + u_{j,i}^{(0)}),\\ \sigma_{ij}^{(n)} &= \lambda_0\delta_{ij}u_{k,k}^{(n)} + \mu_0(u_{i,j}^{(n)} + u_{j,i}^{(n)}) + f_{ij}^{(n)}, \qquad (n \geq 1).\end{aligned} \tag{7.4.8}$$

For particular inhomogeneous material, say λ is a constant and μ is a function of position

$$\mu(x_1, x_2) = \mu_0 + \epsilon\mu_1(x_1, x_2), \tag{7.4.9}$$

the equation (7.4.3) simply reduces to

$$(\lambda + \mu_0)u_{j,ij} + \mu_0 u_{i,jj} + \epsilon\mu_1(u_{j,ij} + u_{i,jj}) + \epsilon\mu_{1,j}(u_{i,j} + u_{j,i}) = 0. \qquad (7.4.10)$$

Using equation (7.4.4) and equating the order of ϵ again, we obtain the equation (7.4.5) with

$$f_{ij}^{(n)} = \mu_1(u_{i,j}^{(n-1)} + u_{j,i}^{(n-1)}). \qquad (7.4.11)$$

The equation (7.4.8) for the stress becomes

$$\begin{aligned} \sigma_{ij}^{(0)} &= \lambda\delta_{ij}u_{k,k}^{(0)} + \mu_0(u_{i,j}^{(0)} + u_{j,i}^{(0)}), \\ \sigma_{ij}^{(n)} &= \lambda\delta_{ij}u_{k,k}^{(n)} + \mu_0(u_{i,j}^{(n)} + u_{j,i}^{(n)}) + f_{ij}^{(n)}, \qquad (n \geq 1). \end{aligned} \qquad (7.4.12)$$

where $f_{ij}^{(n)}$ is given by equation (7.4.11).

Once equation (7.4.5) is solved for the displacements, the stresses can be found through the formula above. The tractions are given by

$$t_i = \sigma_{ij}n_j, \qquad (7.4.12)$$

where n_j denotes the outward normal vectors.

In order to solve the equation (7.4.5a) in the two dimensional case above, let us consider first the equation

$$(\lambda + \mu_0)u_{j,ij}^{(0)} + \mu_0 u_{i,jj}^{(0)} = h_i. \qquad (7.4.13)$$

By assuming ϕ_k as the solution of the above equation and also ϕ_k^* as the solution of the same equation by replacing h_i by h_i^* then by using the divergence theorem and equation (7.4.12), yields

$$\begin{aligned} \int_C t_i\phi_i^*\, dS &= \int_C \sigma_{ij}\phi_i^* n_j\, dS = \iint_R (\sigma_{ij}\phi_i^*)_{,j}\, dA \\ &= \iint_R \sigma_{ij,j}\phi_i^* + \sigma_{ij}\phi_{i,j}^*\, dA. \end{aligned} \qquad (7.4.14)$$

Similarly

$$\int_C t_i^* \phi_i \, dS = \iint_R \sigma_{ij,j}^* \phi_i + \sigma_{ij}^* \phi_{i,j} \, dA. \tag{7.4.15}$$

By subtracting equation (7.4.15) from (7.4.14) we obtain

$$\begin{aligned} \int_C t_i \phi_i^* - t_i^* \phi_i \, dS &= \iint_R [\sigma_{ij,j} \phi_i^* - \sigma_{ij,j}^* \phi_i] \, dA \\ &= \iint_R h_i \phi_i^* - h_i^* \phi_i \, dA, \end{aligned} \tag{7.4.16}$$

since $\sigma_{ij}\phi_{i,j}^* = \sigma_{ij}^* \phi_{i,j}. \sigma_{ij,j} = h_i$ and $\sigma_{ij,j}^* = h_i^*$. Equation (7.4.16) is known as the Betti's Reciprocal Theorem (see Clements and Rizzo [16]).

By choosing ϕ_k as the fundamental solution, $h_i = K_{ij}\delta(\vec{x} - \vec{x_0}), \phi_k^* = u_i^{(0)}, t_k^* = t_i^{(0)}, h_i^* = 0$ for equation (7.4.5a), the reciprocal theorem above leads to an integral solution to equation (7.4.5a) in a region $\mathcal{R}$ bounded by a closed curve C given by (see Rizzo [61])

$$\tau u_j^{(0)}(\vec{x_0}) = \alpha \int_C \left[u_i^{(0)}(\vec{x}) T_{ij}(\vec{x}, \vec{x_0}) - t_i^{(0)}(\vec{x}) U_{ij}(\vec{x}, \vec{x_0}) \right] dS(\vec{x}). \tag{7.4.17}$$

Here t_i denotes the Cartesian tractions, $\vec{x} = (x_1, x_2), \vec{x_0} = (\xi_1, \xi_2)$, $\alpha = (\lambda + 3\mu_0)/(4\pi\mu_0(\lambda + 2\mu_0))$, $\tau = 1$ if $\vec{x_0} \in \mathcal{R}, 0 < \tau < 1$ if $\vec{x_0} \in C$ (note that $\tau = 1/2$ if C has continuously turning tangent).

The functions U_{ij} and T_{ij} are given by

$$\begin{aligned} 2\mu_0(U_{1j} + iU_{2j}) &= \kappa\Omega_j(z) - z\overline{\Omega_j'(z)} - \overline{\omega_j(z)}, \\ \Xi_{22j} - i\Xi_{12j} &= \Omega_j'(z) + \overline{\Omega_j'(z)} + z\overline{\Omega_j''(z)} + \overline{\omega_j'(z)}, \\ \Xi_{11j} + \Xi_{22j} &= 2\left[\Omega_j'(z) + \overline{\Omega_j'(z)}\right], \\ T_{ij} &= \Xi_{ikj} n_k, \end{aligned} \tag{7.4.18}$$

where

$$\begin{aligned} \Omega_j(z) &= -\psi_j \ln(z - z_0), \\ \omega_j(z) &= \kappa\overline{\psi_j} \ln(z - z_0) + \frac{\psi_j \overline{z_0}}{z - z_0}, \end{aligned} \tag{7.4.19}$$

Here the primes denotes the differentiation with respect to the relevant argument, the bar denotes the complex conjugate, n_k denote the normal (outward) vectors, $z = x_1 + \imath x_2$, $\imath = \sqrt{-1}$, $z_0 = \xi_1 + \imath\xi_2$, $\kappa = (\lambda + 3\mu_0)$, $\psi_1 = -\mu_0/\kappa$, $\psi_2 = -\imath\mu_0/\kappa$.

To obtain the stresses in the interior domain $\mathcal{R}$ it is necessary to evaluate the derivative of u_j with respect to ξ_1 and ξ_2. Since the differential operator is a linear operator, it can be applied in a straight forward way to obtain

$$\begin{aligned} 2\mu_0(U_{1j,l} + \imath U_{2j,l}) &= \kappa\Omega_{j,l}(z) - z\overline{\Omega'_{j,l}(z)} - \overline{\omega_{j,l}(z)}, \\ \Xi_{22j,l} - \imath\Xi_{12j,l} &= \Omega'_{j,l}(z) + \overline{\Omega'_{j,l}(z)} + z\overline{\Omega''_{j,l}(z)} + \overline{\omega'_{j,l}(z)}, \\ \Xi_{11j,l} + \Xi_{22j,l} &= 2\left[\Omega'_{j,l}(z) + \overline{\Omega'_{j,l}(z)}\right], \\ T_{ij,l} &= \Xi_{ikj,l}n_k, \end{aligned} \tag{7.4.20}$$

Here the subscripts i, j, k, l take the value 1 and 2. The subscript comma l denotes the differentiation with respect to ξ_1 for $l = 1$ and ξ_2 for $l = 2$ respectively. Once $u_j^{(0)}$ are known, the stresses are calculated by

$$\begin{aligned} \sigma_{ij}^{(0)} = \alpha\mu_0 \int_C u_k[T_{ki,j} + T_{kj,i} + \frac{\lambda}{\mu_0}\delta_{ij}T_{kr,r}] - \\ t_k[U_{ki,j} + U_{kj,i} + \frac{\lambda}{\mu_0}\delta_{ij}U_{kr,r}]\, dS, \end{aligned} \tag{7.4.21}$$

while the tractions are given through equation (7.4.12).

Similarly the integral solution of equation (7.4.5b) in recursive form for ($n \geq 1$) can be calculated. By assuming the displacement field satisfies

$$(\lambda + \mu_0)\phi_{j,ij} + \mu_0\phi_{i,jj} = -f_{ij,j}, \tag{7.4.22}$$

$$t_i = [\lambda\delta_{ij}\phi_{k,k} + \mu_0(\phi_{i,j} + \phi_{j,i}) + f_{ij}]n_j, \tag{7.4.23}$$

also

$$(\lambda + \mu_0)\phi^*_{j,ij} + \mu_0\phi^*_{i,jj} = h^*_i, \tag{7.4.24}$$

$$t^*_i = [\lambda\delta_{ij}\phi^*_{k,k} + \mu_0(\phi^*_{i,j} + \phi^*_{j,i})]n_j, \tag{7.4.25}$$

Using the reciprocal theorem again

$$\begin{aligned}\int_C t_i\phi_i^* - t_i^*\phi_i \, dS &= \iint_R [\sigma_{ij}\phi_i^* - \sigma_{ij}^*\phi_i]_{,j} \, dA \\ &= \iint_R \sigma_{ij,j}\phi_i^* + \sigma_{ij}\phi_{i,j}^* - \sigma_{ij,j}^*\phi_i - \sigma_{ij}^*\phi_{i,j} \, dA.\end{aligned} \tag{7.4.26}$$

And after some simplifications we obtain

$$\iint_R h_i^*\phi_i \, dA = \int_C t_i^*\phi_i - t_i\phi_i^* \, dS + \iint_R f_{ij}\phi_{i,j}^* \, dA. \tag{7.4.27}$$

If we choose ϕ_i^* as the fundamental singular solution, then the solution of equation (7.4.5b) in integral form can be written as

$$\begin{aligned}\tau u_j^{(n)}(\vec{x_0}) = \alpha \int_C \left[u_i^{(n)}(\vec{x})T_{ij}(\vec{x},\vec{x_0}) - t_i^{(n)}(\vec{x})U_{ij}(\vec{x},\vec{x_0})\right] dS(\vec{x}) + \\ \alpha \iint_R f_{ir}^{(n)}(\vec{x})U_{ij,r}(\vec{x},\vec{x_0}) \, dA(\vec{x}) \qquad (n \geq 1).\end{aligned} \tag{7.4.28}$$

By substituting equation (7.4.28) into (7.4.8) we obtain the stresses for the perturbation term of order $n \geq 1$ as

$$\begin{aligned}\sigma_{ij}^{(n)} = \alpha\mu_0 \int_C u_r^{(n)}[T_{ri,j} + T_{rj,i} + \frac{\lambda}{\mu_0}\delta_{ij}T_{rk,k}] - t_r^{(n)}[U_{ri,j} + U_{rj,i} + \frac{\lambda}{\mu_0}\delta_{ij}U_{rk,k}] \, dS + \\ \alpha\mu_0 \iint_R f_{rs}^{(n)}[U_{ri,sj} + U_{rj,si} + \frac{\lambda}{\mu_0}\delta_{ij}U_{rk,sk}] \, dA + f_{ij}^{(n)}.\end{aligned} \tag{7.4.29}$$

Thus the displacement and the stress for the inhomogeneous material can be obtained by substitution back through equation (7.4.4) and (7.4.7).

7.4.2 Two homogeneous materials

We consider an elastic inhomogeneous material with the inhomogeneity made up from two kinds of materials. The first material with $\lambda = \lambda^{(1)}$, $\mu = \mu^{(1)}$ and the

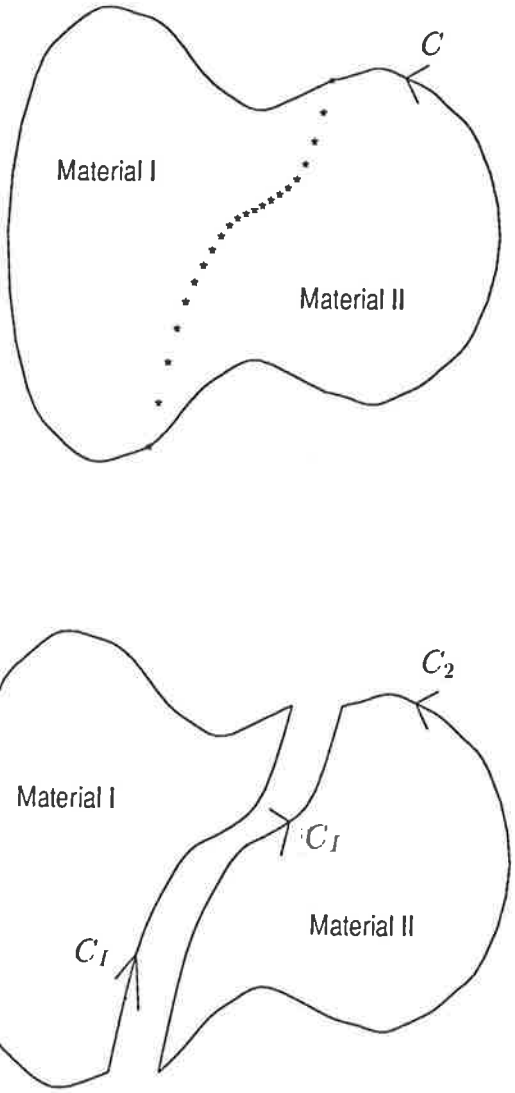

Figure 7.1
Two homogeneous materials with interface boundary
Material I with $\lambda = \lambda^{(1)}, \mu = \mu^{(1)}$ and material II with $\lambda = \lambda^{(2)}, \mu = \mu^{(2)}$

second material with $\lambda = \lambda^{(2)}$, $\mu = \mu^{(2)}$, where $\lambda^{(1)}, \mu^{(1)}, \lambda^{(2)}, \mu^{(2)}$ are constants. Suppose the material have an interface boundary as shown in Figure 7.1.

Thus if we choose the interface boundary as C_I and the pure boundary for the

first material is C_1 then the equilibrium equation should satisfy

$$(\lambda^{(1)} + \mu^{(1)})u^{(1)}_{j,ij} + \mu^{(1)}u^{(1)}_{i,jj} = 0, \tag{7.4.30}$$

with the solution

$$\tau u^{(1)}_j(\vec{x_0}) = \alpha^{(1)} \int_{C_1+C_I} \left[u^{(1)}_i(\vec{x})T^{(1)}_{ij}(\vec{x},\vec{x_0}) - t^{(1)}_i(\vec{x})U^{(1)}_{ij}(\vec{x},\vec{x_0})\right] dS(\vec{x}). \tag{7.4.31}$$

Similarly if we choose the pure boundary for the second material as C_2 then the equilibrium equation should satisfy

$$(\lambda^{(2)} + \mu^{(2)})u^{(2)}_{j,ij} + \mu^{(2)}u^{(2)}_{i,jj} = 0, \tag{7.4.32}$$

with the solution

$$\tau u^{(2)}_j(\vec{x_0}) = \alpha^{(2)} \int_{C_2-C_I} \left[u^{(2)}_i(\vec{x})T^{(2)}_{ij}(\vec{x},\vec{x_0}) - t^{(2)}_i(\vec{x})U^{(2)}_{ij}(\vec{x},\vec{x_0})\right] dS(\vec{x}). \tag{7.4.33}$$

By asumming the materials are perfectly continuous across the interface curve C_I, we have the continuity equations

$$u^{(1)}_i(\vec{x}|_{C_I}) = u^{(2)}_i(\vec{x}|_{C_I}) \qquad i = 1, 2, \tag{7.4.34}$$

and

$$t^{(1)}_i(\vec{x}|_{C_I}) = t^{(2)}_i(\vec{x}|_{C_I}) \qquad i = 1, 2. \tag{7.4.35}$$

Thus if the displacements and/or tractions are known over the pure boundary C we know the displacements and tractions on curve C_I by using the combination of the equations (7.4.31) and (7.4.33). Once the displacements and tractions on the boundary C_1, C_I, C_2 are known, the displacements and tractions in the interior points can be calculated using (7.4.31) and (7.4.33) again.

7.5 Numerical methods

7.5.1 Perturbation technique

Using the boundary element method, the boundary C is discretised into N straight segments. By assuming the displacements and the tractions are constants over a given segment, equation (7.4.5a) can be solved by the approximation

$$\tau u_{jk}^{(0)} = a \sum_{m=1}^{N} \left\{ u_{im}^{(0)} \int_{C_m} T_{ij}(\vec{x}, \vec{p_k})\, dS(\vec{x}) - t_{im}^{(0)} \int_{C_m} U_{ij}(\vec{x}, \vec{p_k})\, dS(\vec{x}) \right\}, \qquad (7.5.1)$$

Here C_m denotes the m^{th} segment of the discretised boundary, $\vec{p_k}$ is the midpoint of C_k and u_{km} and t_{km} are the constant values of u_k and t_k respectively over the segment C_m while $\tau = \frac{1}{2}$ if $\vec{p_k}$ on C and $\tau = 1$ if $\vec{p_k} \in R$.

For certain boundary, we can gain an advantage to reduce the computation time by involving the weight function If the boundary C is divided into m conforming elements C_m. each described by P nodes with $(P-1)$ being the order of the weight function $M_n(\xi), \quad n = 1, 2, \cdots, P$, of the intrinsic variable $\xi, (-1 \leq \xi \leq 1)$ then equation (7.5.1) becomes

$$\begin{aligned} \tau u_{jk}^{(0)} = \alpha \sum_{m=1}^{N} \sum_{n=1}^{P} \Big\{ & u_{imn}^{(0)} \int_{C_m} T_{ij}(\vec{x}, \vec{p_k}) M_n(\xi)\, dS(\vec{x}) \\ & - t_{imn}^{(0)} \int_{C_m} U_{ij}(\vec{x}, \vec{p_k}) M_n(\xi)\, dS(\vec{x}) \Big\}. \end{aligned} \qquad (7.5.2)$$

The integral here can be evaluated by the modified Simpson's rule (see Abramowitz and Stegun [2]) so equation (7.5.1) forms a set of linear algebraic system with $2N$ equations and $2N$ unknowns. Once this system is solved, $u_j^{(0)}$ on the entire boundary are known as well as $u_j^{(0)}$ on the entire domain through the above formula.

Similar approximations are applied for the solution of equation (7.4.5b). The equation (7.4.28) on the boundary is approximated by

$$\begin{aligned}\frac{1}{2}u_{jk}^{(n)} = \alpha \sum_{m=1}^{N} \left\{ u_{im}^{(n)} \int_{C_m} T_{ij}(\vec{x}, \vec{p_k})\, dS(\vec{x}) - t_{im}^{(n)} \int_{C_m} U_{ij}(\vec{x}, \vec{p_k})\, dS(\vec{x}) \right\} \\ + \alpha \sum_{o=1}^{Q} f_{iko}^{(n)} U_{ij,k}(\vec{x}_o, \vec{p_k}) \iint_{R_o} dA(\vec{x}) \qquad (n \geq 1).\end{aligned} \tag{7.5.3}$$

Here $f_{iko}(\vec{x}_o)$ is given by (7.4.6) on the o^{th} subdomain and assumed to be a constant. Q denotes the number of subdomain (domain $\mathcal{R}$ is divided into Q subdomain), $\vec{x_o}$ denotes the interior point of the subdomain, $\vec{x}$ denotes the boundary point. The boundary conditions here are assumed to be superimposed. If we already specify $u_j^{(0)}$ or $t_j^{(0)}$ with the given boundary conditions then $u_j^{(n)}$ and/or $t_j^{(n)}$ are zero. Thus by specifying $u_j^{(n)} = 0$ and $t_j^{(n)} = 0$ on the boundary, equation (7.5.3) form a set of linear algebraic equation with $2N$ equations and $2N$ unknowns again. Once this set of linear algebraic system has been solved, we know $u_j^{(n)}$ and $t_j^{(n)}$ over the boundary. To evaluate the displacement for interior points, it is necessary to evaluate the area integral which contains the singular point. For $x = x_k$, the displacements for the interior points can be obtained by

$$\begin{aligned}u_{jk}^{(n)} = \alpha \sum_{m=1}^{N} \left\{ u_{im}^{(n)} \int_{C_m} T_{ij}(\vec{x}, \vec{x_k})\, dS(\vec{x}) - t_{im}^{(n)} \int_{C_m} U_{ij}(\vec{x}, \vec{x_k})\, dS(\vec{x}) \right\} \\ + \alpha \sum_{o=1}^{Q} f_{iko}^{(n)} \iint_{R_o} U_{ij,k}(\vec{x}, \vec{x_k})\, dA(\vec{x}) \qquad (n \geq 1),\end{aligned} \tag{7.5.4}$$

while for $x \neq x_k$ the displacement for the interior points is given by

$$\begin{aligned}u_{jk}^{(n)} = \alpha \sum_{m=1}^{N} \left\{ u_{im}^{(n)} \int_{C_m} T_{ij}(\vec{x}, \vec{x_k})\, dS(\vec{x}) - t_{im}^{(n)} \int_{C_m} U_{ij}(\vec{x}, \vec{x_k})\, dS(\vec{x}) \right\} \\ + \alpha \sum_{o=1}^{Q} f_{iko}^{(n)} U_{ij,k}(\vec{x}, \vec{x_k}) \iint_{R_o} dA(\vec{x}) \qquad (n \geq 1).\end{aligned} \tag{7.5.5}$$

For $x = x_k$, it is necessary to evaluate $\iint_{R_o} U_{ij,k}\, dA$ and $\iint_{R_o} U_{ij,kl}\, dA$. If the domain is divided into the rectangular shape with width $2a$ and height $2b$ and x_k is chosen

at the center point of the rectangle then $\iint_{R_o} U_{ij,k}\, dA = 0$. $\iint_{R_o} U_{ij,kl}\, dA = 0$, except for

$$
\begin{aligned}
\iint_{R_o} U_{11,11}\, dA &= -4\arctan\frac{a}{b} + \frac{2}{\kappa}\left[\frac{2ab}{a^2+b^2} - 2\arctan\frac{b}{a}\right],\\
\iint_{R_o} U_{22,11}\, dA &= -4\arctan\frac{a}{b} - \frac{2}{\kappa}\left[\frac{2ab}{a^2+b^2} - 2\arctan\frac{b}{a}\right],\\
\iint_{R_o} U_{11,22}\, dA &= 4\arctan\frac{a}{b} - \frac{2}{\kappa}\left[\frac{2ab}{a^2+b^2} - 2\arctan\frac{a}{b}\right],\\
\iint_{R_o} U_{22,22}\, dA &= 4\arctan\frac{a}{b} + \frac{2}{\kappa}\left[\frac{2ab}{a^2+b^2} - 2\arctan\frac{a}{b}\right],\\
\iint_{R_o} U_{12,12}\, dA &= \frac{1}{\kappa}\left[-\frac{4ab}{a^2+b^2}\right],\\
\iint_{R_o} U_{12,21}\, dA &= \frac{1}{\kappa}\left[-\frac{4ab}{a^2+b^2}\right],\\
\iint_{R_o} U_{21,12}\, dA &= \frac{1}{\kappa}\left[-\frac{4ab}{a^2+b^2}\right],\\
\iint_{R_o} U_{21,21}\, dA &= \frac{1}{\kappa}\left[-\frac{4ab}{a^2+b^2}\right].
\end{aligned}
\tag{7.5.6}
$$

7.5.2 Two homogeneous materials

Using the boundary element method with constant coefficients, the boundary C_1, C_I, C_2 (see illustration in Figure 7.1) are discretised into N, M, O straight segments respectively. It is easily to specify the direction for the first material as counter clockwise direction for discretisation purposes. If we use the discretisation rule such as C_1, C_I, C_I, C_2 then we have $N + 2M + O$ discretisation points. Thus equation (7.4.31) on the boundary is approximated by

$$
\frac{1}{2}u^{(1)}_{jk} = \alpha^{(1)} \sum_{m=1}^{N+M} \left\{ u^{(1)}_{im} \int_{C_m} T^{(1)}_{ij}(\vec{x}, \vec{p_k})\, dS(\vec{x}) - t^{(1)}_{im} \int_{C_m} U^{(1)}_{ij}(\vec{x}, \vec{p_k})\, dS(\vec{x}) \right\}. \tag{7.5.7}
$$

Similarly for equation (7.4.33), we approximate by

$$\frac{1}{2}u_{jk}^{(2)} = -\alpha^{(2)} \sum_{m=N+M+1}^{N+2M} \left\{ u_{im}^{(2)} \int_{C_m} T_{ij}^{(2)}(\vec{x}, \vec{p_k})\, dS(\vec{x}) - t_{im}^{(2)} \int_{C_m} U_{ij}^{(2)}(\vec{x}, \vec{p_k})\, dS(\vec{x}) \right\}$$
$$+ \alpha^{(2)} \sum_{m=N+2M+1}^{N+2M+O} \left\{ u_{im}^{(2)} \int_{C_m} T_{ij}^{(2)}(\vec{x}, \vec{p_k})\, dS(\vec{x}) - t_{im}^{(2)} \int_{C_m} U_{ij}^{(2)}(\vec{x}, \vec{p_k})\, dS(\vec{x}) \right\}. \tag{7.5.8}$$

Using the continuity equation (7.4.34) and (7.4.35), equation (7.5.7) and (7.5.8) then form a set of linear algebraic equations with $2(N+2M+O)$ equations and $2(N+2M+O)$ unknowns. Once this linear algebraic system is solved, the displacements and the tractions over the boundary C_1, C_I, C_2 are obtained. Similar approach can be used for calculating the displacements and the tractions of the interior points.

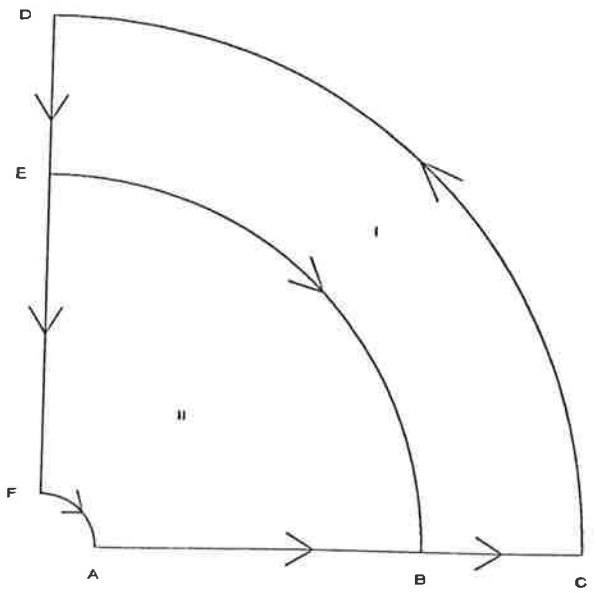

Figure 7.2
A quarter of the disk

7.6 Numerical results

Problem 7.1 : Circular disk with a large hole (comparison for problem 3.1)

We consider the concentrically composite disk which was discussed in problem 3.1 but here we solve the problem using the boundary element method. Because of the symmetric nature of the problem, we consider only a quarter of the disk as illustrated in Figure 7.2. The segments AB and BC is subjected to the boundary conditions $t_1 = 0, u_2 = 0$, the segment CD is subjected with $t_1 = p\cos\theta, t_2 = p\sin\theta$, the segments DE and EF to $u_1 = 0, t_2 = 0$ and the segments FA to $t_1 = 0, t_2 = 0$. The numerical results for the stress concentration factor σ_θ/p obtained using the boundary element method and the analytical results obtained as in problem 3.1 are plotted in Figure 7.3. Here the dots and the dash line represent the numerical results obtained by using the boundary element method and the solid line represents the analytical results. Figure 7.3.a shows the results for radius of the hole $r/r_0 = .1$ obtained by discretising the segments AB into 30 equal segments, BC into 15 segments, CD into 40 segments, DE into 25 segments, EB into 35 segments, EF into 50 segments and FA into 20 segments. Figure 7.3.b, 7.3.c, 7.3,d give the results for the radii $r/r_0 = .2, .3, .4$ respectively using the same discretising points, except for the segment EF which is discretised into $48, 46, 44$ points, segment FA into $23, 26, 29$ points and segment AB into $28, 26, 24$ points respectively.

Problem 7.2 : Inhomogeneous cylinder

We consider here an inhomogeneous cylinder with non dimensionalised material inhomogeneity parameters $\lambda/\lambda_0 = 1$ and $\mu/\mu_0 = 2/(1+r)$. The interior radius is fixed at $r = 1$ and the exterior radius $r = 3$. The pressure $p = 2$ is then applied at the exterior cylinder while in the interior cylinder, zero pressure is applied.

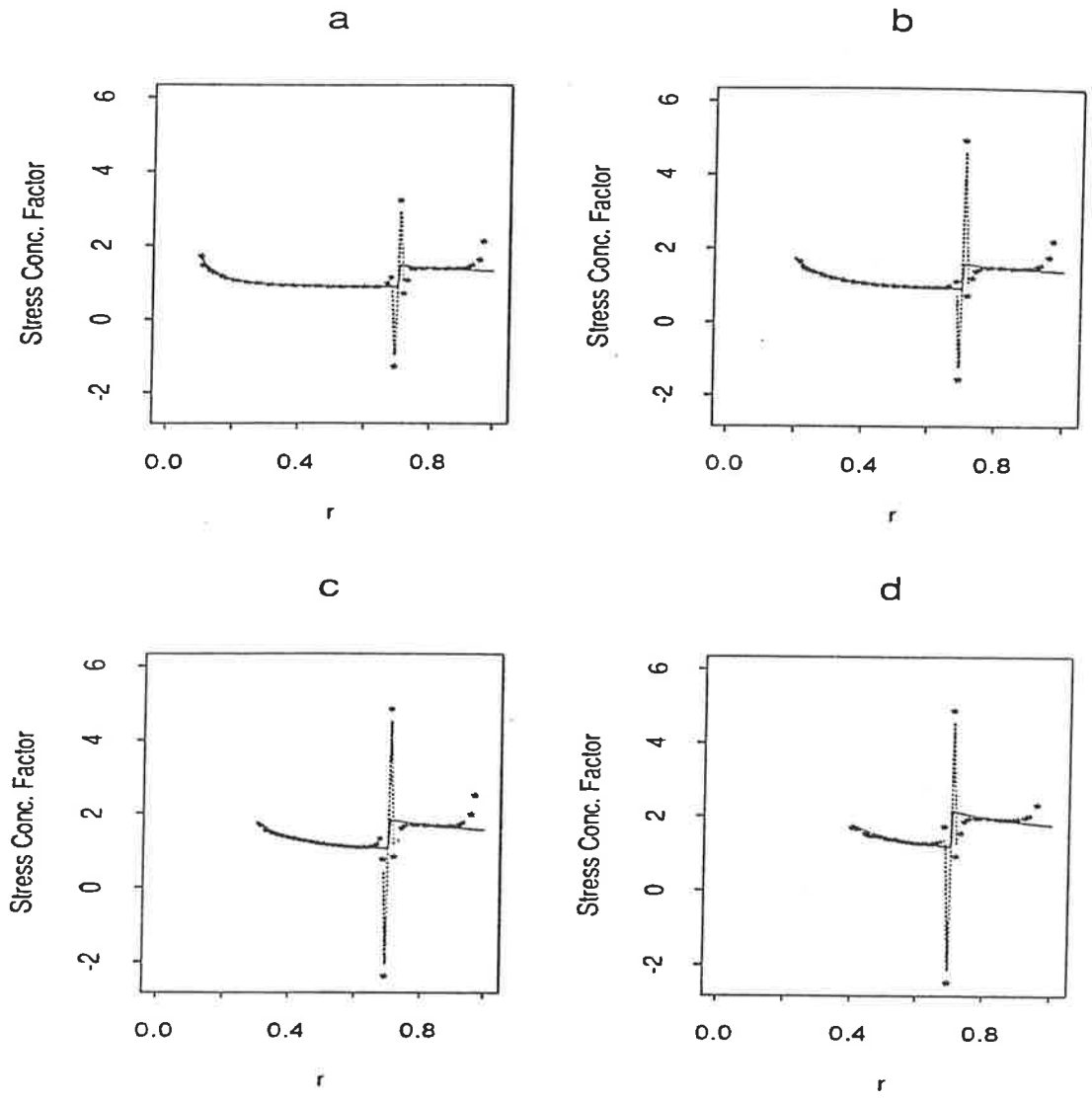

Figure 7.3
Comparison of the stress concentration factor for a disk with
several radii of the hole using boundary element method and analytical method

Using the perturbation technique over a quarter cylinder by specifying 15 segments from the point (0,1) to (1,0), 40 segments from point (1,0) to (3,0), 50 segments from (3,0) to (0,3) and 40 segments from (0,3) to (0,1) or 290 points on the boundary and 141 points at the interior, we obtain the results as shown in Table 7.1. The stress intensity factor for this particular problem, using the boundary element technique and the two point boundary value problem solutions can be compared through Figure 7.2. The solid line in Figure 7.2 represents the results obtained by using the two point boundary value method. The stars denote the results obtained by the boundary element technique using only two perturbation terms, while the dash line are their splines. To this end we note that the materials which is used here is the same material used for the axially symmetric problem discussed in chapter three. Also note that by taking the non dimensionalised quantities $\lambda/\lambda_0 = 1$ and $\mu/\mu_0 = \frac{2}{1+r} = 1 + .01\frac{100(1-r)}{1+r}$, the assumption in (7.4.2) for small variation of λ_1 and μ_1 is violated, however the numerical results obtained in Table 7.1 and Figure 7.4 still show that combination of the boundary element method with the perturbation technique are in a good agreement with the two points boundary value method.

Problem 7.3 : Square plate with circular hole under uniaxial loading

We consider a square plate of width $w = 2$ made up from two kind of materials with a center hole of radius r under uniaxial loading. The first material is bounded by circular boundary with center point $(0, 0)$ and radius $r = .7$ to the edge of the square while the second material is bounded from the circular hole to the circle above. The join of these materials here is assumed to be perfectly continuous.

Because of the symmetrical nature of the problem, we only consider a quarter part of the plate as shown in figure 7.5. Using the boundary element method, we specify the pure boundary of the first material as having 17 segments from (.7,0) to

(1,0), 20 segments from (1.0) to (1,1), 15 segments from (1,1) to (0,1), 18 segments from (0,1) to (0,.7). The pure boundary of the second material is specified by 40 segments from (0,.7) to (0,r), 21 segments from (0,r) to (r,0) and 15 segments from (r,0) to (.7,0) while the interface boundary is specified by 41 segments. Several diameters of the hole in the second material are chosen to observe the behaviour of the stress intensity factor. The stress intensity factor K which is defined as the ratio of the component t_1 of the stress vector at the edge of the hole $(x = 0, y = r)$ to the applied stress (a in Figure 7.5) is plotted in Figure 7.6 for several diameters of the hole relative to the width of the plate ($\frac{2r}{w} = .1, .2, .3, .4, .5$). In Figure 7.6, the same material for the first and the second material with non dimensionalised Young's modulus $E/E_0 = 1.0$ and Poisson's ratio $\nu/\nu_0 = .25$ are chosen for simplification and for testing the result in comparison to the analytical solution for the homogeneous material (see Shilkrut et al [66]) and the numerical solution using a combination between finite elements and the boundary element technique for homogeneous materials (see Wearing and Sheikh [81]).

Figure 7.7. shows the similar problem and the similar discretisation as Figure 7.6 with two different kinds of the materials. Figure 7.7.a shows the graph of the stress concentration factor versus diameter of the hole for $\frac{2r}{w} = .1, .2, .3, .4$ for two kinds of materials. The first material with non dimensionalised Young's modulus $E/E_0 = 1.0$ and Poisson's ratio $\nu/\nu_0 = .25$ and the second material with Young's modulus $E/E_0 = 2.0$ and $\nu/\nu_0 = .25$. By swapping the first material and the second material above, we obtain the results as given in Figure 7.7.b. The results in Figure 7.7.c are obtained by using the first material with $E/E_0 = 1.0$ and $\nu/\nu_0 = .125$ and the second material with $E/E_0 = 1.0$ and $\nu/\nu_0 = .25$, while Figure 7.7.d the first material with $E/E_0 = 1.0$ and $\nu/\nu_0 = .25$ and the second material with $E/E_0 = 1.0$ and $\nu/\nu_0 = .125$.

Table 7.1

Inhomogeneous material with $\lambda/\lambda_0 = 1$ and $\mu/\mu_0 = \frac{2}{1+r}$

$\sigma_r(1) = 0$, $\sigma_r(3) = 2$

R	Traction (BEM)	Traction (TPBV)	Displacement (BEM)	Displacement (TPBV)
2.8750	-2.9870	-2.2782	2.3951	2.4258
2.7750	-2.6427	-2.3058	2.3324	2.3707
2.6750	-2.1604	-2.3350	2.2768	2.3167
2.4750	-2.5808	-2.4088	2.1798	2.2160
2.3750	-2.8877	-2.4537	2.1299	2.1693
2.2750	-2.7215	-2.5057	2.0830	2.1253
2.0750	-2.3619	-2.6346	2.0105	2.0461
1.9750	-2.8973	-2.7125	1.9778	2.0109
1.8750	-3.2684	-2.8069	1.9449	1.9805
1.7750	-3.1398	-2.9168	1.9168	1.9547
1.4750	-3.5561	-3.4203	1.8844	1.9140
1.3750	-4.0114	-3.6731	1.8854	1.9169

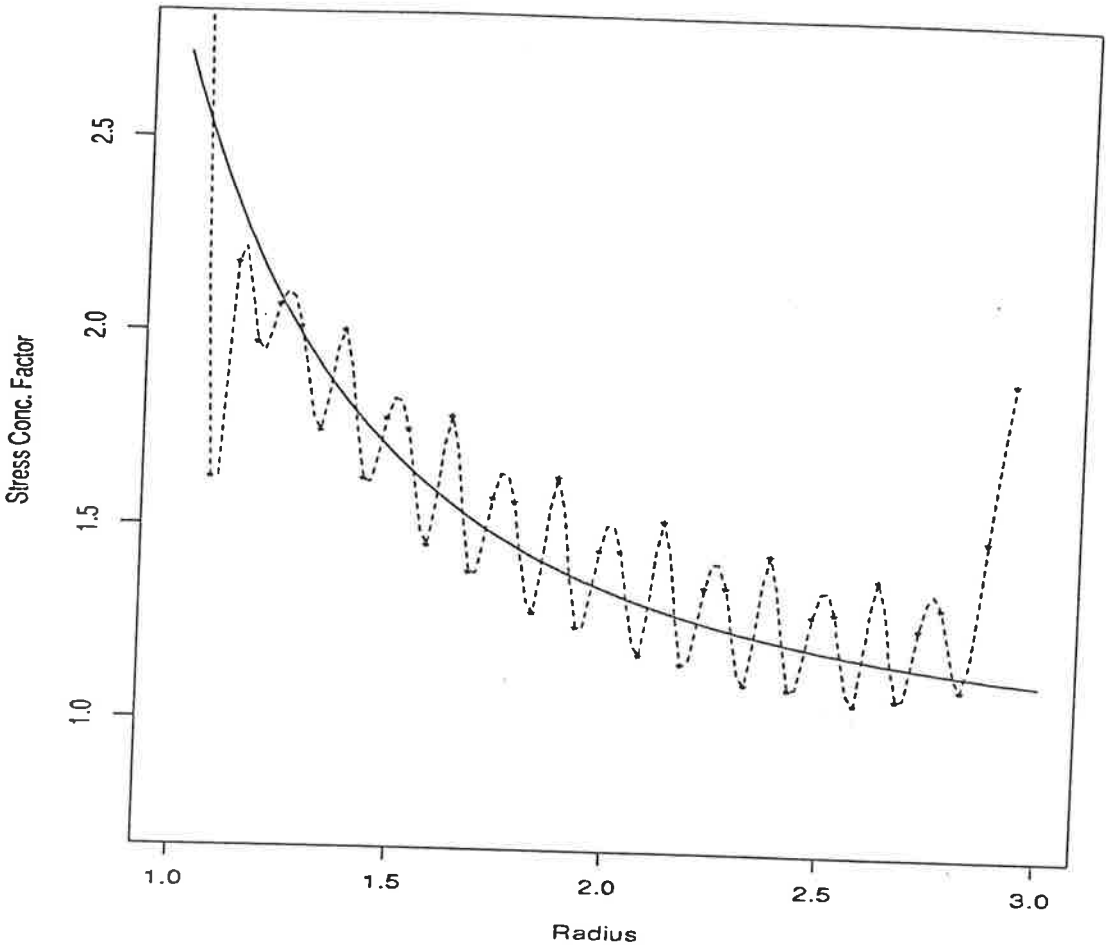

Figure 7.4

Comparison of the stress concentration factor between boundary element method and two point boundary value method for inhomogeneous material with $\lambda/\lambda_0 = 1$ and $\mu/\mu_0 = 2/(1+r)$

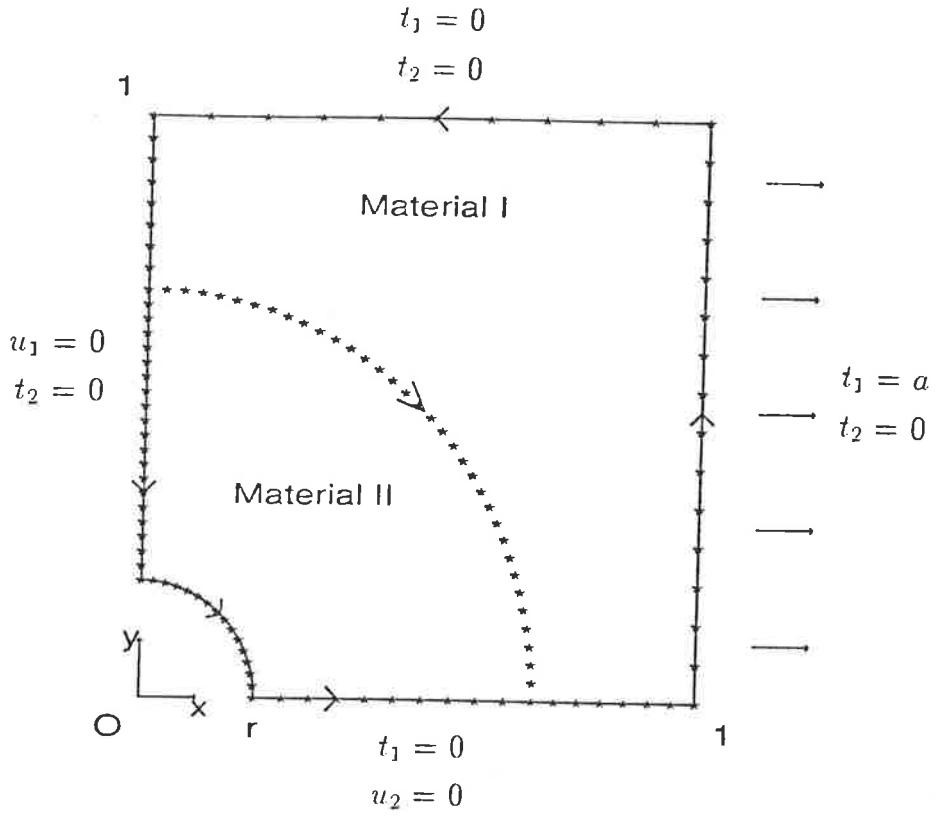

Figure 7.5
A quarter of the plate under uniaxial loading

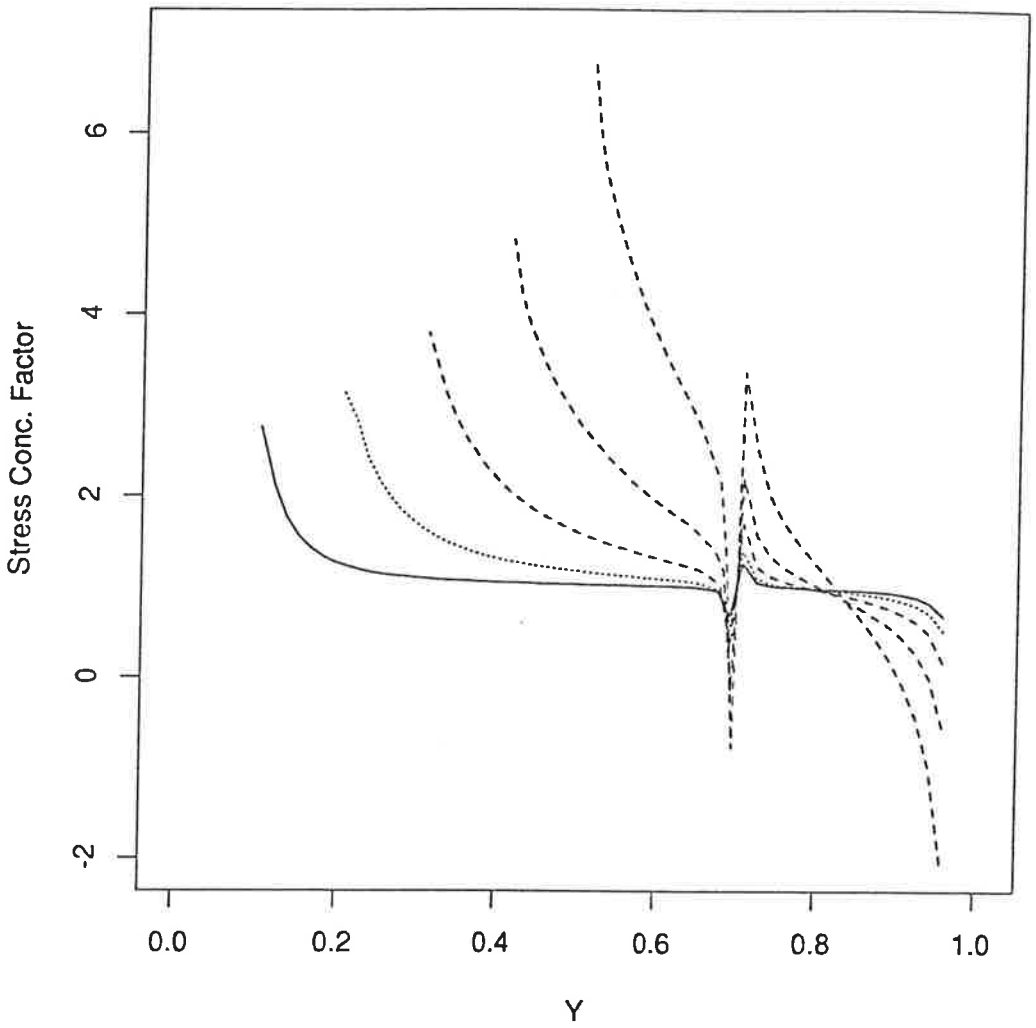

Figure 7.6
The behaviour of the stress concentration factor for homogeneous square plate with several diameters circular hole under uniaxial loading

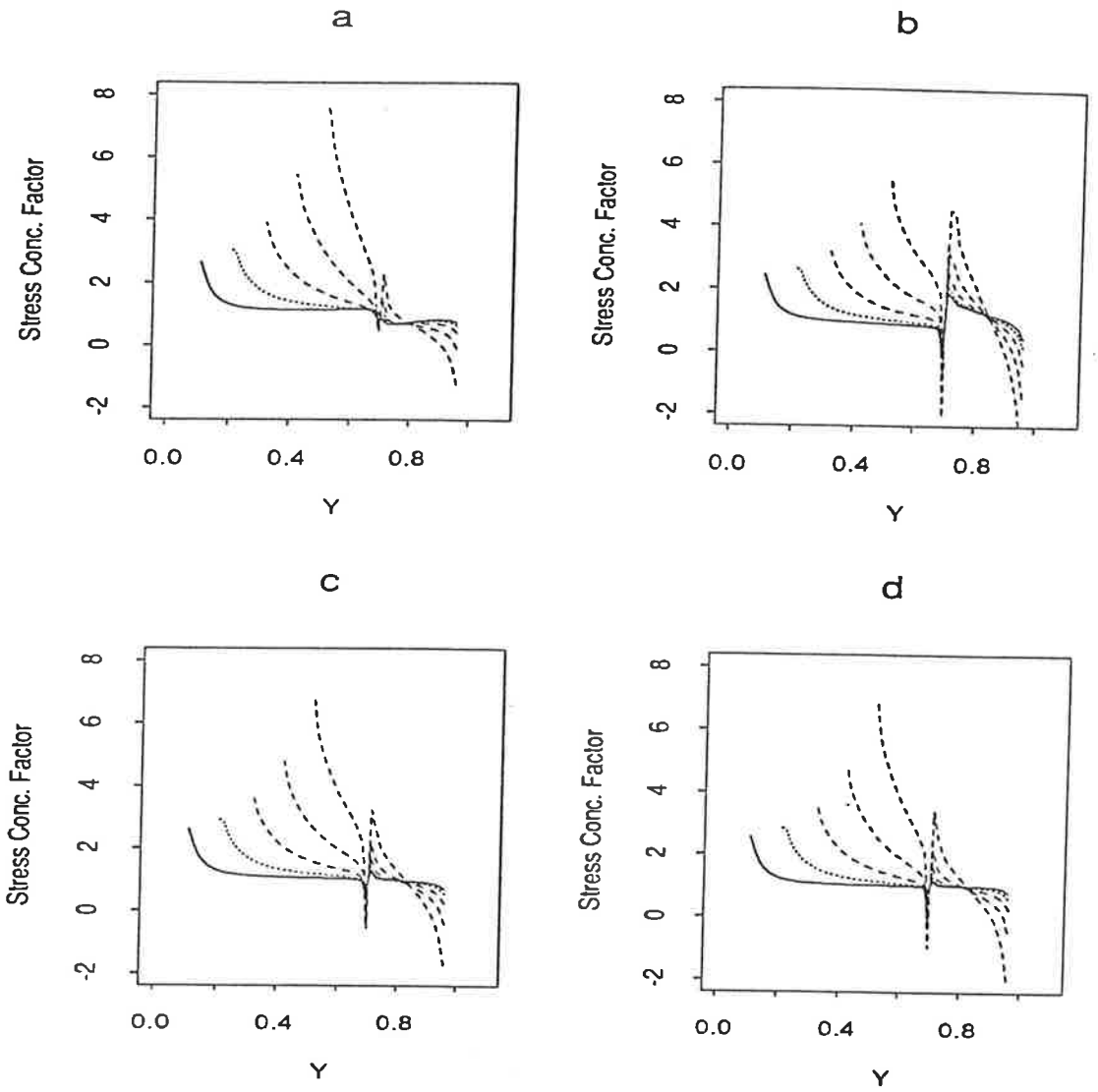

Figure 7.7
The behaviour of the stress concentration factor for two layered homogeneous square plate with several diameters circular hole under uniaxial loading

CHAPTER 8

SURFACE EFFECTS DUE TO INCIDENT PLANE *SH* WAVES

8.1 Introduction

One of the major concern of engineering seismology is to understand and explain vibrational properties of the soil excited by near earthquakes. Alluvial deposits, often very irregular geometrically, may affect significantly the amplitudes of incident seismic waves (see Trifunac [78]).

In the last few years, the ground amplification of seismic wave on alluvial valleys have been studied by numerous authors (see for example, Bravo et al [6], Sánchez–Sesma and Esquivel [64], Trifunac [78], Wong and Jennings [84], Wong and Trifunac [85], [86], Wong et al [87]). Integral equation formulations have been found to be particularly useful in obtaining numerical solutions to problems of this type. In particular, Wong and Jenning [84] have used singular integral equations to solve the problem of scattering and diffraction of incident *SH* waves by canyons of arbitrary cross section. Also Bravo [6] extended the method by considering stratified alluvial deposits. Very recently, Clements and Larsson [14] extended these integral formulation techniques by including the case of homogeneous anisotropic materials.

The work in this chapter can be considered as an extension of the previous work on integral equation formulations to include the case when the alluvial deposits are inhomogeneous anisotropic materials.

8.2 Ground motion on an alluvial inhomogeneous anisotropic valley

8.2.1 Problem formulation

Referred to a Cartesian frame $Ox_1x_2x_3$, we consider an anisotropic elastic half space occupying the region $x_2 > 0$ as illustrated in Figure 8.1. The half space here is divided into two regions in which the first region contains a homogeneous anisotropic material with shear moduli $\mu_{ij}^{(1)} = \lambda_{ij}^{(1)}$ and the second region contains an inhomogeneous anisotropic material with the shear moduli $\mu_{ij}^{(2)} = \lambda_{ij}^{(2)}(a_1^{(2)}x_1 + a_2^{(2)}x_2 + a_3^{(2)})^2$. The materials are assumed to adhere rigidly to each other so that the displacement and stress are continuous across the interface boundary between the first and the second regions and the constants in the shear moduli satisfy the symmetry conditions $\lambda_{ij}^{(\Omega)} = \lambda_{ji}^{(\Omega)}$ for $\Omega = 1, 2$.

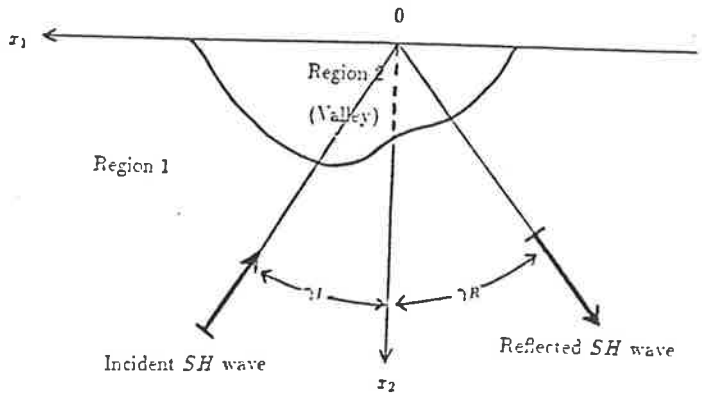

Figure 8.1
The alluvial valley and surrounding half-space

Let $u^{(1)}$ and $u^{(2)}$ be the displacements in the x_3 direction in the half space and the valley respectively. For the propagation of horizontally polarised SH waves, the displacement satisfies the equations of motion

$$\lambda_{ij}^{(1)} \frac{\partial^2 u^{(1)}}{\partial x_i \partial x_j} = \rho_0^{(1)} \frac{\partial^2 u^{(1)}}{\partial t^2}, \tag{8.2.1}$$

for region 1 and

$$\frac{\partial}{\partial x_i}\left[\lambda_{ij}^{(2)}\left(\alpha_1^{(2)}x_1 + \alpha_2^{(2)}x_2 + \alpha_3^{(2)}\right)^2 \frac{\partial u^{(2)}}{\partial x_j}\right] = \rho_0^{(2)}\left(\alpha_1^{(2)}x_1 + \alpha_2^{(2)}x_2 + \alpha_3^{(2)}\right)^2 \frac{\partial^2 u^{(2)}}{\partial t^2}, \tag{8.2.2}$$

for region 2. Here $\rho_0^{(\Omega)}$ denotes the density, t denotes the time and repeated Latin subscripts denote summation from 1 to 2.

In view of assuming the form of time dependence as $\exp(\imath\omega t)$, equation (8.2.1) can be reduced to

$$\lambda_{ij}^{(1)} \frac{\partial^2 v^{(1)}}{\partial x_i \partial x_j} + \rho_0^{(1)}\omega^2 v^{(1)} = 0, \tag{8.2.3}$$

by substituting

$$u^{(1)}(x_1, x_2, t) = v^{(1)}(x_1, x_2)\exp(\imath\omega t). \tag{8.2.4}$$

Similarly with equation (8.2.2). By using

$$u^{(2)}(x_1, x_2, t) = v^{(2)}(x_1, x_2)\exp(\imath\omega t). \tag{8.2.5}$$

we obtain

$$\frac{\partial}{\partial x_i}\left[\lambda_{ij}^{(2)}\left(\alpha_1^{(2)}x_1 + \alpha_2^{(2)}x_2 + \alpha_3^{(2)}\right)^2 \frac{\partial v^{(2)}}{\partial x_j}\right] + \rho_0^{(2)}\omega^2\left(\alpha_1^{(2)}x_1 + \alpha_2^{(2)}x_2 + \alpha_3^{(2)}\right)^2 v^{(2)} = 0. \tag{8.2.6}$$

Of interest is a plane wave of unit amplitude which propagates towards the surface of the elastic half space

$$v_I^{(1)} = \exp \imath\omega\left(t + \frac{x_1}{c_1} + \frac{x_2}{c_2}\right), \tag{8.2.7}$$

where $c_1 = \beta^{(1)}/\sin\gamma_I$, $c_2 = \beta^{(1)}/\cos\gamma_I$, $\beta^{(1)}$ denotes the velocity of the incident waves and γ_I denotes the angle of the incident wave. Since $v_I^{(1)}$ in (8.2.7) propagates in the first material, it must satisfy equation (8.2.3) so that

$$\left[\beta^{(1)}\right]^2 = \frac{\lambda_{11}^{(1)}\sin^2\gamma_I + 2\lambda_{12}^{(1)}\sin\gamma_I\cos\gamma_I + \lambda_{22}^{(1)}\cos^2\gamma_I}{\rho_0^{(1)}}. \tag{8.2.8}$$

Now we consider the case when region 1 and 2 are occupied by the same material. In order to satisfy the traction free surface condition on $x_2 = 0$, it is necessary to have a reflected wave of the form

$$v_R^{(1)} = \exp i\omega\left(t + \frac{x_1}{d_1} - \frac{x_2}{d_2}\right). \tag{8.2.9}$$

Thus if there are no irregularities, the free field solution of the displacement can be written as

$$v_O^{(1)} = v_I^{(1)} + v_R^{(1)}. \tag{8.2.10}$$

The stresses are given by

$$\sigma_{i3}^{(1)} = \lambda_{ij}^{(1)}\frac{\partial v^{(1)}}{\partial x_j}, \tag{8.2.11}$$

so that the stress $\sigma_{23}^{(1)}$ on $x_2 = 0$ is

$$\begin{aligned}\sigma_{23}^{(1)} = &\left(\frac{\lambda_{21}^{(1)}}{c_1} + \frac{\lambda_{22}^{(1)}}{c_2}\right)\exp\left[i\omega\left(t + \frac{x_1}{c_1}\right)\right] + \\ &\left(\frac{\lambda_{21}^{(1)}}{d_1} - \frac{\lambda_{22}^{(1)}}{d_2}\right)\exp\left[i\omega\left(t + \frac{x_1}{d_1}\right)\right].\end{aligned} \tag{8.2.12}$$

This stress will be zero for all time t if

$$\begin{aligned} d_1 &= c_1, \\ \frac{1}{d_2} &= \frac{1}{c_2} + \frac{2\lambda_{21}^{(1)}}{\lambda_{22}^{(1)}c_1}. \end{aligned} \tag{8.2.13}$$

These equations serves to provide d_2 in terms of the unknown quantities c_2, c_1, $\lambda_{21}^{(1)}$ and $\lambda_{22}^{(1)}$. Note that if (8.2.9) is substituted into (8.2.3) then since it represents a solution to (8.2.3) it follows that

$$\frac{\lambda_{11}^{(1)}}{c_1^2} - \frac{2\lambda_{12}^{(1)}}{c_1 d_2} + \frac{\lambda_{22}^{(1)}}{d_2^2} = \rho_0^{(1)}, \tag{8.2.14}$$

and if (8.2.13) is used to substitute for $1/d_2$ in (8.2.14), and then into (8.2.8) so that (8.2.13) ensures (8.2.9) is a solution to (8.2.3) on the assumption that (8.2.7) is also solution to (8.2.3).

Let $d_1 = \beta'/\sin\gamma_R$ and $d_2 = \beta'/\cos\gamma_R$ where γ_R is the angle of the reflection, then

$$\tan(\gamma_R) = \frac{d_2}{d_1} = \frac{\tan(\gamma_I)}{1 + 2(\lambda_{12}^{(1)}/\lambda_{22}^{(1)})\tan(\gamma_I)}, \tag{8.2.15}$$

and once γ_R has been determined from this equation, the wave speed β' of the reflected wave may be readily determined from the equation $\beta' = d_1 \sin(\gamma_R)$.

To include the influence of the inhomogeneous anisotropic alluvial valley in region 2, the solution for the exterior of the deposit is put in the form

$$v^{(1)} = v_O^{(1)} + v_D^{(1)}, \tag{8.2.16}$$

in which $v_D^{(1)}$ is the displacement due to diffracted waves. In region 2, the displacement $v^{(2)} = v_R^{(2)}$ will be caused by the refracted waves.

8.2.2 Integral equation

Proceeding further as in Clements and Larsson [14] for the region $\mathcal{R}_1$ with boundary C_1 and outward pointing normal components n_1 and n_2, the integral equation corresponding to (8.2.3) is

$$\tau v^{(1)}(a,b) = \int_{C_1} \left[\lambda_{ij}^{(1)} \frac{\partial V^{(1)}}{\partial x_j} n_i v^{(1)} - \lambda_{ij}^{(1)} \frac{\partial v^{(1)}}{\partial x_j} n_i V^{(1)} \right] dS, \tag{8.2.17}$$

where $\tau = 1$ if $(a,b) \in \mathcal{R}_1$ and $0 < \tau < 1$ if $(a,b) \in C_1$. The fundamental solution of $V^{(1)}$ is given by

$$V^{(1)} = \frac{i}{4} K^{(1)} \left[H_0^2(\overline{\nu}^{(1)} R^{(1)}) + H_0^2(\overline{\nu}^{(1)} \overline{R}^{(1)}) \right], \tag{8.2.18}$$

where

$$R^{(1)} = \left[(x_1-a)^2 + \frac{\lambda_{11}^{(1)}}{\lambda_{22}^{(1)}}(x_2-b)^2 - \frac{2\lambda_{12}^{(1)}}{\lambda_{22}^{(1)}}(x_1-a)(x_2-b)\right]^{\frac{1}{2}},$$

$$\overline{R}^{(1)} = \left[(x_1-a)^2 + \left(\frac{\lambda_{12}^{(1)}}{\lambda_{22}^{(1)}}\right)^2(x_2-b)^2 - \frac{2\lambda_{12}^{(1)}}{\lambda_{22}^{(1)}}(x_1-a)(x_2-b) + (x_2+b)^2\left(\frac{\lambda_{11}^{(1)}\lambda_{22}^{(1)} - \lambda_{12}^{(1)^2}}{\lambda_{22}^{(1)^2}}\right)\right]^{\frac{1}{2}}, \tag{8.2.19}$$

$$K^{(1)} = \frac{\lambda_{22}^{(1)}}{\lambda_{11}^{(1)}\lambda_{22}^{(1)} - \lambda_{12}^{(1)^2}},$$

$$\overline{\nu}^{(1)} = \rho_0^{(1)}\omega^2 K^{(1)},$$

and H_0^2 denotes the Hankel function of the second kind of order zero.

Proceeding further as in chapter 6, section 6.4 for the region $\mathcal{R}_2$ with boundary C_2 and outward pointing normal components n_1 and n_2, the integral equation corresponding to (8.2.6) is

$$K^{(2)}v^{(2)}(a,b) = \int_{C_2}\left[\lambda_{ij}^{(2)}(\alpha_1^{(2)}x_1 + \alpha_2^{(2)}x_2 + \alpha_3^{(2)})^2\frac{\partial V^{(2)}}{\partial x_j}n_i v^{(2)} - \lambda_{ij}^{(2)}(\alpha_1^{(2)}x_1 + \alpha_2^{(2)}x_2 + \alpha_3^{(2)})^2\frac{\partial v^{(2)}}{\partial x_j}n_i V^{(2)}\right]dS, \tag{8.2.20}$$

where

$$V^{(2)} = \frac{i}{4}(\alpha_1^{(2)}x_1 + \alpha_2^{(2)}x_2 + \alpha_3^{(2)})^{-1}H_0^2(\overline{\nu}^{(2)}R^{(2)}),$$

$$R^{(2)} = \left[(x_1-a)^2 + \frac{\lambda_{11}^{(2)}}{\lambda_{22}^{(2)}}(x_2-b)^2 - \frac{2\lambda_{12}^{(2)}}{\lambda_{22}^{(2)}}(x_1-a)(x_2-b)\right]^{\frac{1}{2}}, \tag{8.2.21}$$

$$\overline{\nu}^{(2)} = \frac{\rho_0^{(2)}\omega^2\lambda_{22}^{(2)}}{\lambda_{11}^{(2)}\lambda_{22}^{(2)} - \lambda_{12}^2}.$$

As in section 6.4, $K^{(2)}$ may be determined by the help of a solution of (8.2.6)

$$w = \frac{i}{4}(\alpha_1^{(2)}x_1 + \alpha_2^{(2)}x_2 + \alpha_3^{(2)})^{-1}H_0^2(\overline{\nu}^2 S^{(2)}), \tag{8.2.22}$$

where

$$S^{(2)} = \left[x_1^2 + \frac{\lambda_{11}^{(2)}}{\lambda_{22}^{(2)}}x_2^2 - \frac{2\lambda_{12}^{(2)}}{\lambda_{22}^{(2)}}x_1x_2\right]^{\frac{1}{2}}. \tag{8.2.23}$$

Thus using (8.2.22) in (8.2.20) we obtain

$$K^{(2)} = \left[w^{(2)}(a,b)\right]^{-1} \int_{C_2} \Big[\lambda_{ij}^{(2)} \left(\alpha_1^{(2)} x_1 + \alpha_2^{(2)} x_2 + \alpha_3^{(2)}\right)^2 \frac{\partial V^{(2)}}{\partial x_j} n_i w^{(2)} - \lambda_{ij}^{(2)} \left(\alpha_1^{(2)} x_1 + \alpha_2^{(2)} x_2 + \alpha_3^{(2)}\right)^2 \frac{\partial w^{(2)}}{\partial x_j} n_i V^{(2)} \Big] dS. \tag{8.2.24}$$

By applying equation (8.2.17) and its fundamental solution (8.2.18) in the region 1 (outside of the valley) then the only non zero integral is the integral over the valley's interface boundary (Sommerfeld radiation condition, see Ursell [79]). If we denote this interface boundary as curve C_I and valley's free boundary as C_F and specifying the normal components n_1 and n_2 pointing outward of the valley's boundary, thus (8.2.17) and (8.2.20) on the valley's boundary are

$$\frac{1}{2} v^{(1)}(a,b) = -\int_{C_I} \left[\lambda_{ij}^{(1)} \frac{\partial V^{(1)}}{\partial x_j} n_i v^{(1)} - \lambda_{ij}^{(1)} \frac{\partial v^{(1)}}{\partial x_j} n_i V^{(1)} \right] dS, \tag{8.2.25}$$

and

$$K^{(2)} v^{(2)}(a,b) = \int_{C_I + C_F} \Big[\lambda_{ij}^{(2)} \left(\alpha_1^{(2)} x_1 + \alpha_2^{(2)} x_2 + \alpha_3^{(2)}\right)^2 \frac{\partial V^{(2)}}{\partial x_j} n_i v^{(2)} - \lambda_{ij}^{(2)} \left(\alpha_1^{(2)} x_1 + \alpha_2^{(2)} x_2 + \alpha_3^{(2)}\right)^2 \frac{\partial v^{(2)}}{\partial x_j} n_i V^{(2)} \Big] dS. \tag{8.2.26}$$

The equations (8.2.25) and (8.2.26) together with the continuity equations

$$v^{(1)} = v^{(2)}, \tag{8.2.27}$$

$$\lambda_{ij}^{(1)} \frac{\partial v^{(1)}}{\partial x_j} n_i = \lambda_{ij}^{(2)} \left(\alpha_1^{(2)} x_1 + \alpha_2^{(2)} x_2 + \alpha_3^{(2)}\right)^2 \frac{\partial v^{(2)}}{\partial x_j} n_i, \tag{8.2.28}$$

and traction free boundary condition on $x_2 = 0$

$$\lambda_{ij}^{(2)} \left(\alpha_1^{(2)} x_1 + \alpha_2^{(2)} x_2 + \alpha_3^{(2)}\right)^2 \frac{\partial v^{(2)}}{\partial x_j} n_i = 0, \tag{8.2.29}$$

may be used to solved for displacement and stress over the interface boundary C_I and the displacement along traction free surface $x_2 = 0$. Once this has been done,

we can obtain the value of the displacements $v^{(1)}$ and/or $v^{(2)}$ at all points (a, b) in the half space $x_2 > 0$ through equations (8.2.17) and (8.2.20).

8.2.3 Numerical results

Suppose we have a semi circular valley (region 2 in Figure 8.1) which is defined by non dimensionalised quantities $(x_1 - 2)^2 + x_2^2 \leq 1$. Also suppose that the material properties $\lambda_{ij}^{(\Omega)}, \rho_0^{(\Omega)}, \alpha_1^{(2)}, \alpha_2^{(2)}, \alpha_3^{(2)}$, $\Omega = 1, 2$ are non dimensionalised quantities and the normalised frequency is defined by

$$\eta = \frac{\omega}{\pi \beta^{(1)}}, \tag{8.2.30}$$

where $\beta^{(1)}$ is given by (8.2.8).

Using the boundary element method by discretising 80 segments on the interface boundary and 70 segments on the free valley boundary, we obtain the numerical results as shown in Figures 8.2–8.9. In Figure 8.2 we used the non dimensionalised material specification as $\lambda_{11}^{(1)} = .12, \lambda_{12}^{(1)} = .00, \lambda_{22}^{(1)} = .12, \rho_0^{(1)} = 3., \lambda_{11}^{(2)} = .02, \lambda_{12}^{(2)} = .00, \lambda_{22}^{(2)} = .02, \rho_0^{(2)} = 2., \alpha_1^{(2)} = .0, \alpha_2^{(2)} = .0 \alpha_3^{(2)} = 1.$ and the incident angle of the wave is chosen to be zero. Note that the results found in Figure 8.2 and the others paper (see for example Sánchez–Sesma and Esquivel [64], Trifunac [78]) are no different. The results in Figure 8.3 are obtained by using the same material for the region 1. For the region 2 (the valley) we used a similar material as in Figure 8.2 also, except we now choose $\alpha_1^{(2)} = .5$, $\alpha_2^{(2)} = .0$, $\alpha_3^{(3)} = .0$. Similarly in Figures 8.4 and 8.5, we used the same material for region 1 and for region 2 the materials inhomogeneities are chosen to be $\alpha_1^{(2)} = .0, \alpha_2^{(2)} = .5, \alpha_3^{(2)} = 1.$ and $\alpha_1^{(2)} = .5, \alpha_2^{(2)} = .5, \alpha_3^{(2)} = .0$ respectively and the angle of the incident wave is specified by zero. Figures 8.6–8.9 are obtained by using the same materials as used for in Figures 8.2–8.5 respectively, except that in this case the incident wave angle is chosen to be 30°.

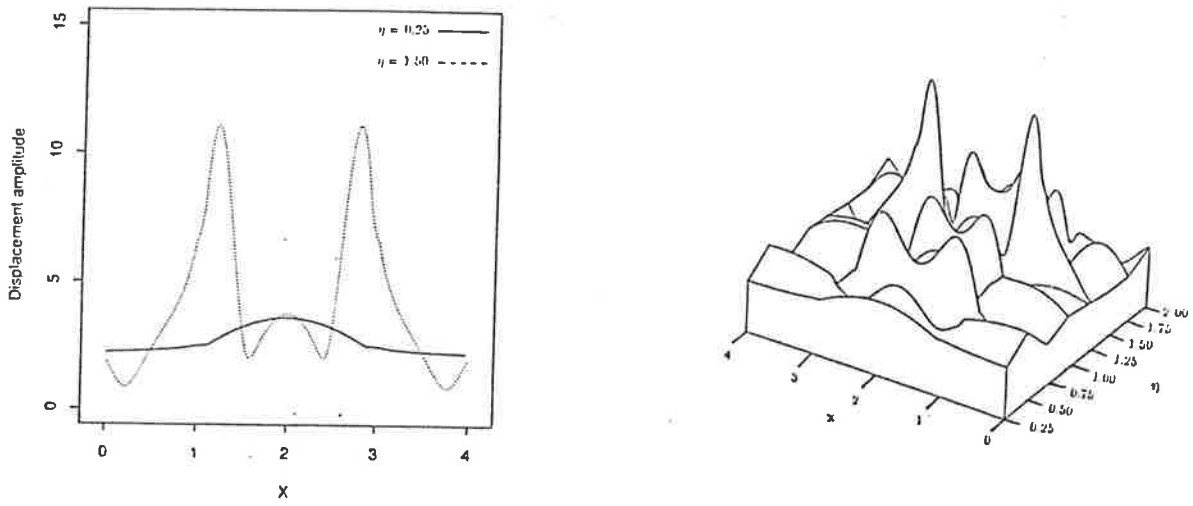

Figure 8.2
Effect of homogeneous valley, $\gamma_I = 0°$

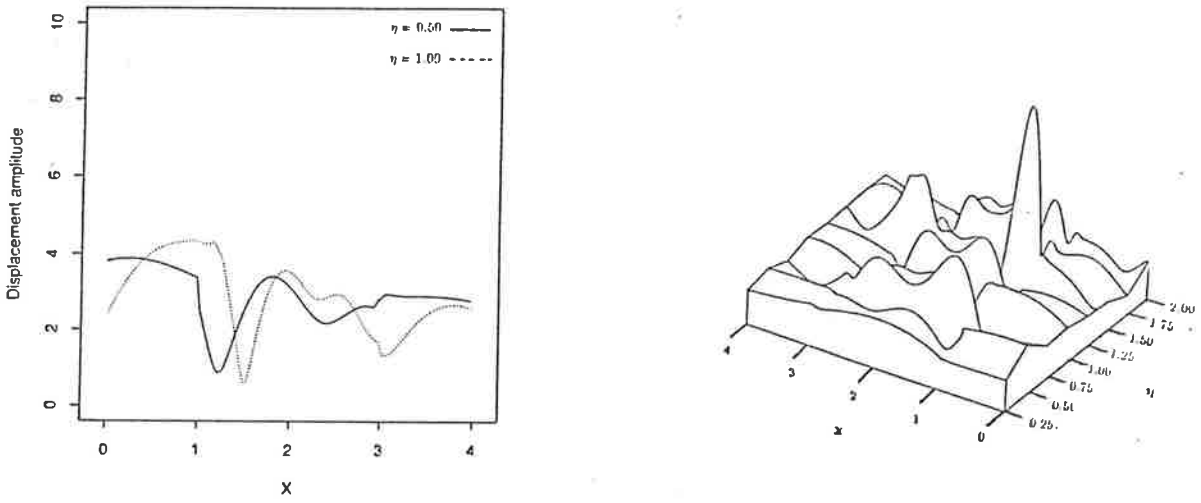

Figure 8.3
Effect of inhomogeneous valley, $\gamma_I = 0°$

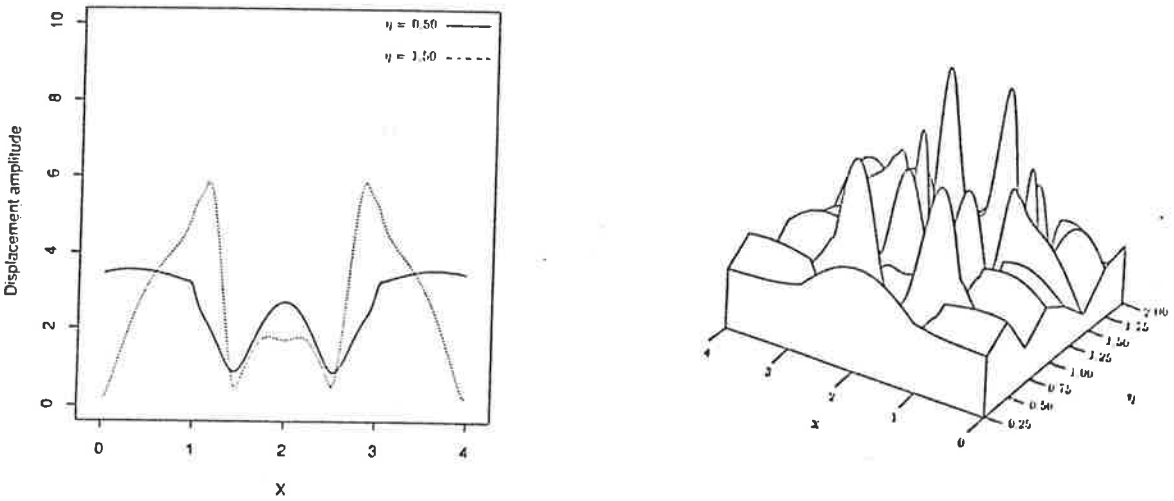

Figure 8.4
Effect of inhomogeneous valley, $\gamma_I = 0°$

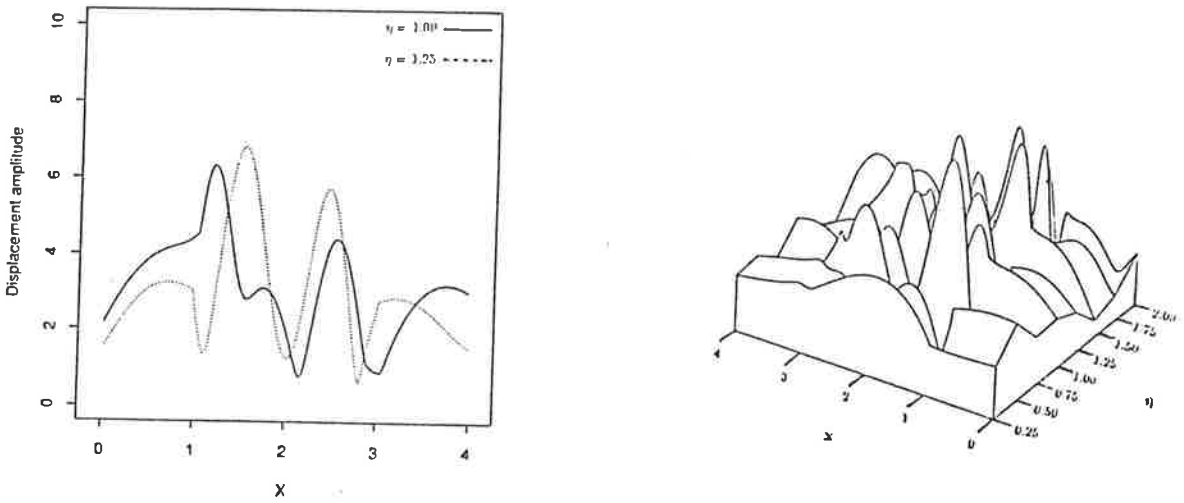

Figure 8.5
Effect of inhomogeneous valley, $\gamma_I = 0°$

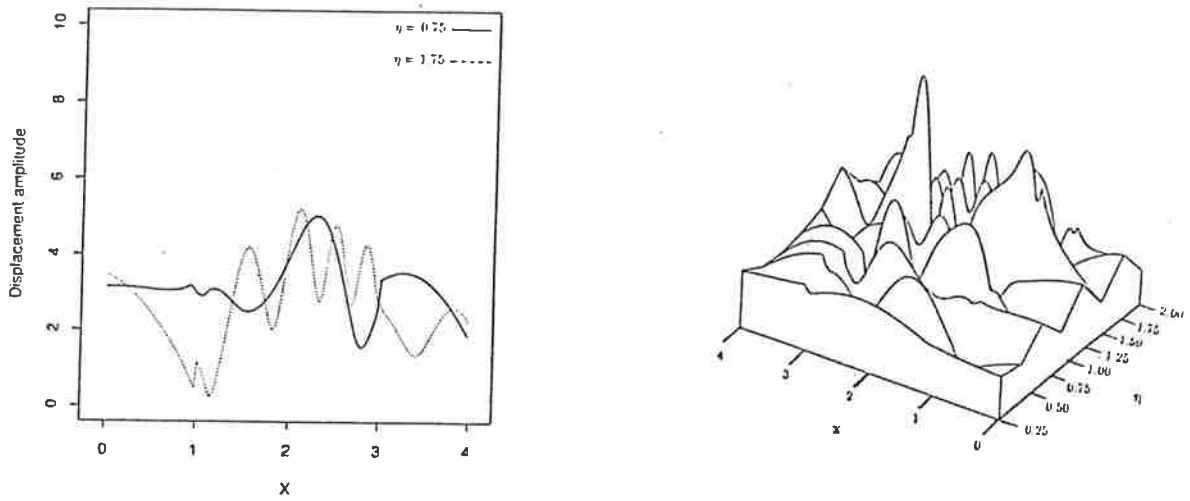

Figure 8.6
Effect of homogeneous valley, $\gamma_J = 30°$

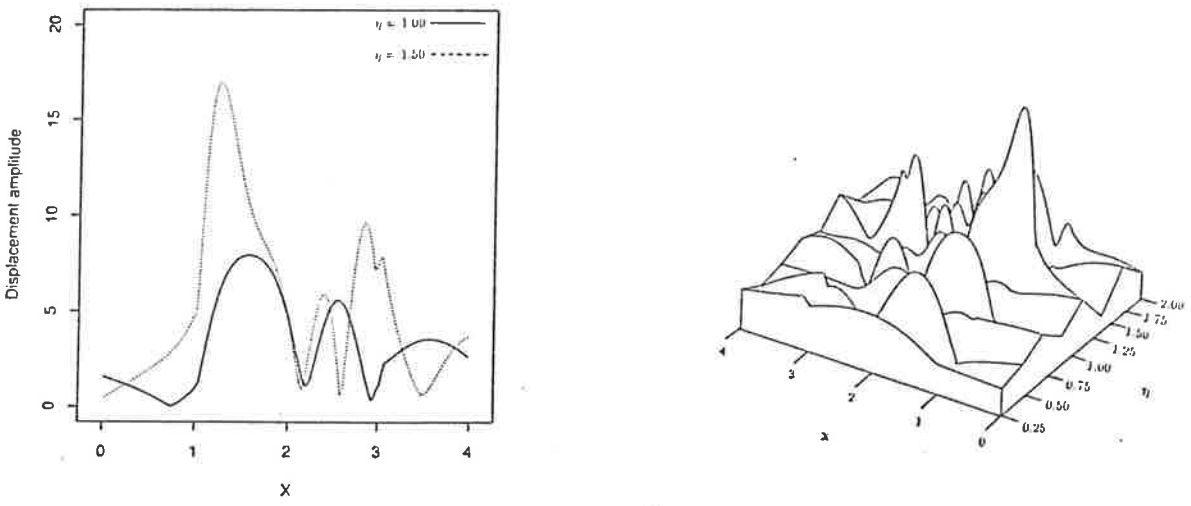

Figure 8.7
Effect of inhomogeneous valley, $\gamma_J = 30°$

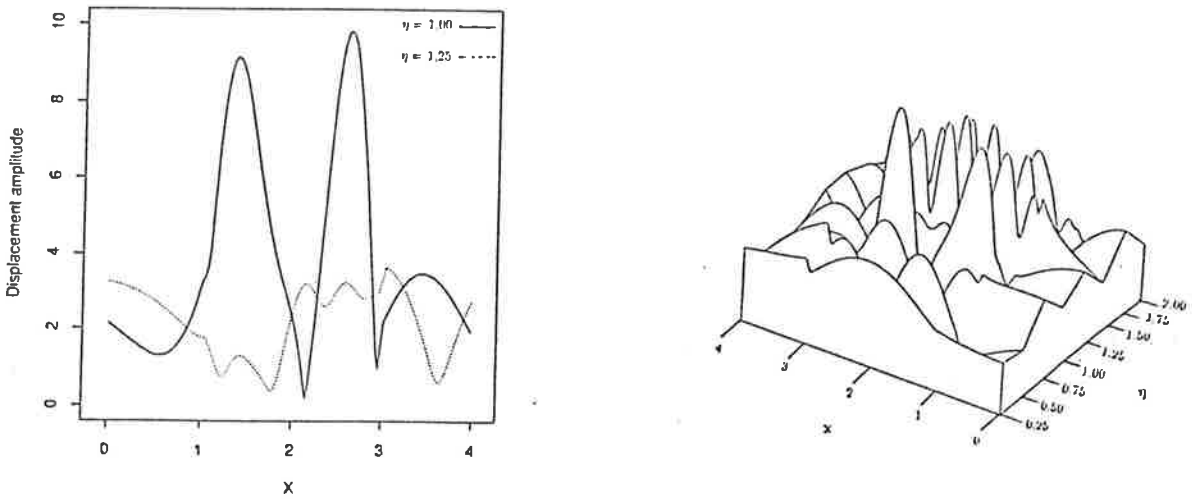

Figure 8.8
Effect of inhomogeneous valley, $\gamma_I = 30°$

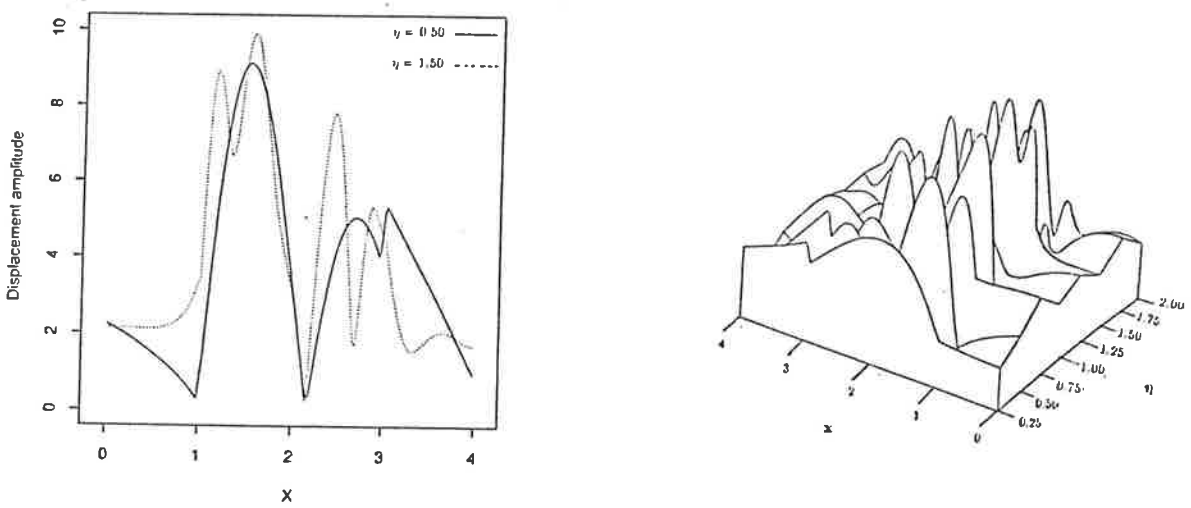

Figure 8.9
Effect of inhomogeneous valley, $\gamma_I = 30°$

8.3 Ground motion effect due to subterranean alluvial deposits

8.3.1 Problem formulation and integral equation

In the case of the alluvial deposits are under the ground (as illustrated in Figure 8.10), we can easily extend the work given in the previous section.

Referring to Cartesian coordinates $Ox_1x_2x_3$, we consider an anisotropic elastic half-space occupying the region $x_2 > 0$. The half space here is divided into two regions. The first region contains a homogeneous anisotropic materials with shear moduli $\mu_{ij}^{(1)} = \lambda_{ij}^{(1)}$. The second region contains an inhomogeneous anisotropic material with shear moduli $\mu_{ij}^{(2)} = \lambda_{ij}^{(2)}(\alpha_1^{(2)}x_1 + \alpha_2^{(2)}x_2 + \alpha_3^{(2)})^2$ and a finite domain bounded by a simple closed curve C_I.

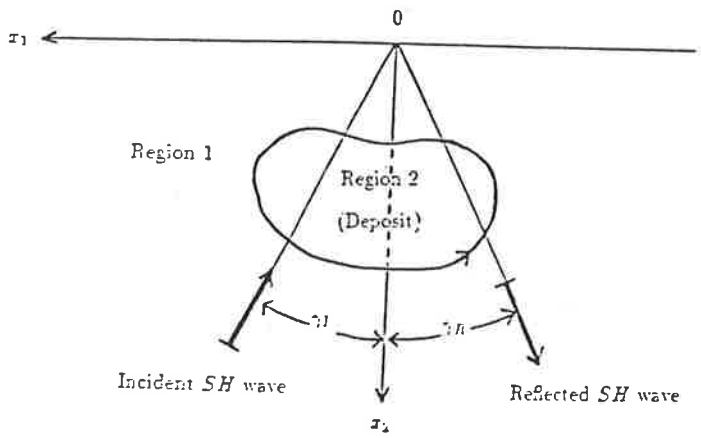

Figure 8.10
The alluvial deposit and surrounding half–space

Let $u^{(1)}$ and $u^{(2)}$ be the displacements in the x_3 direction in the half space and in the deposit respectively then for the propagation of horizontally polarised SH wave, the displacement should satisfy the wave equation (8.2.1) and (8.2.2) for the region 1

and region 2 respectively. Proceeding further as in the previous section the integral equation corresponding to equation (8.2.1) in this case can be written as

$$\tau v^{(1)}(a,b) = -\int_{C_I}\left[\lambda_{ij}^{(1)}\frac{\partial V^{(1)}}{\partial x_j}n_i v^{(1)} - \lambda_{ij}^{(1)}\frac{\partial v^{(1)}}{\partial x_j}n_i V^{(1)}\right]dS, \tag{8.3.1}$$

where $\tau = 1$ if $(a,b) \in$ region 1 and $0 < \tau < 1$ if $(a,b) \in$ boundary of region 1. n_i denotes the outward normal of the simple closed boundary C_I and $V^{(1)}$ is given by (8.2.18). Similarly, the integral equation corresponding to equation (8.2.2) can be written as

$$\begin{aligned} K^{(2)}v^{(2)}(a,b) = \int_{C_I}\Big[& \lambda_{ij}^{(2)}(\alpha_1^{(2)}x_1 + \alpha_2^{(2)}x_2 + \alpha_3^{(2)})^2\frac{\partial V^{(2)}}{\partial x_j}n_i v^{(2)} - \\ & \lambda_{ij}^{(2)}(\alpha_1^{(2)}x_1 + \alpha_2^{(2)}x_2 + \alpha_3^{(2)})^2\frac{\partial v^{(2)}}{\partial x_j}n_i V^{(2)}\Big]dS. \end{aligned} \tag{8.3.2}$$

By using equations (8.3.1), (8.3.2), the continuity equations as given by (8.2.27) and (8.2.28) across the interface boundary C_I, together with traction free condition on $x_2 = 0$ (which is given by (8.2.29)), we can solve for the displacement and stress over the interface boundary C_I. Once this has been done, we obtain all the values of the displacements $v^{(1)}$ and $v^{(2)}$ at all points (a,b) in the half space $x_2 > 0$.

8.3.2 Numerical results

Here we consider a semicircular alluvial deposit which is defined by non dimensionalised quantities x_1, x_2 as in the region $(x_1-2)^2+(x_2+1)^2 \leq 1, x_2 \leq -1$. Suppose we have the non dimensionalised material properties as $\lambda_{ij}^{(\Omega)}, \rho_0^{(\Omega)}, \alpha_1^{(2)}, \alpha_2^{(2)}, \alpha_3^{(2)}, \Omega = 1,2$ and the normalised frequencies defined by (8.2.30). Using the boundary element method by discretising the semi circular boundary into 80 segments and the diagonal of the circle into 70 segments, we obtain numerical results as shown in Figures 8.11–8.13. In Figure 8.11 we used the non dimensionalised material specification as $\lambda_{11}^{(1)} = .12, \lambda_{12}^{(1)} = .00, \lambda_{22}^{(1)} = .12, \rho_0^{(1)} = 3.0, \lambda_{11}^{(2)} = .02, \lambda_{12}^{(2)} = .00, \lambda_{22}^{(2)} = .02, \rho_0^{(2)} =$

$2., \alpha_1^{(2)} = .0, \alpha_2^{(2)} = .0, \alpha_3^{(2)} = 1.$ and the incident angle of the wave is chosen to be zero. The results in Figure 8.12 are obtained by using the same material for the region 1. For the region 2 (the sediment) we used the similar material as in Figure 8.11 also, except by choosing $\alpha_1^{(2)} = .5$, $\alpha_2^{(2)} = .0$, $\alpha_3^{(3)} = .0$ and using zero angle for the incident wave. In Figures 8.13 we used the same material for region 1 and for region 2 as in Figure 8.12 by specifying 30° as the incident angle.

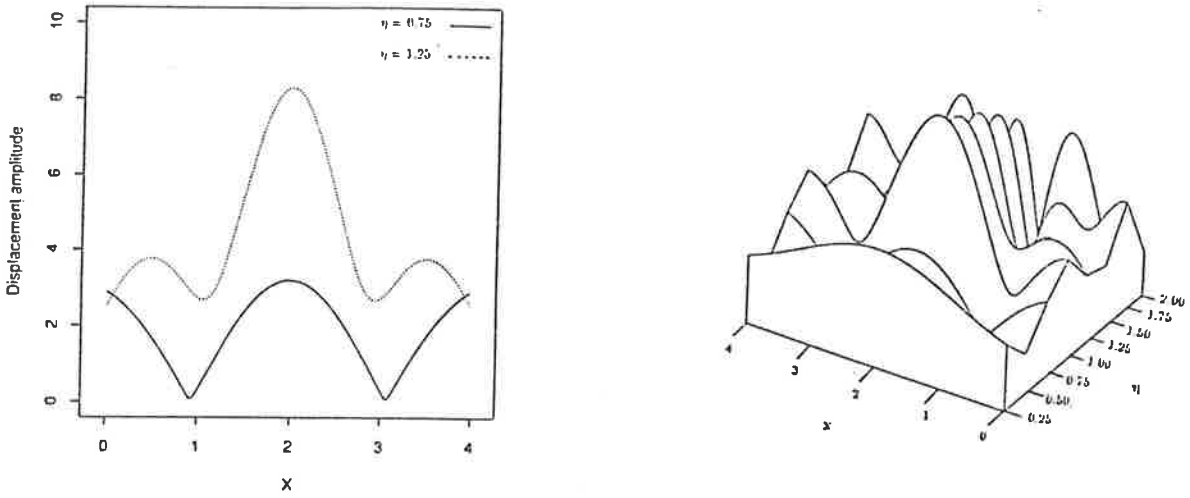

Figure 8.11
Effect of homogeneous deposit, $\gamma_I = 0°$

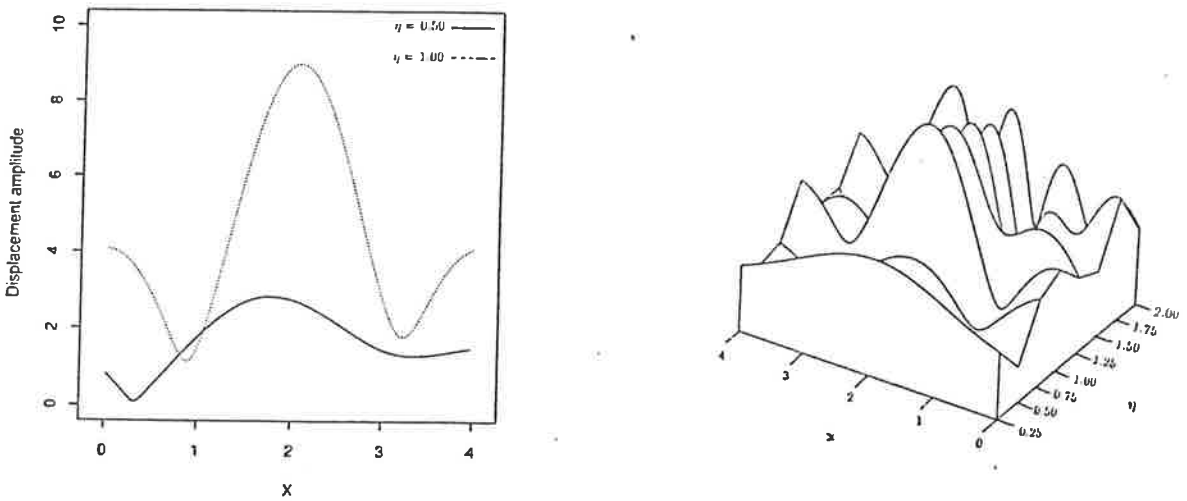

Figure 8.12
Effect of inhomogeneous deposit, $\gamma_I = 0°$

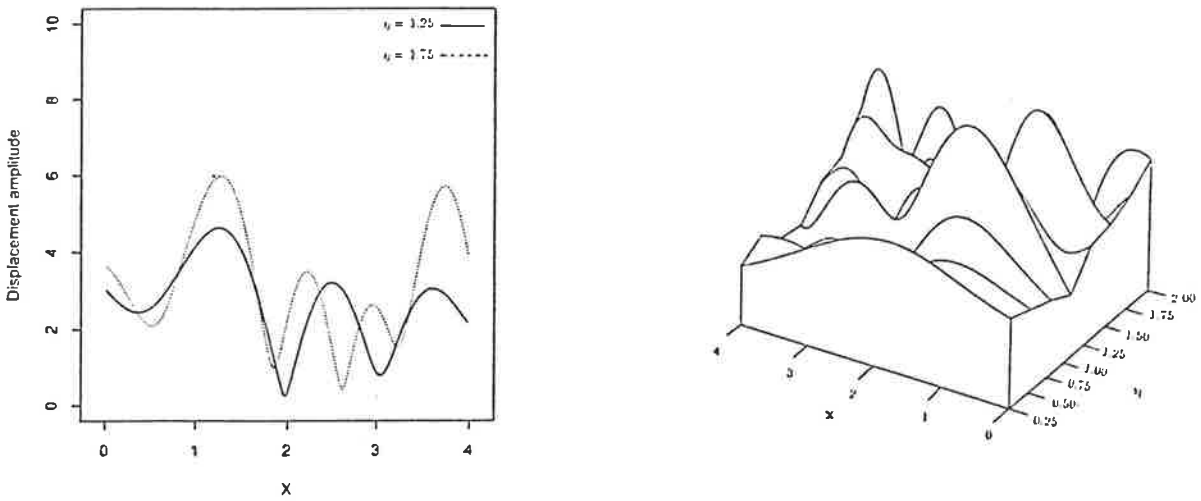

Figure 8.13
Effect of inhomogeneous deposit, $\gamma_I = 30°$

APPENDIX A

Theorem 1 :

Let $u = u(x, y)$ be a solution of

$$\frac{\partial}{\partial x}\left[\mu(x,y)\frac{\partial u}{\partial x}\right] + \frac{\partial}{\partial y}\left[\mu(x,y)\frac{\partial u}{\partial y}\right] + \rho(x,y)\omega^2 u = 0, \qquad (A.1.1)$$

valid in the region R in E^2 bounded by the contour C consisting of a finite number of piecewise smooth closed curves. Also, let u' be another solution of (A.1.1) valid in R, then the reciprocal relation corresponding to (A.1.1) is

$$\int_C \mu(x,y)\left[\frac{\partial u}{\partial n}u' - \frac{\partial u'}{\partial n}u\right] dS = 0. \qquad (A.1.2)$$

Proof :

$$\begin{aligned}
\int_C \mu(x,y)\frac{\partial u}{\partial n}u'\,dS &= \int_C \mu(x,y)\left[\frac{\partial u}{\partial x}u'n_1 + \frac{\partial u}{\partial y}u'n_2\right] dS \\
&= \int_R \left\{\frac{\partial}{\partial x}\left[\mu(x,y)\frac{\partial u}{\partial x}u'\right] + \frac{\partial}{\partial y}\left[\mu(x,y)\frac{\partial u}{\partial y}u'\right]\right\} dA \\
&= \int_R \left[\left\{\frac{\partial}{\partial x}\left[\mu(x,y)\frac{\partial u}{\partial x}\right] + \frac{\partial}{\partial y}\left[\mu(x,y)\frac{\partial u}{\partial y}\right]\right\}u' \right. \\
&\qquad \left. + \mu(x,y)\left\{\frac{\partial u}{\partial x}\frac{\partial u'}{\partial x} + \frac{\partial u}{\partial y}\frac{\partial u'}{\partial y}\right\}\right] dA \qquad (A.1.3) \\
&= \int_R \left[-\rho\omega^2 uu' + \mu\left\{\frac{\partial u}{\partial x}\frac{\partial u'}{\partial x} + \frac{\partial u}{\partial y}\frac{\partial u'}{\partial y}\right\}\right] dA.
\end{aligned}$$

Similarly

$$\int_C \mu(x,y)\frac{\partial u'}{\partial n}u\,dS = \int_R \left[-\rho\omega^2 uu' + \mu\left\{\frac{\partial u'}{\partial x}\frac{\partial u}{\partial x} + \frac{\partial u'}{\partial y}\frac{\partial u}{\partial y}\right\}\right] dA. \qquad (A.1.4)$$

Reciprocal relation in (A.1.2) is obtained by substracting (A.1.4) from (A.1.3).

Theorem 2 :

Let u be a solution of

$$\frac{\partial}{\partial x_i}\left[\mu_{ij}\frac{\partial u}{\partial x_j}\right] + \rho\omega^2 u = 0, \tag{A.2.1}$$

where $\mu_{ij} = \mu_{ji}$ valid in a region R in E^2 bounded by contour C consisting of a finite number of piecewise smooth closed curves. Also let u' be another solution of (A.2.1) valid in R. Then

$$\int_C \mu_{ij}\left[\frac{\partial u}{\partial x_j}u'n_i - \frac{\partial u'}{\partial x_j}un_i\right] dS = 0. \tag{A.2.2}$$

Proof :

$$\int_C \mu_{ij}\frac{\partial u}{\partial x_j}u'n_i\, dS = \int_C \left[\mu_{1j}\frac{\partial u}{\partial x_j}u'n_1 + \mu_{2j}\frac{\partial u}{\partial x_j}u'n_2\right] dS. \tag{A.2.3}$$

Using the divergence theorem in (A.2.3) yields

$$\begin{aligned}
\int_C \mu_{ij}\frac{\partial u}{\partial x_j}u'n_i\, dS &= \int_R \left\{\frac{\partial}{\partial x_1}\left[\mu_{1j}\frac{\partial u}{\partial x_j}u'\right] + \frac{\partial}{\partial x_2}\left[\mu_{2j}\frac{\partial u}{\partial x_j}u'\right]\right\} dA \\
&= \int_R \left\{\frac{\partial}{\partial x_1}\left[\mu_{1j}\frac{\partial u}{\partial x_j}\right] + \frac{\partial}{\partial x_2}\left[\mu_{2j}\frac{\partial u}{\partial x_j}\right]\right\}u' + \\
&\qquad \left\{\mu_{1j}\frac{\partial u}{\partial x_j}\frac{\partial u'}{\partial x_1} + \mu_{2j}\frac{\partial u}{\partial x_j}\frac{\partial u'}{\partial x_2}\right\} dA \\
&= \int_R \left\{-\rho\omega^2 uu' + \mu_{1j}\frac{\partial u}{\partial x_j}\frac{\partial u'}{\partial x_1} + \mu_{2j}\frac{\partial u}{\partial x_j}\frac{\partial u'}{\partial x_2}\right\} dA.
\end{aligned} \tag{A.2.4}$$

Similarly

$$\int_C \mu_{ij}\frac{\partial u'}{\partial x_j}un_i\, dS = \int_R \left\{-\rho\omega^2 u'u + \mu_{1j}\frac{\partial u'}{\partial x_j}\frac{\partial u}{\partial x_1} + \mu_{2j}\frac{\partial u'}{\partial x_j}\frac{\partial u}{\partial x_2}\right\} dA. \tag{A.2.5}$$

By substracting (A.2.5) from (A.2.4) the reciprocal relation (A.2.2) is obtained.

APPENDIX B

Illustration of multivalueness $G_1 = \frac{1}{4}\int_a^x Y_0\left(\nu\left[(t-a)^2+(y-b)^2\right]^{\frac{1}{2}}\right)dt$ around a square boundary. Left graphs and right graphs are obtained before and after the adjustment of the arctan function in the Bessel series expansion respectively.

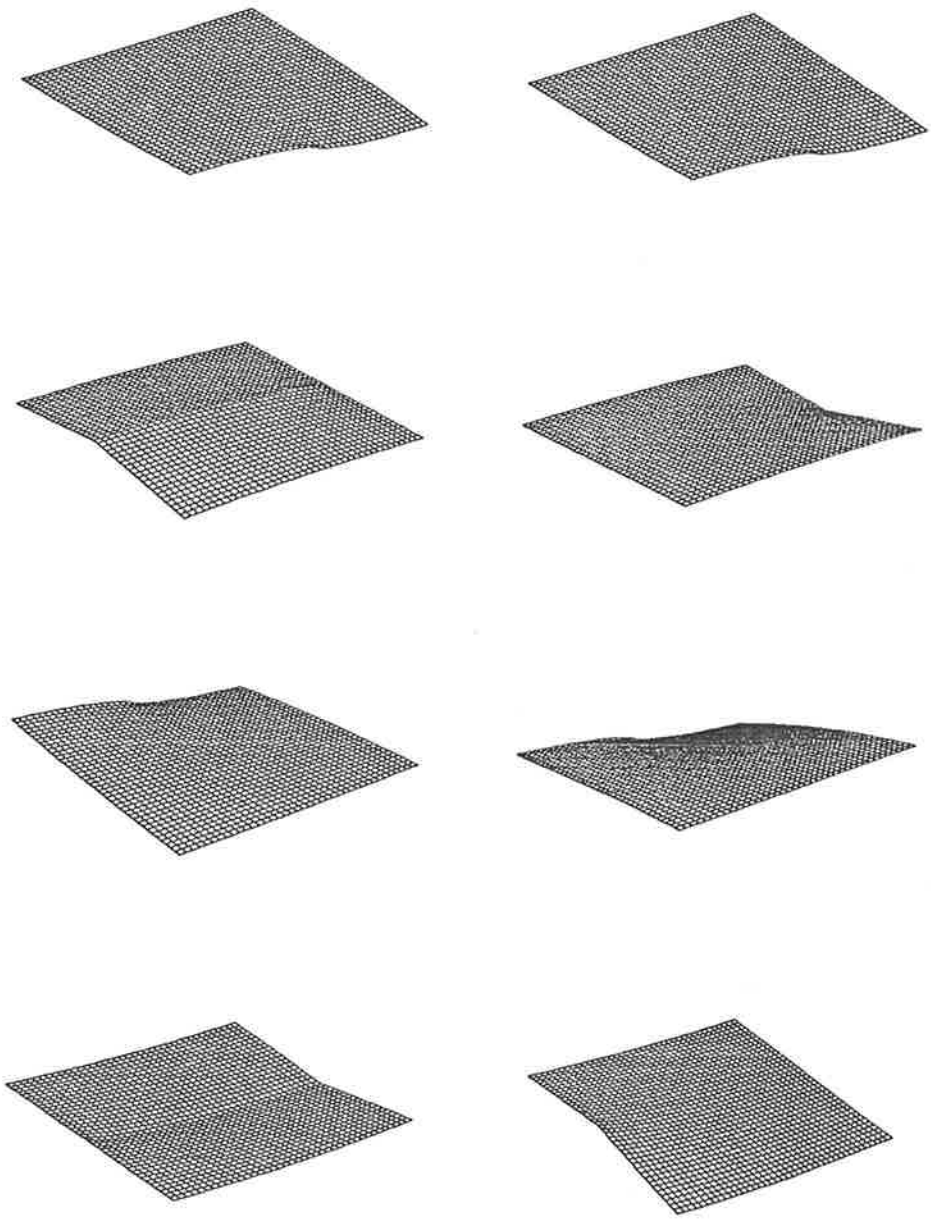

Illustration of multivalueness $\partial G_1/\partial y = -\frac{1}{4}\int_a^x Y_1(\nu\bar{r})(y-b)/\bar{r}\,dt$, with $\bar{r} = \left[(t-a)^2+(y-b)^2\right]^{\frac{1}{2}}$ around a square boundary. Left graphs and right graphs are obtained before and after the adjustment of the arctan function in the Bessel series expansion respectively.

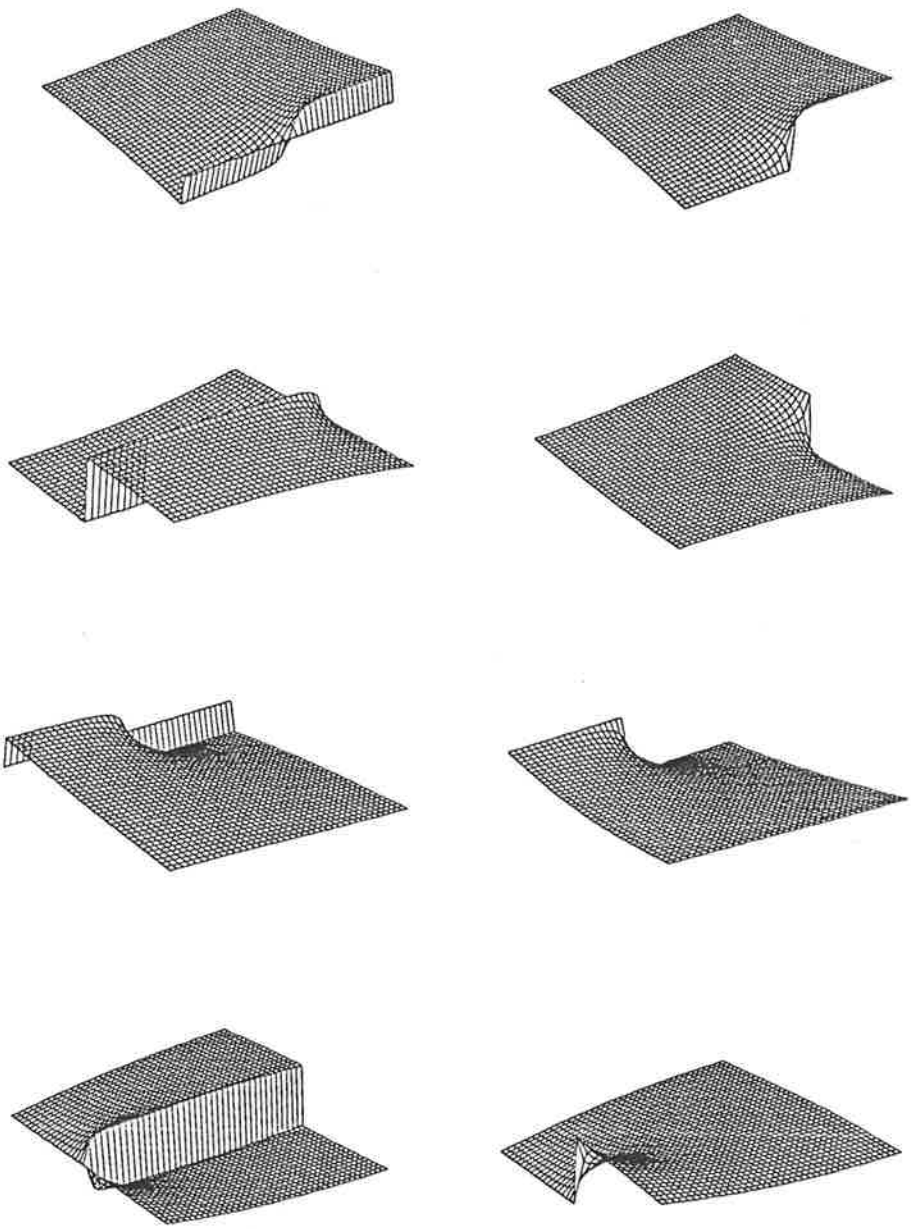

BIBLIOGRAPHY

[1] Abdrabbo, F. M. and Mahmoud, M. A. , Interruption Of A Seepage Flow From A Water Source, *Appl. Math. Modelling* Vol. 15, (1991), 406–415.

[2] Abramowitz, M. and Stegun, I. A. ,*Handbook of Mathematical Functions* Dover, New York, (1970).

[3] Ang, W. T. , A Boundary Integral Equation For Deformations Of An Elastic Body With An Arc Crack, *Quarterly of Applied Mathematics 45*, (1987), 131–139.

[4] Ang, W. T. , *Some Crack Problems*, Thesis, (1987).

[5] Bateman, H. , *Higher Transcendental Functions* Vol. II, Mc Graw-Hill Inc., (1953).

[6] Bravo, M. A. ; Sánchez-Sesma, F. J. and Chávez– García, F. J. , Ground Motion On Stratified Alluvial Deposit For Incident *SH* Waves, *Bull. Seism. Soc. Am. 78*, (1988), 436–450.

[7] Brekhovskikh, L. M. , *Waves In Layered Media*, Academic Press, (1960).

[8] Carnahan, B. , Luther, H. A. , Wilkes, J. O. *Applied Numerical Methods*, John Wiley & Sons Inc., (1969).

[9] Cheng, Alexander H. D. , Darcy's Flow With Variable Permeability : A Boundary Integral Solution, *Water Resources Research* , Vol. 20, (1984), 980–984.

[10] Clements, D. L. , A Boundary Integral Equation Method For The Numerical Solution Of A Second Order Elliptic Equation With Variable Coefficients, *J. Austral. Math. Soc. 22 (series B)*, (1980), 218–228.

[11] Clements, D. L. , *Boundary Value Problems Governed By Second Order Elliptic Systems* , Pitman, (1981).

[12] Clements, D. L. , The Boundary Element Method For Linear Elliptic Equations With Variable Coefficients, *Boundary Element X*, (1989), 91–96.

[13] Clements, D. L. and Kusuma, J. , On The Boundary Element Method For Darcy's Flow With Variable Permeability, *CTAC*, 1991.

[14] Clements, D. L. and Larsson, A. , Ground Motion On Alluvial Valleys Under Invident Plane *SH* Waves, *J. Austral. Math. Soc. Ser. B 33*, (1991), 240–253.

[15] Clements, D. L. ; Moodie, T. B. and Rogers, C. , On The Propagation Of Waves From Spherical And Cylindrical Cavities In Anisotropic Materials, *Int. J. Engng. Sci. 15*, (1977), 429–445.

[16] Clements, D. L. and Rizzo, F. J. , A Method for Numerical Solution of Boundary Value Problems Governed by Second–order Elliptic Systems, *J. Inst. Maths Applics 22*, (1978), 197–202.

[17] Clements, D. L. and Rogers, C. , On The General Solution Of A Linear Second Order Equation With Variable Coefficients, *Mathematika 30*, (1983), 94–103.

[18] Clements, D. L. and Rogers, C. , Wave Propagation In Inhomogeneous Elastic Media With (N+1)-Dimensional Spherical Symmetry, *Can. J. Phys. 52*, (1974), 1246–1252.

[19] Clements, D. L. and Rogers, C. , A Boundary Integral Equation For The Solution Of A Class Of Problems In Anisotropic Inhomogeneous Thermostatics And Elastostatics, *Quarterly of Applied Mathematics* , (1983), 99–105.

[20] Coleman, C. J. ,On The Use Of Particular Solutions In The Boundary Element Approach To The Forced Helmholtz Equation, *CTAC*, 1991.

[21] Cook, R. K. , Some Properties Of Struve Functions, *J. Washington Acad. Sci. 47*, (1957), 365–368.

[22] Cruse, T. A. , *Advanced Boundary Element Methods*, Springer-Verlag, (1987).

[23] Davis, P. J. and Rabinowitz, P. , *Numerical Integration* , Blaisdell Publishing Company, (1967).

[24] Delale, F. and Erdogan, F. , The Crack Problem For A Nonhomogeneous Plane, *J. Appl. Mech. 50*, (1983), 609–614.

[25] Dhaliwal, R. S. and Singh, B. M. , On The Theory Of Elasticity Of A Nonhomogeneous Medium, *Journal Of Elasticity 8*, (1978), 211–219.

[26] Eason, G. , Propagation Of Waves From Spherically And Cylindrical Cavities, *ZAMP 14*, (1963), 12-23.

[27] England, A. H. . *Complex Variable Methods In Elasticity*, John Wiley, London, (1971).

[28] Erguven, M. E. , Torsion of A Nonhomogeneous Transversely Isotropic Half Space, *Lett. Appl. Engng. Sci. 20*, (1982), 675–679.

[29] Erigen, A. C. and Suhubi, E. S. *Elastodynamics*, Academic Press, (1975).

[30] Ewing, W. M. ; Jardetzky, W. S. and Press, F. , *Elastic Waves In Layered Media*, McGraw–Hill Inc., (1957).

[31] Gerasoulis, A. and Srivastav, R. P. , A Griffith Crack Problem For A Nonhomogeneous Medium, *Int. J. Engng. Sci. 18*, (1980), 239–247.

[32] Graff, Karl F. , *Wave Motion In Elastic Solids*, Clarendon Press, Oxford, (1973).

[33] Gray, A. , Mathews, G. B. ,*A Treatise On Bessel Functions*, MacMillan and Co. Ltd., London, (1922).

[34] Green, A. E. and Zerna, W. ,*Theoritical Elasticity* , Oxford, (1954).

[35] Guiggiani, M. and Casalini, P. , Direct Computation Of Cauchy Principal Value Integrals In Advanced Boundary Elements, *Int. J. Numer. Methods Eng. 24*, (1987), 1711–1720.

[36] Head, A. K. , The Galois Unsolvability Of The Sextic Equation Of Anisotropic Elasticity, *Journal Of Elasticity 9*, (1979), 9–20.

[37] Hellwig, G. , *Partial Differential Equations*, Teubner Stuttgart, (1977).

[38] Hui-Ching Wang and Banerjee, P. K. , Axisymmetric Free Vibration Problems By Boundary Element Method, *J. Appl. Mech. 55*, (1988), 437–442.

[39] Kanval, R. P. ,*Linear Integral Equations Theory and Technique*, Academic Press, (1971).

[40] Karageorghis, A. and Fairweather, G. , The Almansi Method Of Fundamental Solutions For Solving Biharmonic Problems, *Int. J. Numer. Methods Eng. 26*, (1988), 1665–1682.

[41] Katsikadelis, J. T. and Sapountzakis, E. J. , An Approach To The Vibration Problem Of Homogeneous, Non–Homogeneous And Composite Membranes Based On The Boundary Element Method, *Int. J. Numer. Methods Eng. 26*, (1988), 2439–2455.

[42] Kohn, W. , Propagation Of Low–Frequency Elastic Disturbances In A Composite Material, *J. Appl. Mech. 41*, (1974), 97–100.

[43] Kohn, W. , Krumhansl, J. A. , Lee, E. H. , Variational Methods For Dispersion Relations And Elastic Properties Of Composite Materials, *J. Appl. Mech. 39*, (1972), 327–336.

[44] Kolsky, H. , *Stress Waves In Solids*, Clarendon Press, (1953).

[45] Lebevev, N. N. , *Special Functions And Their Application*, Printice-Hall Inc., (1965).

[46] Liggett, J. A. ,Liu, P. F. ,*The Boundary Integral Equation Method For Porous Media Flow*, George Allen & Unwin, (1983).

[47] Love, A. E. H. ,*A Treatise On The Mathematical Theory Of Elasticity*, Cambridge Univeristy Press, (1892).

[48] Mase, G. E. ,*Continuum Mechanics*, Mc-Graw Hill book Company, (1970).

[49] McCarthy, M. F. , Hayes. M. A. *Elastic Wave Propagation*, North-Holland Series, (1988).

[50] McLachan, N. W. , *Bessel Function For Engineers* , Oxford University Press, (1941).

[51] Moodie, T. B. , On The Propagation Of Radially Symmetric Waves In Nonhomogeneous Isotropic Elastic Media, *Utilitas Mathematica 2*, (1972), 181–203.

[52] Moodie, T. B. ; Rogers, C. and Clements, D. L. , Radial Propagation Of Axial Shear Waves In An Incompressible Elastic Material Under Finite Deformation, *Int. J. Engng. Sci. 14*, (1976), 585–603.

[53] Muskhelishvili, N. I. , *Some Basic Problems Of The Mathematical Theory Of Elasticity*, (1953).

[54] Myint–U, Tyn, *Partial Differential Equations Of Mathematical Physics*, Elsevier, (1973).

[55] Nasser, S. N. , General variational methods for waves in elastic composites, *Journal of elasticity 2*, (1972), 73–90.

[56] Nayfeh, A. H. and Nasser, S. N. , Elastic Waves In Inhomogeneous Elastic Media, *J. Appl. Mech. 39*, (1972), 696–702.

[57] Ogilvy, J. ,A. , A Layered Media Model For Ray Propagation In Anisotropic Inhomogeneous Materials, *Appl. Math. Modelling* Vol. 14, (1990), 237–247.

[58] Rainville, E. D. , *Special Functions*, Macmillan Company New York, (1960).

[59] Rangogni, R. , A Solution Of Darcy's Flow With Variable Permeability By Means Of BEM And Perturbation Technique, *Boundary Element 9*, (1987), 359–368.

[60] Rangogni, R. , Numerical Solution Of The Generalised Laplace Equation By Coupling The Boundary Element Method And The Perturbation Method, *Appl. Math. Modelling*, Vol. 10, (1986), 266–270.

[61] Rizzo, F. J. , An Integral Equation Approach To Boundary Value Problems Of Classical Elastostatics, *Quarterly of Applied Mathematics 25*, (1967), 83–95.

[62] Rogers, C. and Clements, D. L. , Bergman's Integral Operator Method In Inhomogeneous Elasticity, *Quarterly of Applied Mathematics 36*, (1978), 315–321.

[63] Rogers, C. and Shadwick, W. F. ,*Bäcklund Transformations and Their Applications*, Academic Press, (1982).

[64] Sánchez-Sesma, F. J. and Esquivel, J. A. ,Ground Motion on Alluvial Valleys Under Incident Plane *SH* Waves, *Bull. Seism. Soc. Am. 69*, (1979), 1107–1120.

[65] Schwarz, H. R. , *Numerical Analysis Of Symmetric Matrices*, Prentice Hall, Inc., (1973).

[66] Shilkrut, D. ; Uziel, A. and Gruntman, S. , Elastic Stress Concentrations In A Square Plate With A Large Hole Under Uniaxial Loading, *Journal Of Strain Analysis 22*, (1987), 55–61.

[67] Singh, B. M. and Dhaliwal, R. S. , Asymmetric problem Of A Griffith Crack In A Nonhomogeneous Medium Under Shear, *Journal Of Elasticity 8*, (1978), 313–318.

[68] Sneddon, I. H. , *The Use Of Integral Transforms*, McGraw–Hill, (1972).

[69] Sneddon, I. N. , *Fourier Transforms*, McGraw–Hill, New York, (1951).

[70] Sneddon, I. N. , *Special Function Of Mathematical Physics And Chemistry*, Interscience Publishers Inc., New York, (1961).

[71] Sokolnikoff, I. S. , *Mathematical Theory of Elasticity*, (1956).

[72] Stewart, G. W. , *Introduction To Matrix Computations*, Academic Press, (1973).

[73] Stoker, J. J. ,*Nonlinear Vibrations*, Interscience Publishers Inc., New York, (1950).

[74] Sun, C. T. , Achenbach, J. D. , Herrmann, G. , Continuum Theory For A Laminated Medium, *J. Appl. Mech. 35*, (1968), 467–475.

[75] Synge, J. L. , On The Vibrations Of A Heterogeneous String, *Quar. Appl. Math. 39*, (1981), 292–297.

[76] Tanaka, M. , A Boundary Element Method For Some Inverse Problems In Elastodynamics, *Appl. Math. Modelling* , Vol. 13, (1989), 307–312.

[77] Tranter, C. J. , *The Integral Transforms In Mathematical Physics*, Chapman and Hall Ltd. , (1965).

[78] Trifunac, M. D. , Surface Motion Of A Semi-Cylindrical Alluvial Valley For Incident Plane *SH* Waves, *Bull. Seism. Soc. Am. 61*, (1971), 1755–1770.

[79] Ursell, F. , On The Exterior Problems Of Acoustics, *Proc. Camb. Phil. Soc 74*, (1973), 117–125.

[80] Watson, G. N. , *Treatise On The Theory Of Bessel Function*, Cambridge, (1922).

[81] Wearing, J. L. and Sheikh, M. A. , A Combined Finite Element Boundary Element Technique For Stress Analysis, *Boundary Element X*, (1989), 493–506.

[82] Wilkinson, J. H. , *The Algebraic Eigenvalue Problem*, Clarendon Press, Oxford, (1965).

[83] Wilkinson, J. H. and Reinsch, C. , *Handbook For Automatic Computation*, Springer Verlag, (1971).

[84] Wong, H. L. and Jennings, P. C. , Effects Of Canyon Topography On Strong Ground Motion, *Bull. Seism. Soc. Am. 65*, (1975), 1239–1257.

[85] Wong, H. L. and Trifunac, M. D. , Interaction Of A Shear Wall With The Soil For Incident Plane *SH* Waves : Elliptical Rigid Foundation, *Bull. Seism. Soc. Am. 64*, (1974), 1825–1842.

[86] Wong, H. L. and Trifunac, M. D. , Surface Motion Of A Semi-elliptical Alluvial Valley For Incident Plane *SH* Waves, *Bull. Seism. Soc. Am. 64*, (1974), 1389–1408.

[87] Wong, H. L. ; Trifunac, M. D. and Westermo, B. , Effects Of Surface And Subsurface Irregularities On The Amplitudes Of Monochromatic waves, *Bull. Seism. Soc. Am. 67*, (1977), 353–368.

[88] Yang, W. H. and Lee, E. H. , Modal Analysis Of Floquet Waves In Composite Materials, *J. Appl. Mech. 41*, (1974), 429–433.

[89] Yih-Hsing Pao, Dynamic Stress Concentration In An Elastic Plate, *J. Appl. Mech. 29*, (1962), 299–305.

[90] Yih-Hsing Pao, Elastic Waves In Solids, *J. Appl. Mech. 50*, (1983), 1152–1164.